CARBON POOLS, DYNAMICS, AND BUDGET OF THE BRUCE PENINSULA

KATHLEEN BAO

A THESIS SUBMITTED TO THE
FACULTY OF GRADUATE STUDIES
IN PARTIAL FULFILLMENT OF THE REQUIREMENTS
FOR THE DEGREE OF
MASTER OF SCIENCE

GRADUATE PROGRAM IN GEOGRAPHY
YORK UNIVERSITY
TORONTO, ONTARIO

JANUARY 2024

Abstract

The northern Bruce Peninsula is a UNESCO World Biosphere Reserve, contains the largest continuous forest in Southern Ontario and is a hotspot for biodiversity. However, there is little research done on the carbon pools, their dynamics and the soil carbon budget. A more comprehensive understanding of the processes regulating the uptake and release of carbon dioxide with the atmosphere is needed. This thesis aims to 1) quantify how much carbon is stored in aboveground biomass, soil, roots, litter, and deadwood pools, 2) understand how the carbon moves between these pools and 3) estimate the annual rate of change of the soil carbon budget. Using a LICOR LI8100, measuring soil respiration at 15-minute intervals over the course of two years, the amount of carbon released by heterotrophic (R_h) and autotrophic (R_a) respiration, was determined for litter and soil separately.

Acknowledgements

Table of Contents

List of Figures

List of Tables

1.0 – Introduction

1.1 – The Carbon Pools and Dynamics of the Bruce Peninsula

1.1.1 – The Research Problem

While being a biodiversity hotspot, not much is known about the soil carbon dynamics and carbon pools for the Bruce Peninsula. Globally, the amount of carbon stored in the soil is 3.1 times larger than the amount of atmospheric carbon and is the second largest carbon sink following Earth's oceans. Soil carbon plays a large role in the cycling and storage of carbon on Earth (Ontl & Schulte, 2012). Over 3170 GtC (3170 GtC = 3170×10^9 tonnes) of the total amount of carbon is stored in terrestrial systems with 80% stored in soil (Ontl & Schulte, 2012). The Bruce Peninsula is classified by UNESCO as a World Biosphere Reserve – a hotspot of biodiversity including rare, endangered, and endemic species. It is the northern terminus of the Niagara Escarpment in Ontario and is classified as a Breypen land type comprising predominantly of exposed dolostone bedrock and small patches of soil (Liipere, 2014). Most of the peninsula is classified as poor agricultural land due to the exposed bedrock, although there are areas with soil derived from glacial lake-bed sediments that support agriculture. Both surface and subsurface drainage occurs in the Peninsula with water flowing from northeast to southwest (Liipere, 2014). Karst topography is a result of the subsurface drainage systems due to the chemical weathering of dolomitic limestone (Liipere, 2014).
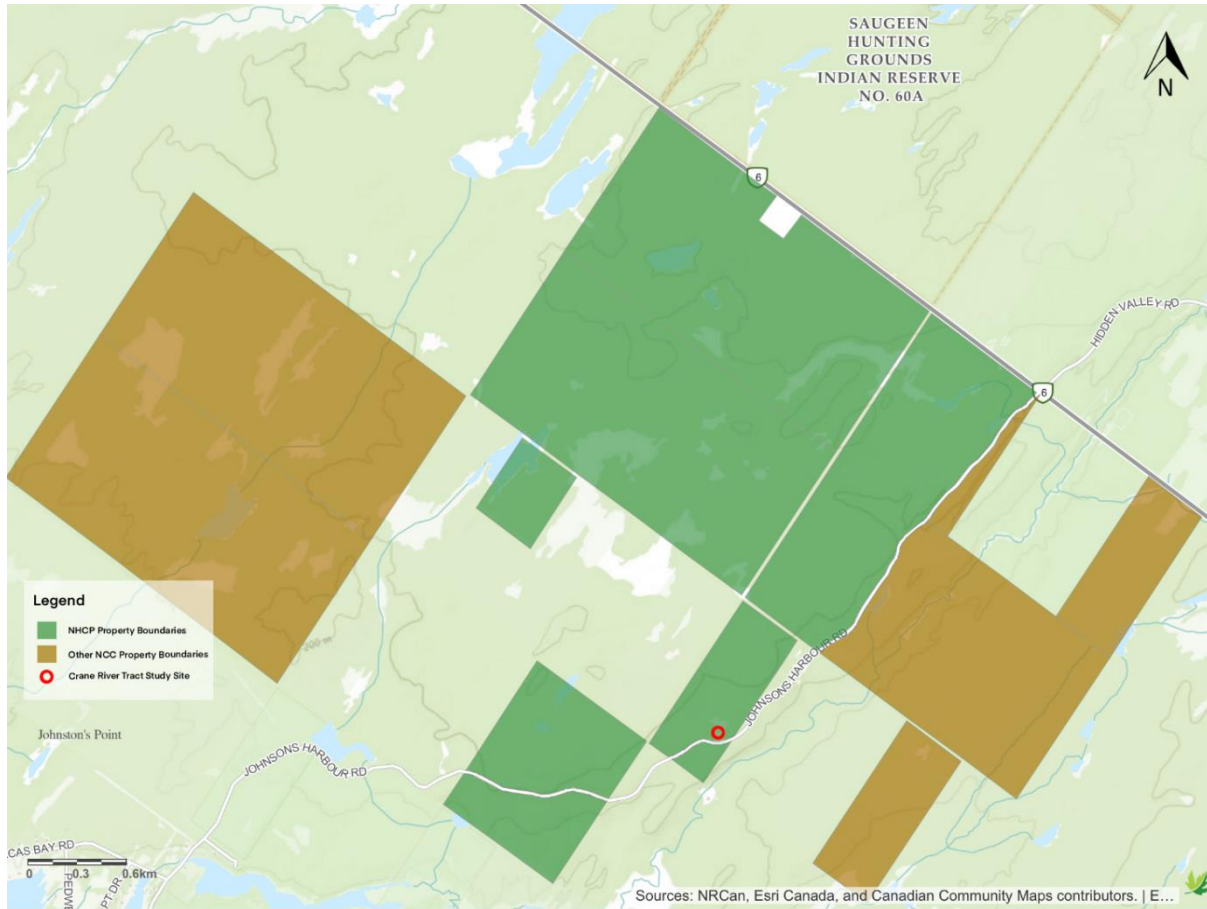
Figure 1: Property boundaries of the Nature Conservancy of Canada including the Crane River Tract (CRT) study site circled in red. *NHCP is the National Heritage Conservation Program and NCC is the Nature Conservancy of Canada.*

In the absence of previous carbon dynamics research within the Crane River Tract (CRT) – owned by Nature Conservancy of Canada – this thesis describes and quantifies the carbon pools of the CRT to evaluate whether the soil carbon budget is in a steady state, positive or negative. If the budget is positive, the soil accumulates more carbon than it loses annually, thereby making it a carbon sink. If the budget is negative, then the soil releases more carbon into the atmosphere and is considered a net carbon source to the atmosphere. Values are compared with a previous study (Bao, 2021) which examined a plot also dominated by Eastern White Cedar, in a shoreline setting on Hay Bay near Tobermory. The carbon dynamics – the transfer of carbon between the pools and the factors affecting the rate of transfer, forms an important focus of the thesis.

The CRT research site is dominated by coniferous forest but grades into alvar habitats containing distinctive zones of coniferous and deciduous vegetation. This provided a convenient opportunity to compare soil forming properties in contrasting habitats under otherwise common climatic conditions.

2

From background research, there is scant mention of coniferous alvars and certainly no data on carbon fluxes or carbon pools of coniferous alvars in the Bruce Peninsula. There is data available on Scandinavian alvars, as this landscape is more common in those regions. This provides a basis for comparisons between the Bruce and Scandinavian alvars.

1.1.2 – Aims, Objectives and Questions

The primary objective is to determine the rate of annual change in the soil carbon budget by measuring or modelling the inputs and outputs of carbon. These gains and losses are related to the magnitude of the various aboveground and belowground carbon pools so their potential to exchange carbon is examined. Because some of the pool sizes and exchange rates change seasonally, their temporal behaviour is described. Because the sampling design extends along a transect, spatial changes in the carbon dynamics can be examined with respect to distance from the forest edge. And because the transect extends beyond the forest edge into an alvar, the bulk characteristic of the carbon pools in two distinct habitats can be compared. Secondarily, the bulk characteristics of the CRT Forest carbon pool are compared to the bulk characteristics of a second forest stand in the Northern Bruce Peninsula at Hay Bay. In addition, a second distinctive alvar habitat dominated by a coniferous prostrate shrub, Creeping Juniper (*Juniperus horizontalis*), is compared to the dominant alvar habitat. Carbon pool sizes and exchange rates are compared to previously published values, when available, but many of those studies are at much larger regional or biome scales.

Carbon pools are defined as large accumulations of organic carbon such as aboveground biomass, belowground biomass, litter, soil carbon and deadwood pools while carbon dynamics are the processes which move carbon between the pools and the environmental factors responsible for the rate of movement.

The overall objective of this research is to account for the estimated rate of change in the soil carbon pool $\Delta C/\Delta t$ (kg[C]/m^2/y). The soil carbon budget is given by:

$$\frac{\Delta C}{\Delta t} = I - O = I_{LF} + I_{RG} + I_{DW} - R_h \pm H_c \pm W_c \tag{1}$$

The inputs (*I*), of organic carbon to the soil pool originate from the living vegetation and hence are dependent on the character (species composition) and size of those pools and their rates of transfer. These include leaf-fall inputs to the soil surface, I_{LF}, the *in-situ* growth of roots, $I_{RG,}$ and the

3

decomposition rate of deadwood comprising fallen branches and trees, I_{DW}. The outputs (O), of organic carbon are primarily dependent on soil decomposition rates which result in the respiratory release of CO_2 to the atmosphere by heterotrophs, R_h. These microorganisms release CO_2 to the atmosphere during the decomposition of litter (duff) to humus near the surface but continue to decompose buried organic soil particles, albeit at a reduced rate, passing CO_2 upwards through the soil profile. These losses are primarily dependent on the character of the soil carbon (labile or recalcitrant) and environmental factors like temperature and moisture. Therefore, important objectives include describing the role these inputs and outputs play in the soil carbon budget. These objectives are met by measuring spatial and/or temporal variations in the components over two field seasons. The exception is the estimate for root inputs, I_{RG} which was obtained by scaling annual root growth to model estimates. Under specific conditions, the soil pool may also gain or lose carbon hydrologically, H_C or may gain or lose carbon because of wind redistribution, W_C. While these mechanisms might be important locally, the resources available for this study did not allow for their direct measurement, although their potential impact is noted.

1.2 – Literature Review
1.2.1 – Carbon Dynamics and Carbon Pools

A carbon pool is defined as a reservoir of organic matter that can accumulate or release carbon. The IPCC subcategorizes terrestrial carbon into five distinct pools: aboveground pool, belowground pool, woody debris pool, litter pool and soil pool (Vashum, 2012). Carbon dynamics refers to how the carbon moves between pools and what factors influence the rate of movement. Photosynthesis is the process in which carbon dioxide is removed from the atmosphere and stored in living biomass in trees and other plants. The carbon can be stored in the branches, bark, roots, foliage, deadwood, and dead organic matter (DOM) in the soil and litter (Kurz et al., 2013). Heterotrophic and autotrophic respiration, forest fires, and decomposition, return the carbon stored in various forest carbon pools, back into the atmosphere. Site productivity characteristics such as stand age, species composition and climate, will determine the amount of photosynthesis (carbon intake) that occurs. The equation for net primary product (NPP) is gross primary production (GPP) subtracted by autotrophic respiration (R_a) (Kurz et al., 2013). The equation for net ecosystem production (NEP) is NPP - R_h (heterotrophic respiration). Over time, the NEP determines if the forest stand is a carbon sink (positive NEP) or a carbon source (negative NEP) (Kurz et al., 2013).

In a review of Northern Hemisphere forest carbon pools, Goodale et al. (2002) indicate that of the Hemispheric total of 390 Pg[C], Canadian forests make up 85 Pg[C] comprising living vegetation (17%), deadwood (4.8%), litter (11.2%), soil (66.5%) and forest products (0.4%). They note while soil dominates the total forest carbon pool in all countries, its estimates likely contain the greatest uncertainties.

Disturbances such as changing length of seasons, forest fires, extreme weather conditions and human-caused disturbances will transfer carbon from the living pools (living above/belowground ground biomass) to the dead pools (litter, soil, deadwood). From 1990 – 2008, the carbon budget of Canadian managed boreal forests varied with an average gain of living biomass pool from the atmosphere at 7±25 Tg[C]/y, and an average gain of the dead biomass pool (deadwood, SOM, litter) of 4±10 Tg[C]/y (Kurz et al., 2013). This places the proportion of the living gains transferred to the soil environment at approximately 57%.

Kurz and Apps (1999) provide a 70-year review of carbon fluxes and pools using the carbon budget model of the Canadian forest sector (CBM-FS2) for eleven Ecoclimatic Provinces. The Cool Temperate province occupies 6.4% of Canada's total forest area of 404 Mha and extends from the Bruce Peninsula eastwards across Southern Ontario and Southern Quebec and includes most of the Maritime Provinces in Canada. Three sets of data from the National Forest Biomass Inventory (NFBI) are used in the model. Scaling factors used in the model projections for the Cool Temperate Province include softwood (coniferous) biomass pool subdivided into [MgC/ha]: AGB 18.6, BGB and 4.3, DOM 165.4 (4.4 Very fast, 20.1 Fast, 23.3 Medium, 117.6 Slow). Annual contributions to the soil DOM pool are estimated as 15% of foliage, 0.67% of stems, 4% of branches and 2% of coarse roots.

The main driver behind carbon dynamics is heterotrophic respiration and differences in microbial communities and the amount of carbon and nitrogen in the soil, will affect the soil carbon turnover rate (Liu et al., 2019). Microbial activity is typically limited by carbon availability; this principal holds true for coniferous soils with high CN ratios (Demoling et al., 2008).

Comparing young (>15 years) and old (divided into 50 year stands and 250-year stands) *Pinus ponderosa* forests, the old forest stored more than twice the amount of carbon than the young forest with 15% of the carbon stored in living biomass for young forest and 61% in old forests (Law et al., 2001). Heterotrophic respiration in old and young *Pinus ponderosa* forests vary with an annual flux of 444 and 389 g[C]/m^2/year respectively (Law et al., 2001). Autotrophic respiration was 571 and 445

g[C]/m^2/year in old and young forests respectively (Law et al., 2001). Coarse woody detritus decomposition flux was 33 and 56 g[C]/m^2/year in old and young forests respectively while fine woody detritus decomposition flux was 3 and 12 g[C]/m^2/year in old and young forests respectively (Law et al., 2001).

1.2.2 – Soil Carbon

Soil carbon is the second largest carbon pool on Earth with approximately 2,344 gigatons of stored organic carbon (Zhang et al., 2020). The amount is greater than the combined carbon pools of both atmosphere and plant biomass. The inputs to the soil carbon pool include the bark, roots, branches, leaves, plant residues and whole trees. The lability between these input sources varies with leaf-fall being highly labile while branches and trunks are less labile due to low and high ratios of CN respectively. Heterotrophic microorganisms produce intracellular and extracellular enzymes that mineralize the soil by converting organic soil carbon to inorganic soil carbon – in the process, consuming the organic nutrients from the soil and producing carbon dioxide as a waste product (Zhang et al., 2020). Fertilization of soils via nitrogen increased hydrolytic enzymes – those that decompose fats, proteins, carbohydrates and nucleic acid, and enzymes that degrade cellulose (Zhang et al., 2020).

Approximately 16–26% of the global soil carbon pool is from forest soils (Su et al., 2021). Carbon that is derived from a high-quality litter input that contain low CN ratios and high decomposition rates, become strongly stabilized soil microaggregates and contribute to heavier SOC fractions greater than 1.8 g/cm^3 (Su et al., 2021). In contrast, poorer quality litter is retained in lighter SOC fractions (less than 1.8 g/cm^3) and contributes to the formation of macroaggregates (Su et al., 2021). The accumulation of SOC includes litter quality and quantity, root exudates and competition of carbon and nitrogen between microorganisms and plants (Zhou et al., 2019). Litter is the primary input of carbon into the SOC. Coniferous forests typically have smaller values of annual leaf-fall, a larger CN ratio for forest litter and coniferous forest soils have smaller concentrations of trace elements aluminum and iron, when compared to broadleaf deciduous forests (Zhou et al., 2019). Annual litterfall differs between deciduous and coniferous forest stands on a yearly basis, with the collection years of 2014–2015 yielding 851±207 kg[C]/ha (deciduous) and 520±102 kg[C]/ha (coniferous), and 2015–2016 yielding 596±143 kg[C]/ha (deciduous) and 430±62 kg[C]/ha (coniferous) (Boča & Van Miegroet, 2017). The average amount of carbon input via litterfall was 250 kg[C]/ha greater under the deciduous species compared to the coniferous species (Boča & Van Miegroet, 2017). The speed of litterfall decomposition for deciduous

aspen ranged from 2–3 years while coniferous litter decomposition averaged at 46 years for the SOC pool (Boča & Van Miegroet, 2017).

There are three subdivisions of SOC, the labile SOC pool, recalcitrant SOC pool and the slow organic carbon pool (Wang et al., 2022). The slow and recalcitrant pools have slow carbon turnover rates ranging from a decade to hundreds and thousands of years. The labile pool has the shortest turnover rate ranging from days to months, is very sensitive to small changes in the environment such as temperature and moisture and is the most active soil pool out of the three (Wang et al., 2022). The labile pool is one of the first indicators of changes in overall SOC based on the following, crucial indicators: dissolved organic carbon (DOC), microbial biomass carbon (MBC), easily oxidizable carbon (EOC), and light-fraction organic carbon (LFOC) (Wang et al., 2022). DOC is typically carried by water, absorbed by plants and microorganisms. It aids in processes of microorganisms converting organic carbon to inorganic carbon. LFOC contains easily mineralizable organic matter not protected by soil colloids, from physical or chemical processes such as UV radiation and microbial enzymes, respectively. EOC contains easily oxidizable components in the soil such as humic acid that react heavily with an unstable environment. MBC contains microbes such as fungi and bacteria that are the main contributors to nutrients flowing to and from the soil carbon pool (Wang et al., 2022).

The main influence on the labile SOC pool are the environmental changes including temperature, precipitation, pH, and microbial decomposition. Environmental factors such as a decrease in pH towards more acidic soils, cause an increase amount of biotoxic cations such as Al^{3+} and Mn^{2+} (Wang et al., 2022). Soil microbes will be affected by temperatures with higher temperatures leading to increased rates of decomposition and carbon dioxide emission. In a Southern Ontario Forest plantation dominated by White Cedar, the soil organic carbon was 83.23 t[C]/ha (Wotherspoon et al., 2014). Hybrid Poplar (*Populus deltoides × Populus nigra*), Red Oak (*Quercus rubra*), Black Walnut (*Juglans nigra*) and Norway Spruce (*Picae abies*) have SOC of 86.86, 83.77, 76.84, and 78.33 t[C]/ha, respectively (Wotherspoon et al., 2014).

In predominantly aspen (*Populus tremuloides*), deciduous forests, the SOC was larger than coniferous forest with values of 93.7±16.11 and 82.9±27.9 Mg[C]/ha respectively (Boča & Van Miegroet, 2017). Deciduous aspen forest soils produce lower levels of CO_2 emissions compared to coniferous soils with 146.2 mg/g soil C (8.5% total SOC) and 231.4 mg/g soil C (18% total SOC), respectively (Boča & Van Miegroet, 2017). The data indicates a lower rate of decomposition of deciduous aspen forest soil pool. With an average forest stand age of 100 years for both deciduous and coniferous forests, there is an

annual net average accumulation of SOC by 225 kg[C]ha/year for the two types of forests (Boča & Van Miegroet, 2017).

A study in Spain showed the SOC being higher in deciduous broadleaf forest soils (59±1 Mg[C]/ha) while coniferous SOC stocks were 56±1 Mg[C]/ha within the top 30 cm of soil (Chiti et al., 2012). Chiti (2012) compared their SOC stocks with other forests of the same classification in other European countries. In Turkey, coniferous forests had SOC of 172±26 Mg[C]/ha from 0–30 cm soil depth while coniferous SOC in Greece contained 72±39 Mg[C]/ha (Chiti et al., 2012). Predominantly Histosol soil in forest environment in France showed an average SOC of 267 Mg[C]/ha for a depth of 0–30 cm (Arrouays et al., 2006). Luvisol SOC at the same depth and environment averaged 65 Mg[C]/ha (Arrouays et al., 2006).

A study in Beijing China showed the SOC at five different coniferous forest averages as 226.6, 150.4, 409, 356.2 and 198.3 Mg[C]/ha from 0–40 cm (Geng et al., 2009). The same study showed broad leaved forest SOC as 259.7, 280, 441.9, 509.5, and 303.7 Mg[C]/ha at five different forest averages from 0–40 cm (Geng et al., 2009). A study of Eastern Red Cedars (*Juniperus virginiana*) showed average SOC accumulation rates of 0.30 Mg[C]/ha/year in forest stands aged between 22–59 years (Sauer et al., 2023).

Kriiska (2019) found soil carbon flux was 73% and 76% accountable by changes in temperature in Pine and Spruce forests respectively. The amount of precipitation and VMC was not significantly impactful on the R_h or R_a respiration rate of the soil. Maximum soil respiration occurred in August in line with the highest temperatures during the year and the average annual soil respiration was 5.73±0.25 Mg[C]/ha/y and 6.54±0.30 Mg[C]/ha/y in Scots Pine (*Pinus sylvestris*) and Norway Spruce forest stands respectively (Kriiska et al., 2019). Heterotrophic soil respiration made up of 82% (Norway Spruce) and 78% (Scots Pine) of total soil respiration (Kriiska et al., 2019).

The effect of temperature on soil respiration cannot be understated. In a temperate coniferous forest comprised of Alfisol soil, with an average SOC of 166±10 Mg[C]/ha from a depth of 0–100 cm, an increase in temperature of 4°C caused a spike of soil respiration by 34–37% annually (Hicks Pries et al., 2017). In the experiment by Hicks Pries (2017) showed the soil carbon stock in the first five and fifteen centimeters of soil as 6052±478 and 3048±399 g[C]/m^2 respectively. With annual temperature increase of 4°C globally, soils (excluding Histols, Cryosols and Aridisols) could lose 3.1 Pg[C]year, globally (Hicks Pries et al., 2017) because of respiration.

1.2.3 – Aboveground & Belowground Biomass and Litter Pools

Aboveground biomass refers to any plant biomass aboveground such as branches, foliage, bark, wood, shrubs in both coniferous and deciduous forest stands (Dymond et al., 2016). Belowground biomass refers to living biomass underground such as structural and fine roots and rhizome systems. As forest density increases, the biomass and carbon stocks increase as well. A study on temperate forests of Pakistan showed the average aboveground and belowground biomass in a predominantly coniferous forest comprised of *Pinus roxberghii* (Chir pine), *Pinus wallichiana* (Himalayan White Pine), *Abies pindrow* (West Himalayan Fir), and *Picea smithiana* (West Himalayan Spruce) (Khan et al., 2020). The average aboveground biomass in the study was 149±40.77 t/ha and ranged from 280 t/ha to 46 t/ha (Khan et al., 2020). The amount of carbon in aboveground biomass ranged from 131 t/ha to 22 t/ha and had an average of 70±19.16 t/ha. The ratio of belowground to aboveground biomass was 47%. Total aboveground and belowground biomass was 6.7 Mt and 1.74 Mt, respectively while the total aboveground and belowground carbon was 3.15 Mt and 0.82 Mt (Khan et al., 2020). The total amount of carbon dioxide emitted from the whole forest stand using remote sensing techniques from 2000–2015 (15 years) was 14.53 Mt (Khan et al., 2020).

The IPCC (2006) report states the aboveground biomass of temperate forests in North America as 60 tonnes of dry matter per hectare in forests younger than 20 years and 130 tonnes of dry matter per hectare in forests older than 20 years. Temperate coniferous forests in Europe and Asia contain 150–200 and 25–30 tonnes of dry matter per hectare in stands older than 20 years and younger than 20 years, respectively (IPCC, 2006). The percentage of carbon in a 25-year-old, White Cedar agricultural land in southern Ontario, in aboveground biomass was 52±0.4 % while belowground comprised 47±1 % (Wotherspoon et al., 2014). The mean carbon content per tree in White Cedar is 146±24 kg[C] and 239±62 kg[C] in Poplar (Wotherspoon et al., 2014). Peichl et al., (2006) assumed the proportion of carbon in falling leaves varies between deciduous (assumed 43% carbon concentration) or coniferous (assumed 50% carbon concentration) leaves.

Figure 4 shows the patterns of above-ground biomass in the Bruce Peninsula generated using reflectance characteristics of the plant canopy (Puric-Mladenovic and Clark, 2010; Puric-Mladenoivc et al., 2016). This forms a basis for comparison with the ground-based estimates of tree biomass at specific locations. These estimates also provide an impression of the spatial variability in AGB within the Peninsula and may serve as a means of extrapolating those carbon dynamics processes which are dependent on above-ground biomass.

Litterfall contains the shed remains of once living plant biomass and is the largest contributor to the soil carbon budget (Wotherspoon et al., 2014). It includes leaves, twigs, roots, branches, bark, wood, fruiting bodies and seeds. In mature Eastern Red Pine stands, the average annual litterfall was 5000 kg/ha/year (Sauer et al., 2023).

Litterfall C inputs from Hybrid Popular, Red Oak, Black Walnut, Norway Spruce and White Cedar are 1.63, 1.07, 1.50, 1.49, 0.68 t[C]/ha/year, respectively with White Cedar having the lowest litterfall input (Wotherspoon et al., 2014). Litterfall C outputs from the same study (2014) showed R_h carbon outputs as 1.04, 0.54, 1.44, 0.63, and 0.26 t[C]/ha/year for Hybrid Popular, Red Oak, Black Walnut, Norway Spruce and White Cedar, respectively. The aboveground and belowground assimilation of carbon for White Cedar was 0.53 and 0.12 t[C]/ha/year, or 82% and 18% of total annual assimilation, respectively (Wotherspoon et al., 2014).

Calamagrostis grass alvars (deciduous) have an annual litter fall that ranges between 2080±30 and 1470±170 kg/ha/year (Kriiska et al., 2019). Annual leaf-fall was higher in Norway Spruce than Scots Pine forest with averages of 4620±380 kg/ha/year and 4030±410 kg/ha/year respectively (Kriiska et al., 2019). The amount of carbon stored in a *Pinus ponderosa* forest stand foliage was 2700 and 600 kg[C]/ha for old (50–250 years) and young (<15 years) forests, respectively (Law et al., 2001). The total carbon stored in aboveground biomass including wood, bark, branches, stems in the young *Pinus ponderosa* forest was 5190 kg[C]/ha while the old forest stored 105210 kg[C]/ha of carbon (Law et al., 2001). The litter layer of ~1 cm contained 12330 and 7080 kg[C]/ha of carbon in old and young forests respectively (Law et al., 2001).

Coniferous alvars of the Bruce Peninsula have shallow soils, less than 10 cm deep, atop bedrock composed of dolostone (Reschke et al., 1999). Through frost heaving, the dolostone bedrock surface is broken up into many small, cracks and crevasse ranging from 1 cm to 1 m long. Patches of Creeping Juniper range from 2 to 220 ha and typically grow in a mosaic pattern with other shrubs. Other types of alvar include juniper alvar shrubland, tufted hairgrass wet alvar grassland and little bluestem alvar grassland (Reschke et al., 1999).

1.2.4 – CN ratios

The losses of forest C after a fire range from approximately 62–80% in deciduous forests and 29–57% coniferous forest, from pre-fire forests (Kauffman et al., 2009). A 2001 California study showed various soil and litter CN ratios as well as carbon and nitrogen concentrations in the soil (g/kg). The CN litter ratio in forests comprised predominantly of coniferous White Fir and Ponderosa Pine ranged from

32.2 to 44.4 (Quideau et al., 2001). The CN ratio in coniferous, low density soil fractions (A horizon) ranged from 24.8 – 34.1 while whole mineral soil (B horizon) ranged from 10.9 – 19.5 (Quideau et al., 2001). The nutrient patterns of decomposition varied between coniferous and deciduous forests with coniferous vegetation showing highly recalcitrant carbon while intensive oxidation in the litter occurred in the deciduous oak soil organic matter. The former shows slow release and decomposition of litter due to low bioavailability while the latter shows increased microbial and decomposition activity with rapid nutrient release (Quideau et al., 2001).

Nitrogen derived from branches, stems and foliage, is greater in deciduous Aspen forests than coniferous forests. Nitrogen concentrations (percent dry mass) for litter were 0.021 in Aspen forests compared to 0.005 and 0.007 in Jack Pine and Black Spruce forests respectively (Gower et al., 2000). Percent dry mass nitrogen concentrations for foliage were 2.50±0.35 (Aspen), 1.48±0.034 (Jack Pine), and 0.72±0.08 (Black Spruce) (Gower et al., 2000). The average amount of time nitrogen spends in the forest canopy as a leaf range from 1.3 – 1.6 years (Aspen), 5.9 – 9.8 years (Jack Pines) and 14.1 – 16.8 years (Black Spruce). Foliage litterfall differed for all three species with 2170±167, 860±85 and 785±121 kg/ha/year for Aspen, Jack Pine and Black Spruce, respectively (Gower et al., 2000).

CN ratios vary between the top five and fifteen centimeters of soil with ratios of 28.1±2.7 and 24.8±1.5 respectively (Hicks Pries et al., 2017). The percentage of carbon (%C) in the first five centimeters of soil was 8.3±0.8 (%C) compared to the percentage in the first fifteen centimeters of soil 3.0±0.3 (%C) (Hicks Pries et al., 2017). In the Cascade Mountain range with the dominant species of Ponderosa Pine (*Pinus ponderosa*), the total amount of carbon and nitrogen in the soil (0–20 cm) of young forests (<15 years) was 2.62 and 0.171 kg/m^2 respectively (Law et al., 2001). In old forests of 50 and 250 years, the soil (0–20 cm) carbon and nitrogen were 2.79 and 0.104 kg/m^2 respectively (Law et al., 2001).

A study by Baird (1999) showed how CN ratios in coniferous forests changed from 3 months and 1 year after a fire event. The organic layer was completely burned away in the ground fire while the 3-month A and B horizons had a CN ratio of 19 and 14, respectively. The 1-year A and B horizons had a CN ratio of 21 and 15 respectively and an organic horizon CN ratio of 42 (Baird et al., 1999). Nitrogen saturated sites show the highest amount of respiration (Tietema, 1998).

1.2.5 – Deadwood

The deadwood pool contains all dead material that is not found in either litter pools or buried in the soil carbon pools. This includes coarse roots, coarse dead woody debris (branches, fallen trees), and

snags (dead trees not fallen to the ground). The R_h from this pool is particularly difficult to quantify due to practical limitations associated with attempting to estimate the rate of decomposition – which vary based on forest type, geographical location and tree species/density – and carbon transference from the deadwood to soil pools or atmosphere. The quantity of deadwood present depends on the amount of time since the last disturbance and type of disturbance, as well as natural decay and mortality rates (IPCC, 2006). The IPCC (2006) does not have default values for carbon stocks in deadwood for any climate ranging from boreal to tropical to temperate to subtropical. Kurz and Apps (1999) provide values of 0.67% of stems, 4% of branches and 2% of coarse roots that annually contribute to the dead organic matter (DOM) pool in forests. A proportion of this would be buried while some would be in contact with or suspended above the soil surface. Deadwood classification involves a five-class system with class one as a freshly fallen tree while class five contains small, broken pieces of wood splinters. This classification system was developed by Maser (1979) and is still used to characterise the stage of decay to the present.
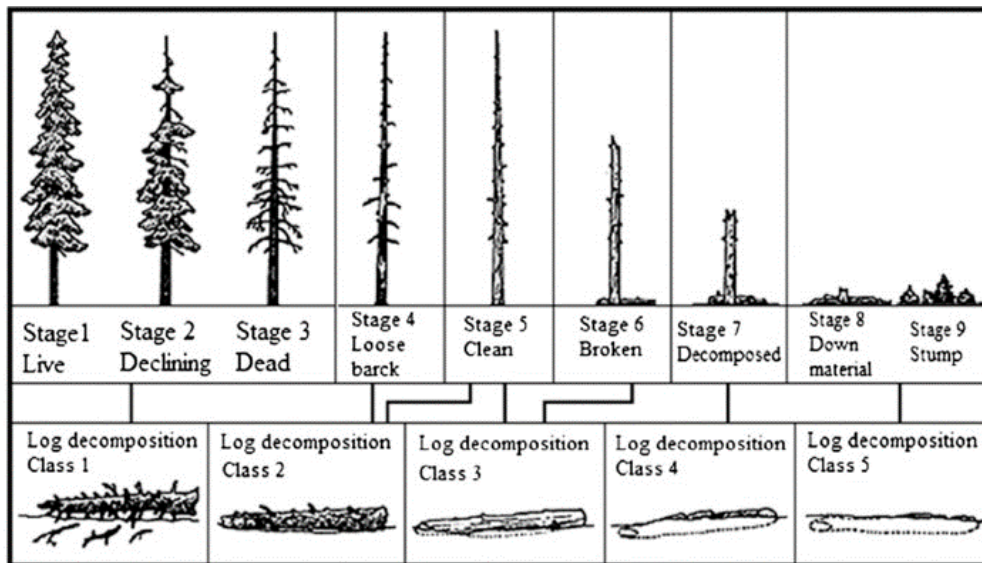
Figure 2: Visual representation of deadwood decay classification one through five. Class one is the least decayed. Class five is the most decayed.

1.2.6 – Significance and Justification

There is a dearth of available information regarding the carbon within the soils of the Bruce Peninsula (WoSIS Soil Profile Database, November 2023). Much of the Bruce Peninsula is distinctive in the respect that the soils of the entire region are very shallow and yet contain the largest continuous forest in southern Ontario. Being a narrow Peninsula separating Georgian Bay from Lake Huron, its climate is strongly modified by those water bodies. Tobermory was a dominant refuelling port on the

Great Lakes for steamships up until the early 1900's during which time it was heavily logged. Subsequently in 1908, a major wildfire burned the entirety of the northern Bruce Peninsula except for the northern tip. Other than a few enclaves of surviving trees on cliff faces and adjacent to swamps, all the present-day vegetation and possibly most of the soil is younger than 115 years old. It is remarkable that today's forests support a biodiversity they do. This study aims to add a small piece to the puzzle regarding its soils and may supplement information needed for environmental conservation efforts.

1.3 – The History and Introduction to the Bruce Peninsula
1.3.1 – Geographical Features of the Bruce Peninsula

Alvars are defined as areas of relatively flat, dolomitic bedrock containing small pockets of soil (0–20 cm deep) and less than 60% tree canopy cover (Liipere, 2014). The shallow soil allows for fast water evaporation with little drainage to bedrock. According to the Southern Ontario Ecological Land Classification system, there are three categories of alvar: Open Alvar, Shrub Alvar and Treed Alvar. Open and Shrub Alvars contain less than 25% tree and shrub cover while Treed Alvars contain more than 25% tree cover (Liipere, 2014). Over 60–75% of alvars in North America are located in Ontario, specifically, the Great Lakes St. Lawrence region and the highest quality alvars are located in the Bruce Peninsula and Manitoulin Island. The landscape is defined as an extreme landscape with droughts, annual flooding and surface temperatures reaching up to 53°C. Despite the extreme environment, there are many species of flora and fauna that are found inhabiting and migrating through the alvars. Over 376 vascular plant species, 58 moss taxa, 52 lichen taxa and over 62 algae species inhabit the alvars of Bruce Peninsula (Liipere, 2014). Endemic species such as the Lakeside Daisy (*Tetraneuris herbacea*) and Dwarf Iris (*Iris lacustris*) inhabit the alvars.

Aside from its distinctive topographic features and landscape, the Bruce Peninsula is classified as a UNESCO Biosphere Reserve and is home to a variety of flora and fauna. Over 872 taxonomic groups of vascular plants have been found in the Bruce Peninsula including rare plant taxa such as 44 taxas of orchids, 10 insectivorous plant taxa and 20 fern taxa (Liipere, 2014). The Lakeside Daisy has 95% of its global population in the Bruce Peninsula while the Dwarf Lake Iris has 50% of its global population in the Peninsula. Over 355 species of lichen and symbiotic fungi have been discovered in the Bruce Peninsula. Aside from being a large host to flora species, the peninsula is home to 56 species of endangered and threatened fauna, including the spotted turtle (*Clemmys guttata*), Northern Long-eared Bat (*Myotis septentrionalis*) and Gray-cheeked Thrush (*Catharus minimus*) (Liipere, 2014). Other non-endangered or threatened species which have been found on the peninsula include over 39 species of mammals, 29

taxa of reptiles and amphibians, 60 species of fish and over 3300 insect species. The common Black Bear (*Ursus americanus*) and Massasauga Rattlesnake (*Sistrurus catenatus*) are two species with a high population in the Bruce Peninsula owing to the unbroken forests. The black bears are genetically distinct from other populations in Ontario owing to this phenomenon.

1.3.2 – 1908 Fire

Fire plays an important ecological role from promoting nutrient cycling in the soil to ecological succession for pyrophytic plant species. For instance, Jack Pine (*Pinus banksiana*) require fire to germinate as the cones are coated in a waxy resin that melts at 50°C or higher (Alexander & Cruz, 2012). Fire severity has been empirically measured by inventorying the amount of carbon and organic matter lost from both aboveground and belowground. Aboveground biomass lost due to fire centers around how much crown has been scorched, plant mortality and remaining twig diameter around terminal branches. Belowground biomass loss centers around how much litter and soil were burned off as well as the characteristics of ash after the fire has run its course (Keeley, 2009). The intensity and severity of the fire will be impacted by pre-fire characteristics of the forest stand such as soil substrate, topography, climate, forest age and species composition (Keeley, 2009). After a fire, pioneer species such as Aspen, Jack Pine and White Birch, are established alongside various moss, lichen and plants with easily dispersed seeds, become established. The primary successional species are typically fast growing, fast colonizing and require full sunlight. Species such as Eastern White Cedar, White Spruce and Balsam Fir have no adaptations to forest fire and will typically only recolonize a stand if either the seeds are transported into the stand or, from unburned refugia (Canada, 2020).

The August 1908 fire, swept through the Bruce Peninsula. It came from the direction of Lake Huron and crossed over to Georgian Bay (Hepburn, 1981). The townships of Amabel, Albemarle, Eastnor, Lindsay (containing the Crane River Tract), were completely burned while in the northernmost township of St. Edmund where Hay Bay is located, only the southern half was burned (Hepburn, 1981). The 1908 fire cleared much of the species that were once dominated such as Hemlock, Oak and Pine, and secondary succession has allowed cedars to dominate the area at present.

Consequently, there are parts of the study site in the Crane River Tract that were burned and show evidence of fire scarring such as charcoal on fallen logs and stumps. Since the 1908 fire was the last major wildfire in the Bruce Peninsula, it is possible that the fire reset the amount of soil organic matter in the form of litter.

2.0 – Methodology

2.1 – Introduction to the Study Site

2.1.1 – Crane River and Hay Bay

Two sites were studied: The Crane River Tract (CRT) and Hay Bay (HB) sites. Both are in the northern Bruce Peninsula in Ontario Canada. (Figures 3 & 4) The CRT is located at 45°07'59.2"N, 81°29'59.4"W while HB has coordinates of 45°14'36.2"N, 81°41'19.2"W. CRT is the main focus of this study as much of the data from HB had already been collected, catalogued and used previously (Bao, 2021). It is supplemented here with current measurements. The HB study site was located on private property on a single 20 × 20m plot, extending approximately five to twenty-five meters from the shoreline of Hay Bay on Georgian Bay approximately 10 km from the Tobermory townsite (Figure 5). It was classified as a lakeshore environment due to its proximity to the water, with a single dominant tree species of Eastern White Cedar. Although heavily logged up to the early–to mid–1900's, the 1908 fire reportedly did not extend this far northward.
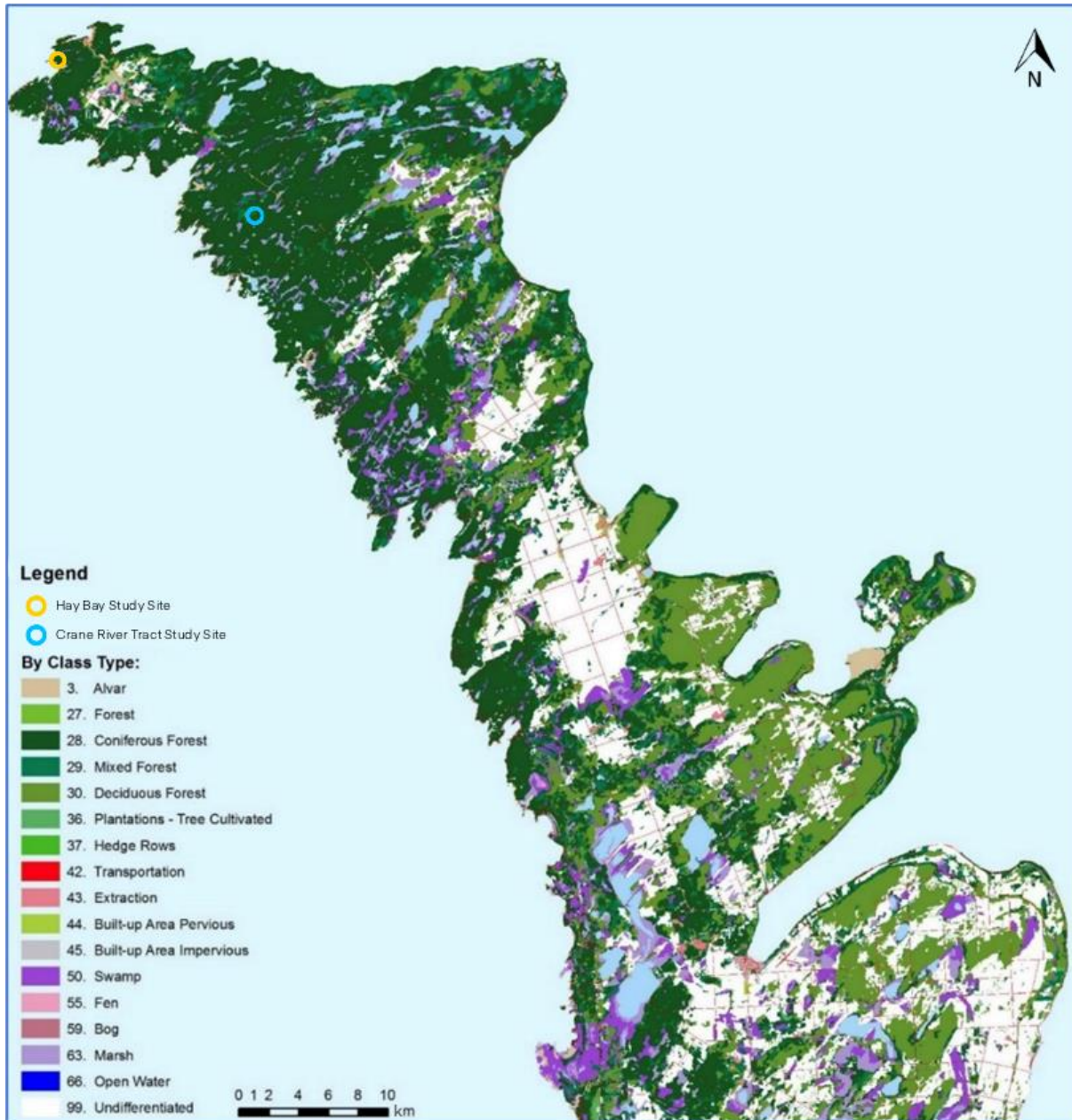
Figure 3: Map of the Bruce Peninsula showing landscape cover types (Obbard et al., 2016). The Hay Bay (HB) and Crane River Tract (CRT) research sites are shown in yellow and blue circles, respectively.
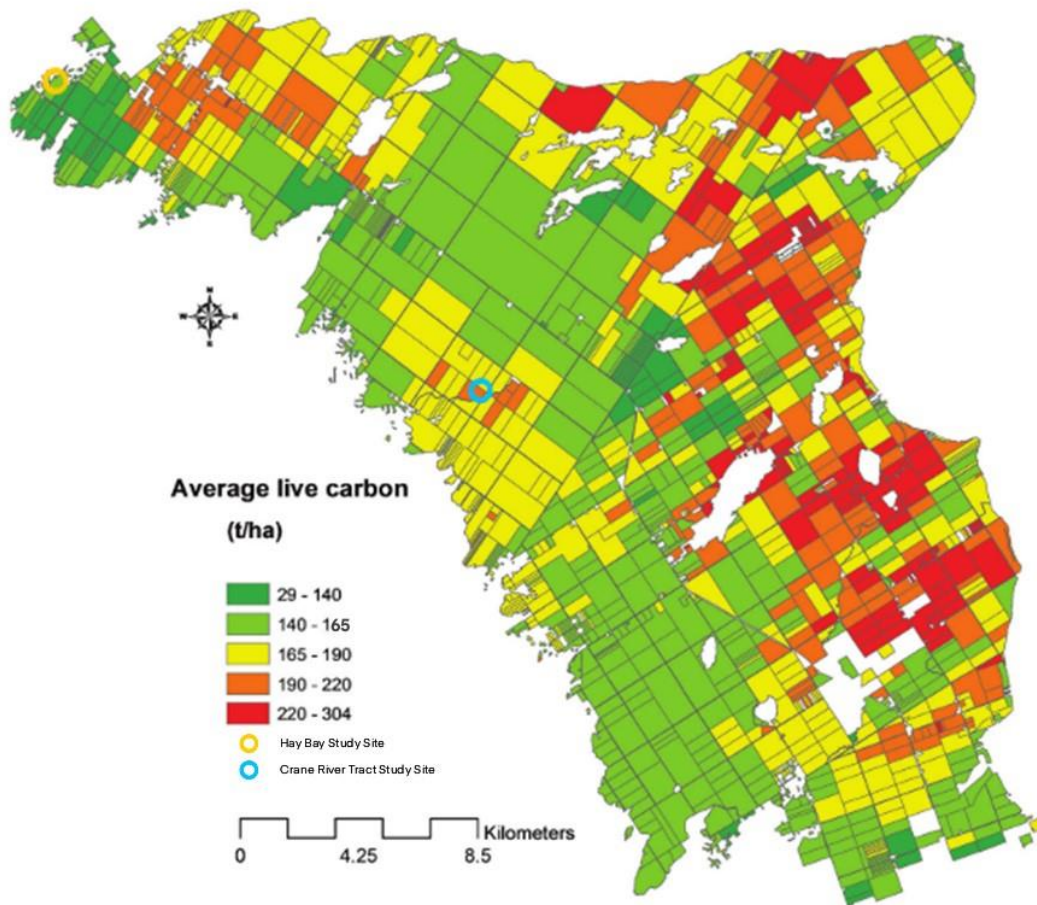
Figure 4: Map of Northern Bruce Peninsula (Eco-district 6e14) showing remote sensing derived estimates of living biomass [t[C]/ha]. (Puric-Mladenovic et al., 2016). Yellow circle represents the Hay Bay site while blue circle represents Crane River Tract site.

Figure 5: Hay Bay study site. HB M2 plot measured 7 × 7 m. Twin white collars represent the living and dead collars for respiration measurements using LICOR LI8100 (red trailer). Black baskets were used to measure litterfall.

The Crane River Tract is owned by the Nature Conservancy of Canada which granted research access (NCC#12345678/2019) in 2019. It comprises 819 hectares of Great Lakes Mixed Forest subtype (Propriété Crane River Tract, 2022) approximately 20 km south of the Tobermory townsite. The forest was comprised predominantly of Eastern White Cedar (*Thuja occidentalis*) but had a sizeable and variable fraction of White Pine, Red Pine and Balsam Fir. Eastern White Cedar is coniferous and grows in both organic and mineral soils with a preference for nutrient rich soils near streams, cooler soil temperatures and moist soils (Johnston, 1979). It can grow in extreme regions such as limestone cliffs in the Bruce Peninsula where one of the oldest Easter White Cedar in Ontario was found to be over 700 years old (Johnston, 1979).

Figure 6: The Crane River Tract study site extracted from the Bruce County Maps mapping system, showing a) the entirety of the gradient from alvar to forest study site, total area, length and width, b) the forested area from plot B – D, subclassified as a transitional zone from alvar to forest, to calculate the aboveground forest biomass pool. Plots A – H contained the main study site while plots Y and Z contained the coniferous alvar (red dotted line). Numerals in brackets show the coordinate system used for sample locations. Image taken April 2015 before the deciduous tree leaves emerged.

The CRT site contains eight contiguous 20×20m plots that stretch along the 160 m transect, highlighted in yellow in Figure 6. The surficial geology comprises dolomitic limestone in the form of glacial furrows and ridges dipping gently to the south-west towards the Crane River. Plot A contains the deciduous alvar site where there are no coniferous species save for a few White Spruce (*Picea glauca*) seedlings. Plot A contained shallow soils in comparison to the other forested plots, was covered with deciduous shrubs, forbs, grasses mosses/lichens and bare rock. Plot B contained a long 'finger' of Eastern White Cedar that were at a higher elevation (~45 cm) than the sides of the ridge which were furrow depressions of the alvar. This marks the first of the transitional zones B, C and D between the alvar plot A and the exclusively forest plots of E, F, G and H. Plots C and D were similar to B with D being more heavily forested than C. Plots E, F, G, and H contained a variety of coniferous tree species including Eastern White Cedar (*Thuja occidentalis*), Red Pine (*Pinus resinosa*), White Pine (*Pinus strobus*), Balsam Fir (*Abies balsamea*), with minor presence of Tamarack (*Larix laricina*), White Spruce (*Picea glauca*), and unidentifiable dead snags. There was the occasional isolated paper birch (*Betula papyrifera*) and Trembling Aspen (*Populus tremuloides*) scattered amongst the conifers.

Alongside the eight transect plots, there were adjacent 20×20m plots used for microtopographic, soil and biomass sampling. A distinctive feature was a patch of alvar dominated by Creeping Juniper (*Juniperus horizontalis*). This was subsequently referred to as the coniferous alvar plot (CA) and straddles two adjacent plots labelled Y and Z in Figure 6 (red dotted line).

2.1.2 – Historical Temperature and Precipitation

Mean Monthly Historical weather data was downloaded from the Environment Canada website. While the climate normal period is currently classified from 1981–2010, there were no close weather stations with continuous data during that period. The closest weather station to the study sites with data over the entire climate normal period was Wiarton A, however, it is over 75 km from the study site which can cause some discrepancies in weather data with the study sites.

The selected weather stations were chosen via proximity to the study site as well as how much continuous data the weather station contained. Tobermory RCS is an inland station while Cove AUT was a weather station on Cove Island. A comparison of the temperature records at these sites showed a thermal lag at Cove Island as Lake Huron and Georgian Bay water bodies both act as heat sinks as with approximately four times the volumetric heat capacity than land. Cove AUT data station has been abandoned since April 2021. Tobermory RCS data station is still active.
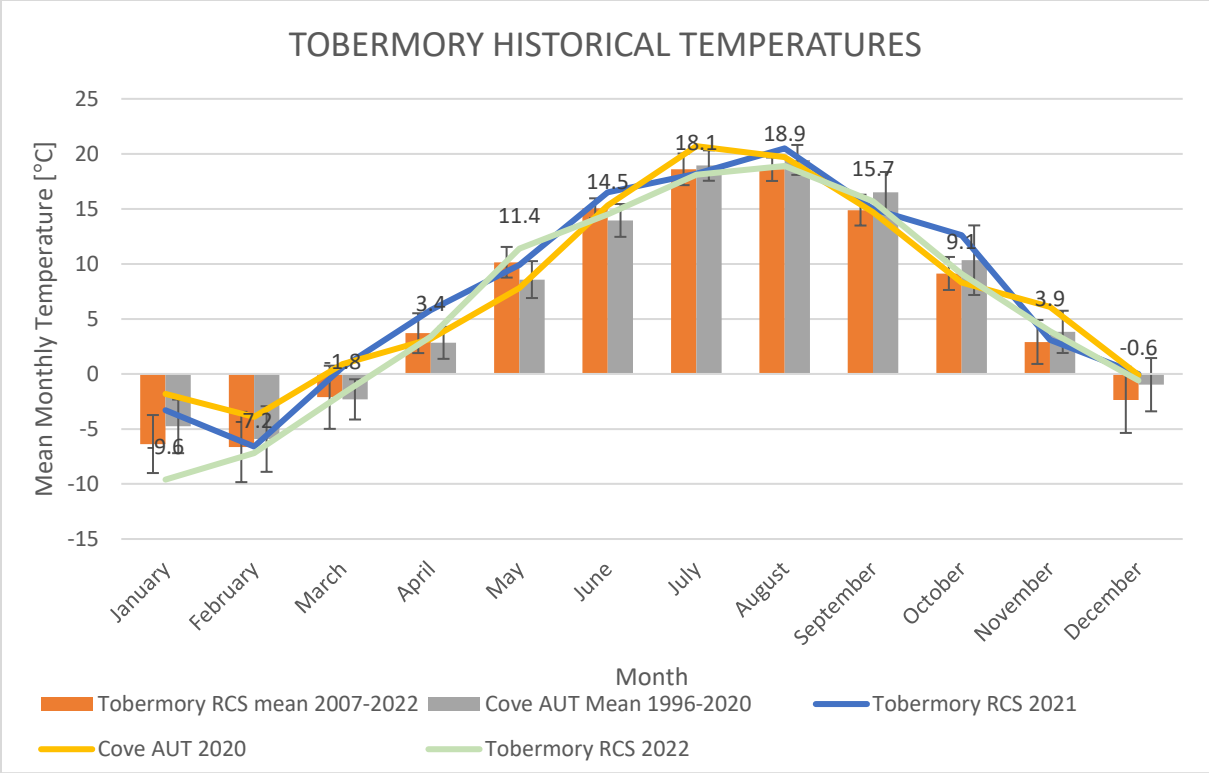
Figure 7: Tobermory mean monthly historical temperatures from two weather stations, Tobermory RCS and Cove AUT, plotted side by side for comparison. Error bars represent ±1 standard deviation (SD). Cove AUT weather station stopped collecting data after 2020.

From historical temperature data extrapolation (Figure 7) it can be stated that monthly mean temperatures in 2022 were consistently cooler than in 2021 but both years were within ±1 standard deviation of normal.
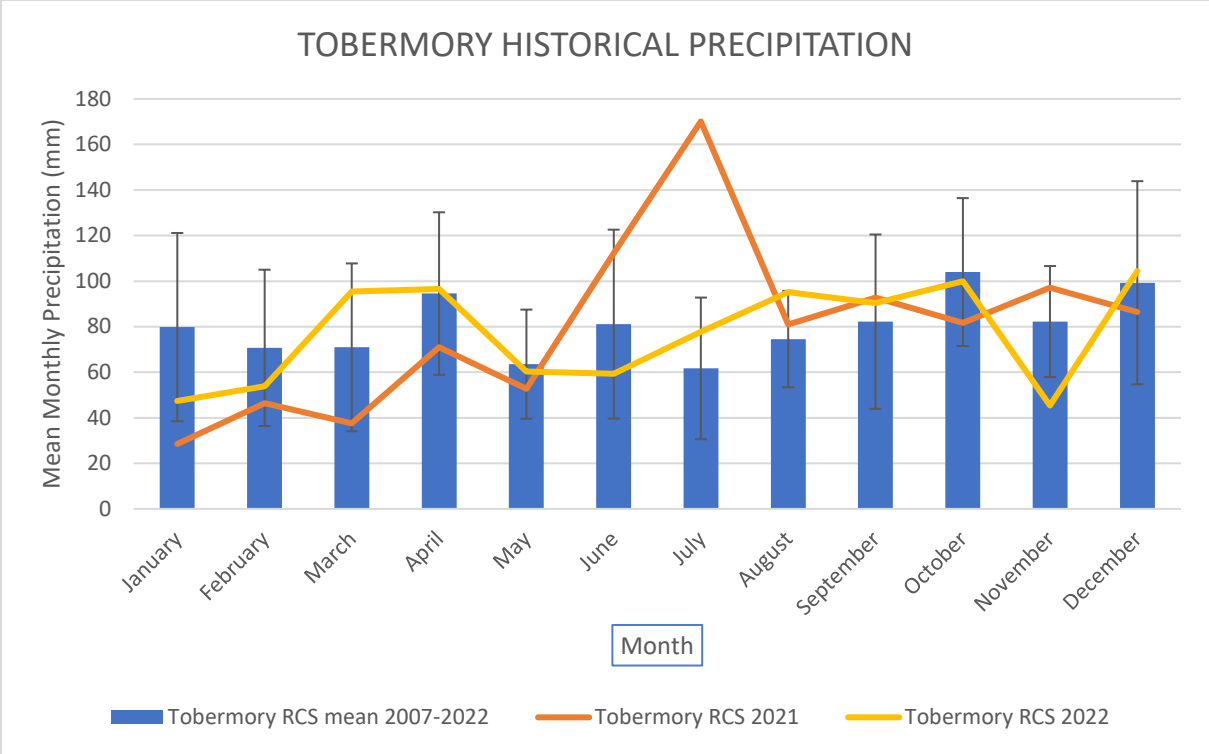
Figure 8: Mean monthly historical precipitation for the weather station Tobermory RCS. Error bars represent ±1 standard deviation (SD) of uncertainty.

Comparing the mean historical precipitation with the measured monthly precipitation for 2021, January had less precipitation in 2021 compared to the historical data. Conversely, July had exceptional high precipitation in 2021. Conversely November of 2022 was unusually dry. The rest of the months for 2022 and 2021 fall within the ±1 standard deviation margin considered normal. Cove AUT precipitation data was not included due to the lack of reliable monthly precipitation means.

2.2 – Field Data Collection
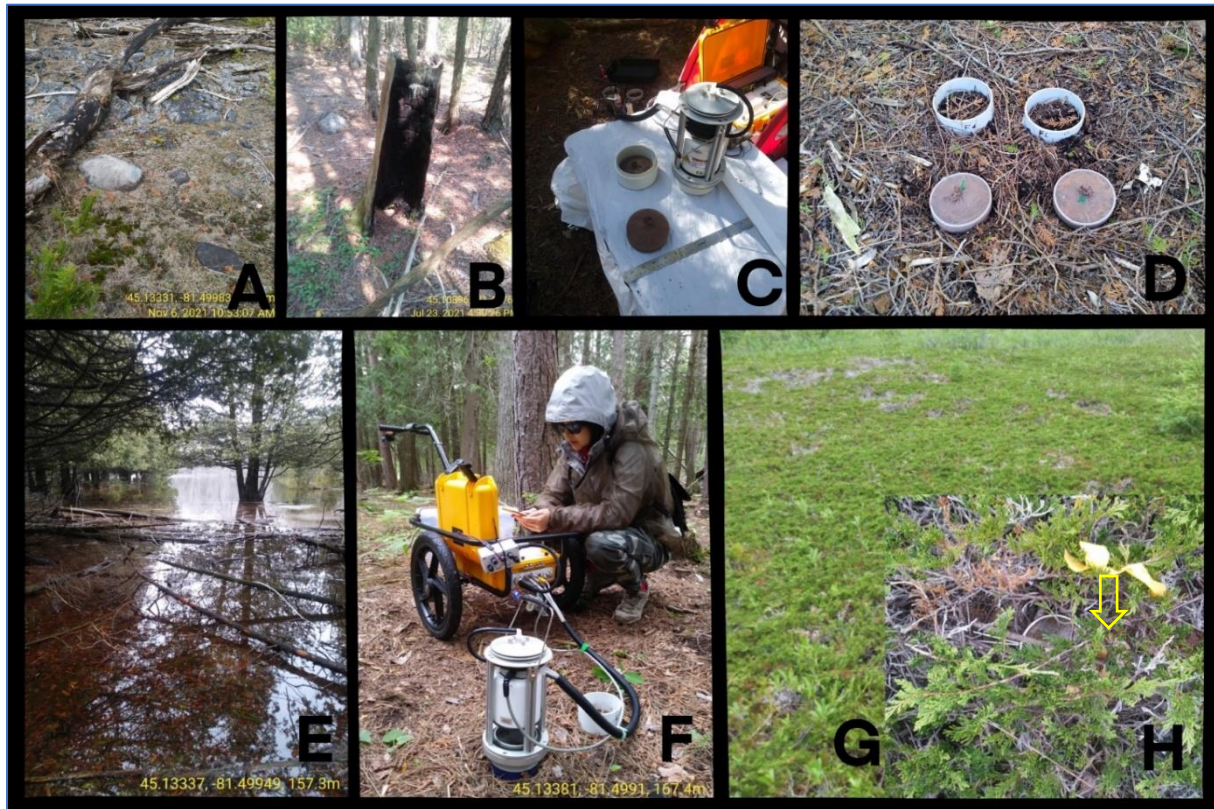
Figure 9a,b,c,d,e,f,g,h: Collage of CRT study site photos featuring A) Charred White Cedar trunks B) Charred White Cedar stump showing evidence of fire, C) Litter puck flux measurements using the LI8100 in the field, D) Litter pucks and soil collars on the forest floor, E) Pronounced spring flooding in 2021 as a result of winter snow melt on the alvar sites that stretch into parts of the forest, F) Kathleen taking soil collar flux measurements using the LI8100, G) Uniformity of the coniferous alvar Creeping Juniper , H) Close-up of the litter collection sieves of the coniferous alvar buried under the branches of Creeping Juniper.

2.2.1 – Microtopography and Elevation

In order to understand the possible role of microtopography and soil depth on carbon dynamics at CRT, survey measurements were taken at 1 m intervals along an x-axis transect extending from alvar to forest. (Figure 6, yellow spine, from (0, 10) to (160, 10)) at 161 locations. This entailed suspending a chalk-line with bubble level, at 10 m intervals between two anchors and measuring the distance to the ground (±1 cm) with a graduated fiberglass measuring rod. At the same locations, a graduated (±1 cm) steel metal probe was inserted into the soil until the distinct ping of metal hitting bedrock was heard. The depth from the top of the soil to the bedrock was recorded. This data was used to generate an elevation profile and soil depth profile along the alvar-forest transect. Microtopography and soil depth data were also collected along ten selective orthogonal transects of the site where surface cover (tenths) estimates were also taken.

2.2.2 – Soil Cores

Soil cores were extracted to determine the amount of carbon in the soil. Soil samples were taken along the x-axis transect at 5 m intervals with a manual corer measuring 24 cm long with a diameter of 2 cm. A square metal wire quadrat (25 cm × 25 cm) was placed at each location to sample litter. Everything within the wire quadrat was gently raked including any living plants and the litter layer to isolate the litter from soil below. The soil corer was then twisted down to the bedrock and the core was extracted. In deeper soils – particularly in the deeper forest – there were two visible layers of soil; A horizon and B horizon. Each soil horizon subsample was measured for length, then bagged separately and labelled.

The soil sub-samples from horizon A, B and C, were weighed (±0.1 g) and dried in convection ovens at 60°C for over 72 hours. At only one location (150, 10) did the soil exhibit a C horizon. Gravimetric Moisture Content (GMC, g[H_2O]/g[dry soil]), and bulk density (ρb, g/cm^3) was calculated for each subsection. Approximately 20 g of the dry sub-samples were used for loss-on-ignition (LOI) tests at 450°C for six hours to determine the mineral (MF) and organic fractions (OF). Prior to Incineration, dried samples were weighed (±0.1 mg) after grinding to a fine powder with a mortar and pestle and pebbles or wood pieces were removed.

$$SOC\ (kg[C]m^{-2}) = \sum_{i=1}^{n} OF_i \rho_{bi} \Delta z_i\ CF \qquad (2)$$

The soil organic carbon, (SOC), [kg[C]/m^2] is given by Equation (2) where the soil depth of each layer is (Δz) and bulk density is (ρb) to obtain SOM, and then multiplied by the carbon fraction (CF = 0.5) of soil organic matter and then summed for all layers.

2.2.3 – Litter collection

Litter biomass samples were collected from the same 5m intervals at which soil cores were subsequently extracted (N = 33). Additional litter samples were also collected along the y-axis orthogonal transects (e.g., (0, 0) to (0, 20)) at 5 m intervals (N = 5) and at locations where gas flux collars were installed on the forest floor (N = 7). Collar locations were constrained to locations where access was possible with the LI8100. Within the forested plots the mean distance from collars to the nearest five trees was 168±39 cm.

Within each quadrat, any living above ground biomass (AGB) was clipped beforehand at ground level and sorted into twigs and leaves. This was done in August 2021 near peak biomass. Then the soil surface was gently raked to lift the litter from the soil surface, which was bagged and labelled separately. Typically, living AGB was only found in the deciduous alvar in Plot A. Most litter on the forest floor comprised fallen tree foliage (needles, leaves and twigs) as there was very little living understory vegetation.

The litter samples were processed in the lab using similar techniques used for soil analysis. The exception being that LOI was not required as all the organic matter is assumed to have an organic fraction of 1.0. The organic matter contents for litter and soil were summed to provide an estimate of total belowground SOM at a given location.

2.2.4 Ground Cover

The forest and alvar differed considerably in terms of living vegetation growing near the ground surface. Although both habitats contained areas of exposed bare rock, subjectively the living understory in the forest was so minimal that the magnitude of the understory carbon pool was not measured and considered negligible. This absence of living understory vegetation was likely the result of the deep shade and rainfall interception offered by the forest canopy and the extensive amounts of needle litter blanketing the ground. Conversely, areas in the alvar that did not comprise bare rock, were densely covered with plants of varying growth forms which would be benefitting from full sunlight and rainfall.

To characterize the contrasting ground cover, surveys were conducted along orthogonal transects at one metre intervals within 25 × 25 cm quadrats within Plots A, B and C. Ground cover (in tenths) was classified into bare rock/soil, moss/lichen, deadwood, leaf litter, grasses, forbs and shrubs for both forest and alvar habitats. Cover estimates represented the consensus of at least two observers. Soil depth (±1 cm) and microtopography (±1 cm) were also recorded at these locations.

2.3 – Above Ground Biomass

2.3.1 – Forest-Stand Living Biomass Allometric Estimates

Within the 160m × 20m alvar to forest transect, tree inventory included species identification, height (H, m), and diameter at breast height (DBH, cm) was observed. The inventory was divided into 20m × 20m at plots B through H. Every tree – living or dead (taller than 1.3 m) – within the plot was marked with a tag ID. DBH was measured with tree calipers or DBH tape at ~1.3m from the ground. Tree height was calculated through trigonometry using a clinometer to calculate the angle θ between the top of the tree and eye level at a distance, x from the base of the tree measured using a tape measure. Since

eye level was different for each person using the clinometer and the base of the tree could have sat in a depression or elevated mound of soil, base corrections were implemented to determine the correct height of the tree. The biomass of living wood, bark, branches and foliage was estimated using the measured DBH and H, from empirical formulae with species-specific coefficients from Lambert et al. (2005) for each tree. Total living tree biomass is the sum of the individual biomass components for each tree and the sum of tree biomass (kg) for all trees was computed for each plot (400 m^2) to derive estimates of above ground living biomass (kg/ha) in the forest. The living belowground structural root (> 5mm) biomass was estimated as a constant proportion of the aboveground biomass for each tree.

2.3.2 – Tree Age

Tree coring was used to determine the age of the largest diameter trees of each species in each plot in August 2021. Twenty cores were extracted again in October 2023 from each of White Cedar, White Pine and Red Pine over as wide a range in DBH as possible within the research site. Cores were mounted on wooden pallets, sanded with progressively finer sandpaper and rings counted with 10× binocular microscope. Age was estimated by at least two individuals, and when discrepancies greater than 2–3 years occurred, growth rings were recounted. Once age is established, then the long-term apparent rate of carbon accumulation (LARCA, kg[C]/y) can be estimated for individual trees.

2.4 – Below Ground Biomass

2.4.1 – Deadwood

Deadwood can be classified as any woody debris or standing woody tissue that does not undergo cellular growth anymore. Deadwood can come in the form of snags (standing deadwood), logs (deadwood that touches the ground) or coarse woody debris. The amount of carbon stored in deadwood is relatively unknown and throughout the literature, there were no cases of quantifiable deadwood decay rates per species. There are five classes of deadwood decay described in Chapter 1 (Maser et al., 1979).

To obtain deadwood biomass, all of the stems and branches within three randomly selected 4×4m quadrats per plot, were collected and weighed within a tarp using a handheld scale (±1 kg). Since the full weight of all deadwood in a 4×4m quadrat was too bulky to bring to the lab, a subsample of deadwood was collected for oven-drying (7 days at 100°C), to scale up as a moisture correction for the entire sample. Any snags or logs that were too large to weigh manually were evaluated instead by measuring, the diameter and length to obtain wood volume and then published wood densities were

applied to get mass. These volume-based values were added to the directly weighed samples to obtain total deadwood biomass per plot in kg/ha.

2.4.2 – Roots

One of the most elusive carbon pools is roots for the obvious reason that they are not directly observable (Vogt et al., 1998). The biomass of structural roots, like branches, can be obtained from allometric relationships as a proportion of above ground biomass. This is based on the premise that trees allocate resources below ground to support their continued ability to grow upright in the presence of environmental stressors. The larger issue is the biomass of fine roots which grow and senesce seasonally drawing on translocated photosynthates produced in the leaves in order to extract nutrients from the soil for tree growth and maintenance. There are several different field methods of determining fine root biomass and their turnover rates which complicates drawing generalizations about forest root dynamics from numerous comprehensive studies. No single method is ideal for all applications, but in reviewing numerous direct and indirect methodologies, Vogt et al. (1998) identify two indirect methods, one based on the Carbon Balance Approach and another based on the Carbon Fluxes Approach which are utilized here. As well Chen et al. (2004) have analysed a large number of comprehensive root datasets and have generated a family of empirical formulas for calculating fine root biomass, their turnover rates and their annual growth rates, based on representative basal tree diameters, forest age and average temperature conditions. which are used for comparison.

Nevertheless, fine root samples were collected at the CRT and HB sites although this was not done extensively, in order to provide some generalized context. Five 10 cm cores of soil were extracted from the Hay Bay site down to bedrock at plot M2 in 2020. These cores were split into a 10 cm surface layer and remaining layer. And seven similar 10 cm cores of soil were extracted at the Crane River Tract in 2022 and 2023, at Plots B through H adjacent to the collars where gas flux sampling occurred. These samples were not subdivided into layers based on depth. Soil sub-samples were sieved, and spray-washed on 0.5 mm sieves, after which fine roots (<2 mm and <5 mm) were separated from coarse structural roots manually with tweezers. Roots were oven-dried at 60°C for four days to remove moisture and then the total and fine root biomass was expressed on a mass per unit area basis.

2.4.3 – Leaf Fall Collection

Both CRT and HB leaf-fall collection utilized plastic baskets (25 cm × 35 cm) lined with screen mesh (Figure 5). HB contained twenty-four leaf litter baskets in total with eight baskets per subplot M1 through M3. Samples were collected approximately four times per year and all samples from eight

baskets per plot were merged before oven-drying and lab processing. The rate of litterfall carbon inputs to the soil surface (g[C]/m^2/y) at Hay Bay are now available for three collection years from April 2020–April 2023.

At Crane River Tract, initially, litterfall collection made use black landscaping fabric (5 m × 0.76 m = 3.8 m^2) pinned into the ground with spikes in each plot. However, flooding in the alvar and transitional regions of forest (Plots A, B, C, D), washed away part of the tarps and the leaf litter that had been collecting on the tarp. After this incident, 45 litter baskets (25 cm × 35 cm) identical in design to those at Hay Bay, were anchored to stakes in the ground to prevent the baskets from shifting. Plots at CRT contained on average six baskets except at plot A which was entirely alvar. Here litterfall was estimate by collecting all AGB within 25×25 cm quadrats, sorting into leaf and stem and assuming all deciduous leaves fell to the ground annually. Plot B contained 4 leaf-fall trap baskets, Plot C contained 5 leaf-fall trap baskets, Plot D contained 8, Plot E contained 6, Plot F contained 8, Plot G contained 6 and Plot H contained 8. Basket traps were placed adjacent to (~30 cm) the flux collars. Throughout the field season, leaf-fall collection would occur approximately every 3–4 months over a year when samples were processed for moisture content and then summed to get an annual estimate of leaf-fall biomass (g/m^2/y).

At the coniferous alvar site where the predominant species was Creeping Juniper (*Juniperus horizontalis*) eight 8 cm diameter metal sieves were used to collect leaf-fall over the study period. The 8 cm metal sieves were placed approximately a meter apart from each other and were buried within the interlocking branches and stems of the Creeping Juniper directly on the soil surface. The contents were collected every 3–4 months, processed within one week and combined to obtain annual estimates of leaf-fall biomass (g/m^2/y) from the Creeping Juniper canopy.

2.4.4 – Alvar Vegetation
To determine foliage biomass for the remainder of the alvar, all of the living vegetation on the ground within a 25×25 cm square quadrat, was pruned, collected and separated into woody tissue or leafy material. These samples were then weighed separately after oven-drying for moisture correction. While the predominant plant matter in the deciduous alvar were grass species (40%), there were some seedlings of white spruce which overhung into some of the 25×25 cm quadrats. Any overhanging vegetation into the quadrat was pruned and added into the AGB of that alvar sample.

2.5 – Soil Respiration: Time Series and Surveys

The soil CO_2 flux time series, to our knowledge, is the first of its kind to be collected in the Bruce Peninsula. These were measured with a series of 10 cm diameter static chambers using Licor LI8100a Soil CO_2 Flux Systems and Licor's Soil Flux Pro processing software. Phillips and Nickerson (2015) review various methods of obtaining soil respiration fluxes and the method employed here minimizes errors generated by other static chambers arising from modifying the environment to be measured. The measurement procedure involves placing the survey chamber on a collar anchored into (~ 1 cm) the soil surface, allowing the automated chamber to seal closed and then recording the rise in the CO_2 concentration (ppm) of air pumped through tubing into an infrared gas analyzer (IRGA). The chamber then reopens to allow ambient air exchange with the soil surface. The rise in concentration over time $\Delta C/\Delta t$ (ppm/s) is typically very precise ($R^2 > 0.997$) indicating thorough mixing in the headspace and the absence of air leakage with the outside. The fitted slope is converted into an equivalent CO_2 flux ($\mu mol/m^2/s$) based on the surface area sampled (78 cm^2) and the volume of air being exchanged, which includes a correction for the variable volume of air contained within the protruding collar (collar offset). This system also corrects for the accumulation of CO_2 in the headspace whenever a non-linear slope is encountered. This happens periodically when sampling coincided with bursts in the CO_2 flux generated by root respiration. In this case the rapid rise in concentration is fitted to an exponential curve and the rate of release is evaluated at the ambient CO_2 concentration when the chamber first closes. Eight collars were employed at the Hay Bay Forest, seven collars were employed at the Crane River site within the forest (one in each forest plot), and six additional collars were installed, three each in the deciduous and coniferous alvar sites. This configuration measures the total belowground CO_2 flux, R_t, including heterotrophic respiration, R_h, from the surface litter and soil matrix and autotrophic root respiration, R_a. Care was taken to remove new seedlings as they emerged from collars and to avoid trampling around collars while measurements were being taken. An additional environmental variable measured simultaneously by the IRGA was air water vapour concentration (ppt). The rise in water vapour concentration (H_2O range) over the interval when the chamber was closed is due solely to evaporation from the surface which is partly regulated by moisture availability in the surface emitting CO_2.

A second set of collars was paired at each sampling site in order to isolate the heterotroph respiration from root respiration. Phillips and Nickerson (2015) review several methods of partitioning root respiration from total soil respiration including the use of isotopes, girdling the phloem on the trunks of trees, sampling in both forest gaps and continuous canopy, and trenching. All methods possess advantages and disadvantages for specific applications. The trenching method is employed here which

involves severing the tree roots to kill them, and as a result they no longer release CO_2 within the soil zone treated. A core of the entire soil profile is excavated down to bedrock and the soil column is enclosed in a collar of the same length, which is sealed at the bottom, then returned *in situ* to the excavated hole. In theory, the *dead root* collars only release carbon dioxide due to heterotrophic decomposition of soil carbon within the litter and soil matrix. This is in contrast with the living root collars which also release autotrophic respiration (Phillips & Nickerson, 2015). Because the collars are installed within 20 cm of each other, the assumption is that everything else being equal, the difference between the two fluxes is due to root respiration.

The value of partitioning total belowground respiration into heterotrophic and autotrophic respiration is significant. R_h is a process which consumes soil carbon and therefore represents a net loss in the soil carbon budget. Root growth comprises a proportion of root respiration (the remainder being utilized for root maintenance) and annual fine root growth represents a net input to the soil carbon budget. Published values of forest net primary production, NPP represent the difference between forest gross primary production, GPP, minus forest respiration, R_a, which includes all the autotrophic respiration from both above-ground and below-ground biomass pools of trees. Conversely, published values of net ecosystem production, NEP, measured using eddy covariance systems mounted above the forest canopy represent the difference between GPP (sometimes labelled GEP) and ecosystem respiration, ER, which includes both heterotrophic losses as well as autotrophic losses.

Forest floor respiration can also be measured with a ground-based eddy covariance (EC) system. Lavigne et al. (1997) compared CO_2 fluxes measured with chambers against EC estimates and found there was a very good correspondence between the R_t fluxes measured with a system very similar to the one used here and F_c from eddy covariance. Exceptions occurred when the upwind fetch of the EC system shifted to include shrubs growing on the forest floor which were respiring and photosynthesizing. A critical limitation of the EC system is its inability to distinguish between R_h and R_a and therefore was not used in this study.

The trenching method however has several limitations (Phillips and Nickerson, 2015). The main one involves the degree to which the collars themselves could be modifying the environment to be measured. A sealed soil column of soil may become too moist if excess water percolates downwards and accumulates at the base, depriving decomposers of oxygen. The sealed soil column may also become too moist as roots no longer extract soil water for transpiration. Third, in the undisturbed soil, mycorrhizal exudates, associated with fine roots, mineralize organic matter which then serve as

nutrients for root growth. But some fractions of these nutrient are scavenged by heterotrophs to consume carbon within the soil matrix. This *pumping* of heterotrophic decomposition would be absent within the isolated chamber soil, thus depressing the real-time rate of measured R_h compared to that occurring naturally. It is unclear how large this influence may be and to some extent it is a matter of definition whether the difference between the two fluxes (R_t and R_h) is termed autotrophic or *root-mediated* respiration. Trenching is a commonly used technique and fits with the resources available for this study. In this application, the excess water concern was mediated by puncturing the bottom seal of the chambers with a 0.25 mm hole to allow for gravity drainage.

For a limited time, two LI8100's were available at Hay Bay to measure R_t and R_h synchronously from each pair of collars. After one flux system was permanently located at CRT a single unit was used to measure the flux from each collar, sequentially. At each location, a survey was conducted which would typically last four hours. Each collar was sampled in triplicate with each sample interval lasting 60 seconds. After both collars were sampled, the apparatus was moved to the next set of collars. This was repeated approximately biweekly during the growing season. Data pairs were compared, and the root component of respiration was determined from $R_a = R_t - R_h$. The averages, proportions and their standard deviations during the surveys were computed. Then flux values of R_a and R_h were binned in 5°C increments and regressed against air temperature which was measured simultaneously. The resulting regressions were generally excellent. Subsequently, regression estimates of monthly R_h and R_a were calculated based on Environment Cananda measured monthly temperatures, to generate annual CO_2 flux totals which were converted to their carbon equivalents The conversion of flux ($\mu mol/m^2/s$) to carbon equivalent biomass ($g[C]/m^2/year$) was to convert micromoles to moles by dividing by 1,000,000. Then multiply by 12.01, the atomic weight of carbon. Multiply by 86400, the number of seconds in a day and then by 365, the number of days in a year.

Before leaving a site, the flux system was left positioned on one of the collars and programmed to generate a time series of the soil flux every 15 minutes at a fixed location. The length of the time series would depend on the interval between site visits which varied from daily to biweekly. If precipitation occurred between site visits, rainfall collected *in situ* by a rain gage was reintroduced to the collar affected to maintain the moisture content of the soil as close to undisturbed as possible. The apparatus was then moved to a new collar. This protocol progressed through the entire forest site, such that fluxes and the corresponding temperature were being recorded almost continuously from early spring to late fall. However, numerous interruptions occurred when three or more consecutive overcast

days occurred in which case the solar pV panels were incapable of charging the 12V batteries sufficiently. This problem became more acute as increasing lengths of cable had to be used to provide power at plots deeper into the forest. Other interruptions to the time series occurred when components required repair or when the IRGA's required calibration. These latter two issues also occurred at Hay Bay where 110V AC power was available to charge the batteries. Very few readings were obtained in the winter as site access was prohibitive and drifting snow became problematic for the operation of survey chambers. Due to the uneven collection of data from different locations and under various temperature regimes, the entire flux record from all R_h and R_a time series was binned in 5°C increments and regressed against temperature to estimate the annual respiration fluxes from monthly mean temperatures in a manner like the survey measurements. These annual flux totals were calculated independently for the forest at Hay Bay and for the forest, deciduous alvar and coniferous alvar at the Crane River Tract.

2.6 – Litter Respiration
2.6.1 – Field Litter Experiments

One objective of the research was to compare the rate of decomposition of the newly fallen carbon in the form of leaf litter to the rate of decomposition in the soil itself. To achieve this, we measured the CO_2 emissions from the forest floor which included litter and soil and then measured separately the emissions from litter alone, to isolate the soil decomposition by residual. On 6 June 2022, litter was sampled from both CRT (N = 7) and HB (N = 8) forest study sites next to the flux collars using a serrated corer which permitted the collection of all litter down to the soil surface. Four replicate 78 cm^2 samples were collected and homogenized and then one-quarter of the litter biomass was placed into 10 cm rings approximately 2 cm deep and enclosed in nylon mesh. These *litter pucks* were returned to the soil surface where they would be exposed to ambient temperature and moisture conditions throughout the field season. Periodically, the samples were gathered next to a sampling station located in a shaded portion of the forest. The samples were first weighed (±0.1 g) to determine their moisture gravimetric content (GMC) in a windproof enclosure and then inserted into a custom respiration chamber onto which the LI8100 survey chamber was mounted. The measurement protocol involved taking a series of triplicate 60 second flux and temperature readings, taking care that the operator was downwind of the apparatus so as not to alter ambient CO_2 levels by breathing. Prior to each flux reading, air was purged from the gas lines for 20 seconds to eliminate residual air. Samples were then returned to their original locations at each plot. This entire procedure would take approximately two to three hours. This was repeated seven times from 6 June 2022 to 27 November 2022.

While the wildlife at CRT were fairly courteous throughout the study season, the HB red squirrels and chipmunks had a field day chewing through nylon stockings which contained the litter pucks. HB puck A was severely damaged while HB puck B and C showed some damage.

The other three replicate litter samples were identical in all respects to the ones used for the litter pucks and therefore one was used in oven drying to determine litter biomass. A second sample was used to repeat the litter respiration experiments in a growth chamber under controlled temperature and moisture conditions while the third could be used for nutrient analysis.

Litter respiration in the field was analyzed for its sensitivity to temperature, GMC and biomass. Because it was collected in close proximity to the flux collars it could be used to partition total collar R_h into litter R_h and soil R_h revealing spatial variations in the effectiveness of fast versus slow decomposers. Or it could be used to estimate how the soil efflux would respond, for example, to a fire which burned the litter layer. Because it was also collected in close proximity to leaf-fall baskets it could be regressed against annual leaf-fall to determine litter turnover rates, and also regressed against canopy foliage biomass to determine the extent to which spatial variations in forest floor litter biomass were dependent on potential litter inputs from the canopy. By reweighing the samples at the end of the field season, the moisture-corrected loss of biomass due to decomposition could be estimated at each location.

2.6.2 – Lab Litter Experiments

While field litter pucks are a great indicator of the flux at a specific time, temperature, and moisture condition, they do not isolate for each of the factors affecting the flux individually. However, in a controlled lab environment, it is possible to account for each of the factors (biomass, temperature, moisture content) that affect the flux, individually and determine which one has the dominant effect. These experiments used one-quarter of the total litter collected from each forest sample location at HB and CRT, enclosed in identical litter pucks which were kept frozen until mid-December 2022.

The growth chamber was calibrated to maintain temperatures of 5, 10, 15, 20, 25 degrees Celsius which corresponded to the temperature range which the samples in the field experienced. The entire apparatus and all samples were situated within the chamber to minimise temperature differences between the set temperature and sample temperature. Nevertheless, it would take at least an hour for everything to come into steady state at the set temperature, so samples were enclosed in sealed bags to control for weight loss due to evaporation over that extended period of time. Replicate temperature runs were taken at varying moisture contents corresponding to GMC values of average, median, mode,

minimum and maximum GMC as experienced in the field. Water was added to each sample after a temperature run to achieve these moisture levels.

In this way the sensitivity of respiration could be regressed against temperature and moisture independently within the ranges experienced in the natural environment. The effect of the spatial variations in litter biomass on respiration could also be evaluated using this procedure.

2.7 – Nutrient Analysis – CN & pH

Carbon (C) and Nitrogen (N) are important constituents of soil carbon dynamics as they effect the rate of decomposition, nutrient cycling and physical properties of the soil (Palmer et al., 2017). A high CN ratio suggests slower decomposition rates and soils with low lability while a low CN ratio indicates faster rates of decomposition and high lability. To account for differences in decomposition rates and, by extension, to determine the soil CN ratios, CRT soil samples from (0, 10) to (0, 160) were gathered every 5 meters (refer to 2.1.2 – soil cores methodology). Acid fumigation technique was performed to remove inorganic carbon. Then CN ratio was measured with an Elemental Analyzer (EA). The time elapsed between sample collection and sample analysis was approximately a year. It was not necessary to preserve the soil samples against decomposition as the litter layer with the fastest decomposition rate was removed, the moisture was evaporated out of the soil samples before storage. The litter layer was removed to separate the soil carbon from litter carbon and the lack of litter standard samples to compare our litter CN to, in the EA. The sealed samples had no exposure to sun or oxygen other than the limited amount of oxygen inside the sealable plastic bag used for storage.

Thirteen locations were selected adjacent to the flux collars in November 2023 to collect surface (5 cm) soil samples. In the laboratory, 22 ml of soil was mixed with 22 ml of distilled water to form a slurry which was stirred for a half-hour. Triplicate measurements of pH were taken with a hand-held calibrated OakIon (±0.01) meter.

2.8 – Acid Fumigation

The purpose of acid fumigation was to remove the inorganic carbon from the soil samples. Since the research project focused on organic carbon, contamination of inorganic carbon would interfere with the EA (Elemental Analyzer) as it cannot differentiate between inorganic vs organic carbon.

The 52 soil sediment samples had been oven dried for over 48h at 60°C to remove moisture content prior to fumigation. Standard operating procedures were employed in the Farquarson lab at

York University in the acid fumigation and acid removal processes prior to centrifuging and freeze drying.

2.9 – CN Analysis

CN data was collected by adding the soil sediment samples into an Elemental Analyzer EA cube. Once the samples are loaded on the EA cube carousel, each individual sample was dropped into a small chamber where combustion occurs. The gaseous state which accompanies combustion was transferred to an analyzer inside the cube which records how much carbon and nitrogen were in each soil sample.

Samples are divided into three categories: A) Run-in (sulfanilamide) 2.0 mg, B) Soil standard at 12.5 mg, C) Actual Sediment Samples at 12.5 mg. There were 52 sediment samples, 15 Run-in samples and 9 soil standard samples. Of the soil sediment that came from the acid fumigation procedure, some did not have the required 12.5 mg mass, post fumigation. For those, the entire tube of soil sediment was weighed. The samples were loaded into the EA carousel which can hold 60 samples at a time (2 blanks and 58 samples) and left to combust, analyze and record overnight. Excel data was downloaded directly.

3.0 – Results

In the results section, statistical significance is denoted by asterisks. No asterisks denote a $P >$ 0.05 or not significant. One asterisk (*) denotes a $P < 0.05$, or a 95% confidence level. Two asterisks (**) denote $P < 0.01$, or a 99% confidence level. Three asterisks (***) denote $P < 0.001$, or 99.9% confidence level.

3.0.1 – Temperature and Precipitation

Figure 10 shows average temperature and precipitation from the weather station closest to the study site for the year of 2021–2022. The data in figure 10 was from Government of Canada Historical Data site (https://climate.weather.gc.ca). Figure 10 is not typical for CRT/HB for a typical temperature moisture perspective as data from 2007–2020 (Figure 7) shows a reduction in precipitation for summer months of May – August and increase of precipitation in winter months of January – March. Average temperatures were higher in the study year than the 2007 – 2020 data by 2.6% while average precipitation was higher in 2007 – 2020 compared to the study year by 1.7%.
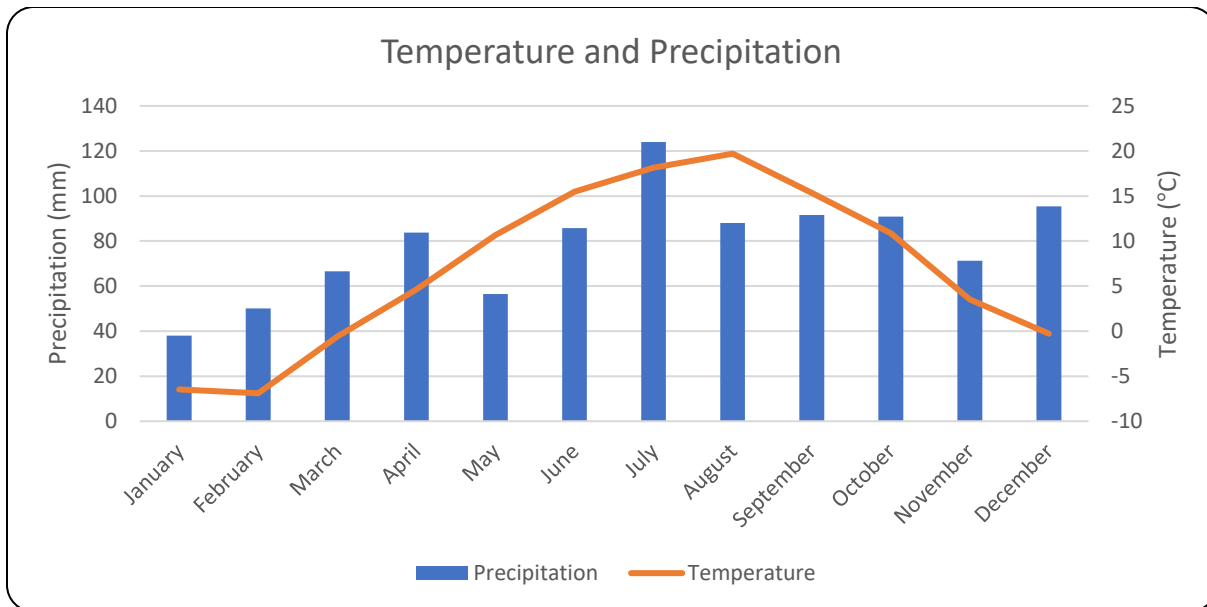
Figure 10: Average temperature and precipitation for Tobermory RCS weather station from 2021 – 2022.

Figure 11 compares the forest and alvar ground cover at CRT. At the deciduous alvar, grasses make up 39% of the ground cover while needle leaf litter comprises 44% of the forest ground cover. While exposed bedrock makes up a similar proportion of both habitats, the green vegetation understory in the forest makes up only 7.5% whereas in the alvar about 68% comprises shrubs, forbs and grasses. Moss and lichens make up 6% of the forest floor, compared to 3% of the alvar surface.
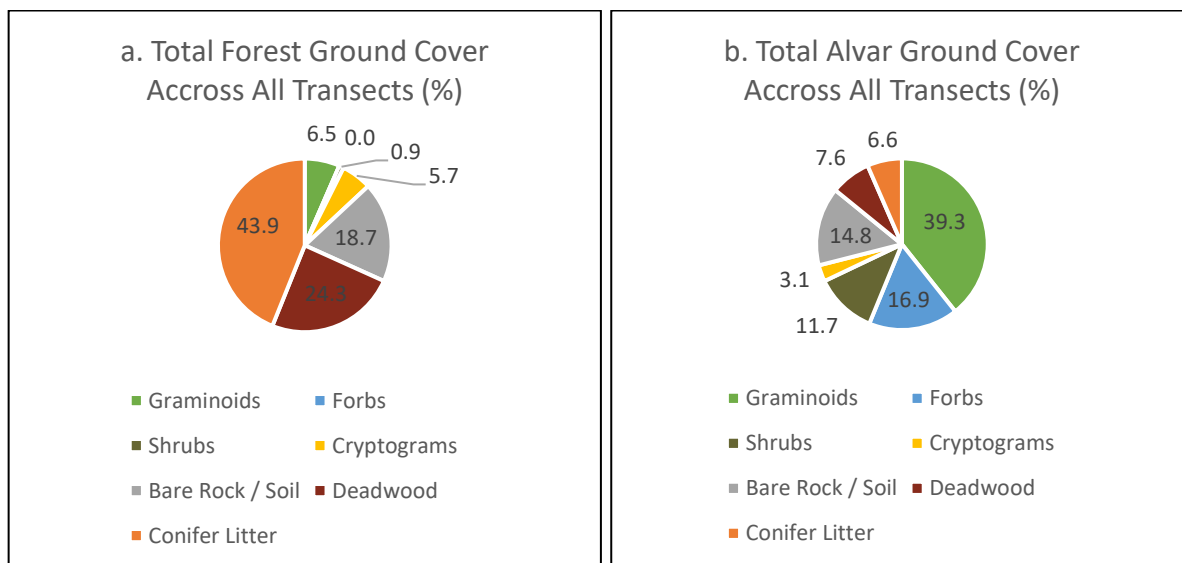
Figure 11a,b: Ground cover (%) for coniferous forest *(a)* and deciduous alvar *(b)* landscapes at CRT. (N = 70).

3.1 – Carbon Pools

3.1.1 – Crane River Tract (CRT) Pools

Figure 13 shows the soil at CRT comprises the largest biomass pool (43%) followed by living aboveground biomass (41%), litter (5%), deadwood (3%) and root (8%). Figure 12 shows, at plot G (120–140), the aboveground biomass pool is larger than the soil pool. Plot H has the largest number of Balsam Fir trees and the largest number of dead snags in the CRT. In my BSc thesis (Bao, 2021), the living understory biomass pool was considered to equal to zero due to the absence of noticeable living understory plants. The assumption is mirrored in the CRT hence the lack of an understory pool.
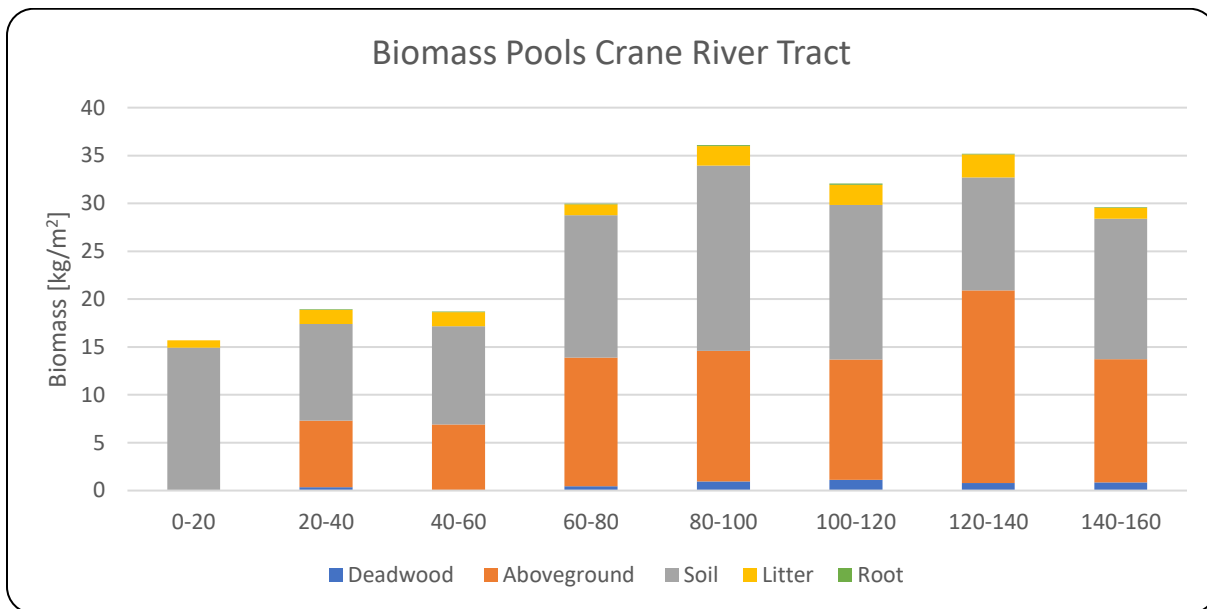
Figure 12: The biomass pools (kg/m^2) at the CRT classified into soil, living aboveground biomass, litter, deadwood and roots. Numbers indicate the distance in meters of the 20 × 20 m plots along the transect extending from the alvar (0–20), through the transition zone (20–60) and into the forest (60–160). Root biomass is not available for the 0–20 alvar plot.

Table 1 shows the root biomass for fine roots (<2mm diameter), coarser roots 2–5mm diameter) and the total fine root biomass which is the combination of both coarse and fine roots. The root samples were taken from each of the seven forested plots from the entire soil profile in 2023.

Table 1: The root biomass (kg/m^2) for CRT separated into fine roots, coarse roots and total roots for plots B – H in 2023.

ROOT BIOMASS (kg/m^2)	B	C	D	E	F	G	H	MEAN	SD
(2023) FINE ROOT	1.15	0.58	0.85	0.52	0.67	0.49	0.37	0.66	0.24
(2023) COARSE ROOT	0.30	0.50	0.69	0.18	0.50	0.20	0.09	0.35	0.20
(2023) TOTAL ROOT	1.45	1.08	1.54	0.70	1.17	0.68	0.46	1.01	0.38

Table 2 and Figure 13 shows the aboveground and soil carbon pools are almost identical at 41% and 43%, respectively. The deadwood pool is the smallest. The root pool Is divided into structural (>2mm diameter) and fine (<2mm diameter) roots.

Table 2: The carbon pools (kg[C]/ha) of CRT for the coniferous forest aboveground biomass, soil, litter, deadwood and root pools. These averages include the forest in the transitional zones (plots B and C) and were scaled to the proportions of tree cover of 231m^2 and 109 m^2, in plot B and C respectively.

Coniferous Forest Pools	Crane River Tract (kg[C]/ha)
Aboveground	61763
Soil Carbon	64689
Litter	7898
Dead wood	3660
Structural Roots	15441
Fine Roots	1991
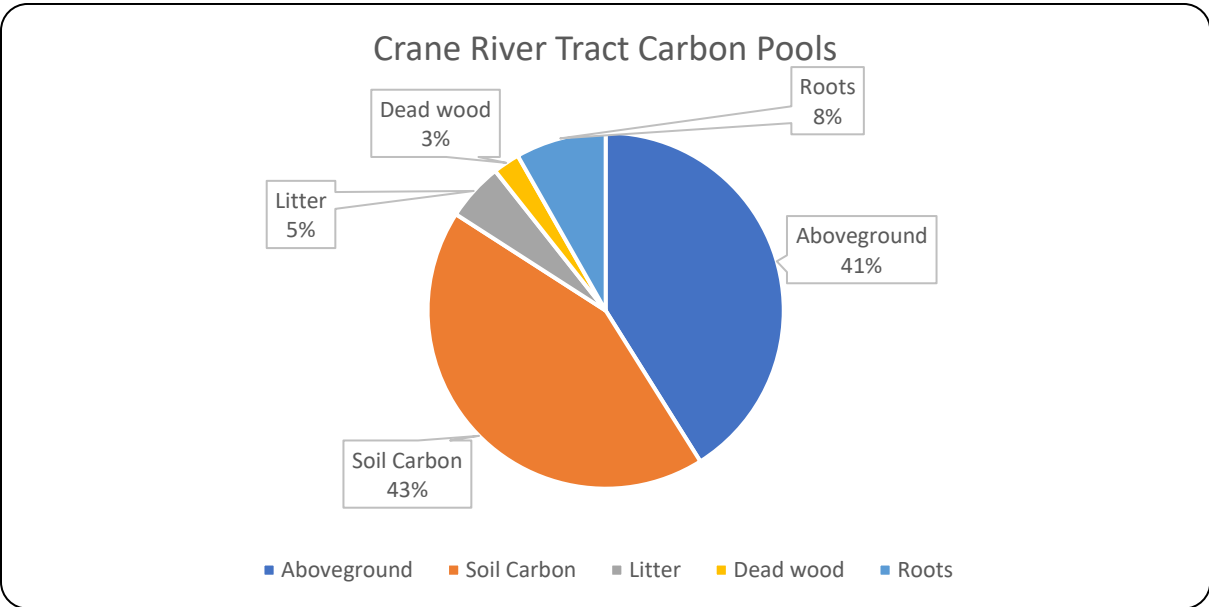
Figure 13: Crane River Tract (CRT) forest carbon pools for aboveground, soil, litter, deadwood and root pools expressed as percentages.

Figure 14 shows the soil organic carbon (SOC) content of the entire soil profile at numerous (x, y) coordinate locations within the study site. There is an incredibly large value of SOC at coordinate (110, 10). Field notes were re-examined to evaluate the possibility of a lab processing error and none was found. At this coordinate, there is a C horizon layer. On average, the SOC in the forest and alvar are not significantly different (Table 3).
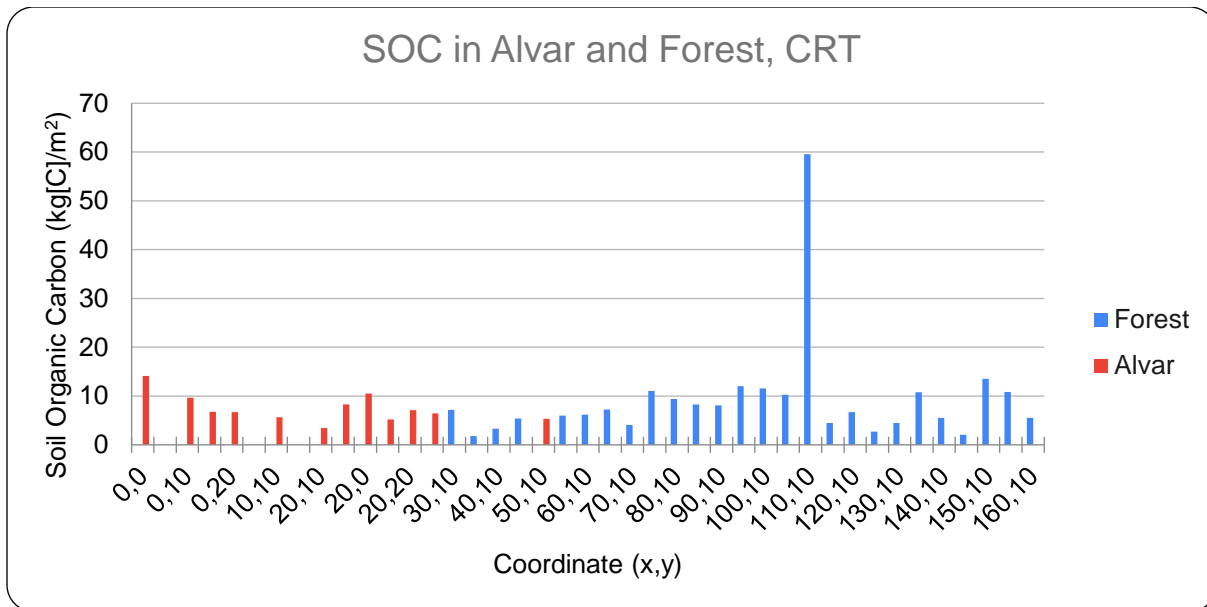
Figure 14: Soil organic carbon ($kg[C]/m^2$) at CRT for alvar (red) and forest (blue).

Table 3 indicates SOC at plot F is approximately 45% larger than the average coniferous forest pool. Plot F incorporates the extreme value in Figure 14. Plot B SOC is approximately 38% smaller than the average in the coniferous forest pool as a whole. Plot B is a transitional plot between alvar and forest and had the lowest average soil depth for all of the plots. Plot C was a transitional zone but had almost double the soil depth compared to plot B.

Table 3: The plot averages for soil organic carbon (SOC) at CRT for the coniferous forest and deciduous alvar. Plot A corresponds to coordinates (0,0–20,10), B (20,10–40,10), C (40,10–60,10), D (60,10–80,10), E (80,10–100,10), F (100,10–120,10), G (120,10–140,10), and H (140,10–160,10).

Plot Coordinate Averages	SOC kg[C]/m^2	Bulk Density Average (g/cm^3)	Organic Fraction	Soil Depth Average (cm)
A (0,0 – 20,10)	6.55	1.14	0.10	8.7
B (20,10 – 40,10)	3.99	0.51	0.42	4.8
C (40,10 – 60,10)	5.14	0.68	0.25	8.9
D (60,10 – 80,10)	5.89	0.90	0.16	7.0
E (80,10 – 100,10)	7.77	0.42	0.28	10.5
F (100,10 – 120,10)	11.89	0.83	0.47	8.7
G (120,10 – 140,10)	5.59	0.70	0.21	8.8
H (140,10 – 160,10)	5.02	0.54	0.33	5.0
Average Deciduous Alvar	**6.55**	**1.14**	**0.10**	**8.71**
Average Coniferous Forest	**6.47**	**0.64**	**0.26**	**7.67**

Figure 15 shows the total aboveground biomass for all trees within each plot for the CRT study site using Lambert et al., (2005), formulas. These employ species-specific empirical coefficients and utilize measured tree height and DBH to compute wood, foliage, branch, and bark biomass for each tree taller than breast height.
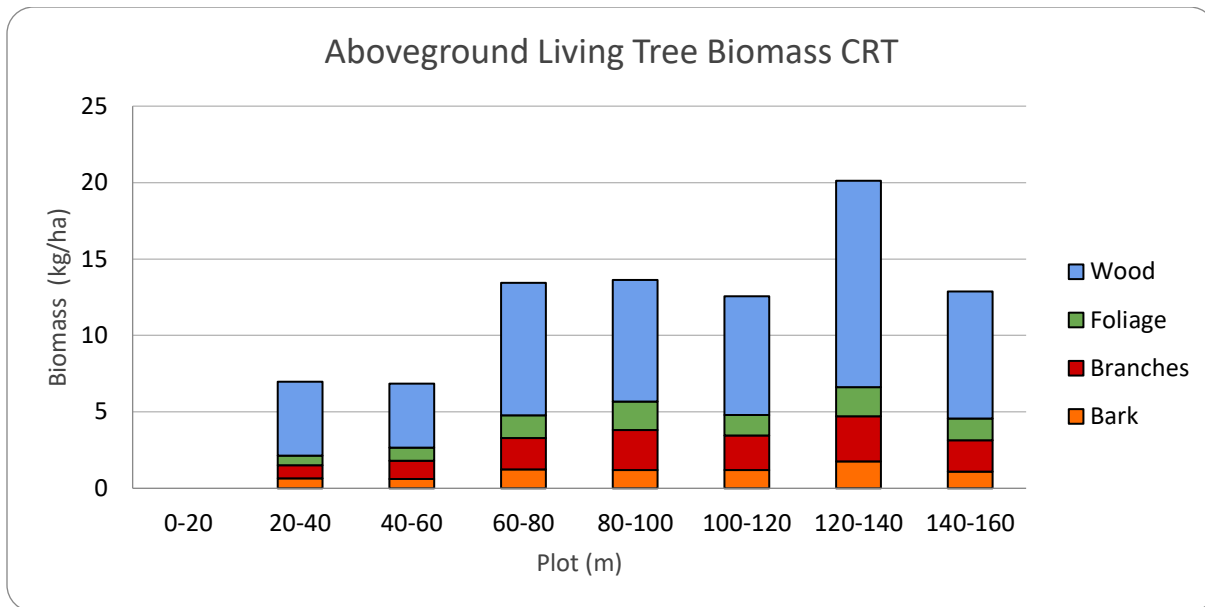
Figure 15: Overall CRT aboveground biomass (kg/ha) per plot, separated into proportions of wood biomass (blue), foliage biomass (green), branch biomass (red), and bark biomass (orange). Average AGB at CRT is 123525 kg/ha (61762.5 kg[C]/ha).

Most of the aboveground living biomass of the trees at CRT is comprised of woody tissue 63.9%, while the bark comprises the smallest amount of living biomass 9%. Foliage and branches comprise 11% and 16.2% of AGB tree biomass, respectively. Plot A (0–20) is alvar. Plots B (20–40) and C (40–60) are transitional zones between alvar and forest. Values for transition plots were scaled to the actual forest covered portion. Plots D through H (60–160) are entirely forest and they do not appear to exhibit a gradient in biomass with distance into the forest. Plot G (120–140) stands out as possessing the highest above-ground living biomass. It exceeds the fully forested plots average AGB by approximately 50,000 kg/ha and the transitional forest plots by a factor of three.

Figure 16 shows the number of trees (#/ha) belonging to each species within each plot and Figure 17 the same species-specific data for biomass (kg/ha). Figure 18 shows the corresponding pattern in mean DBH (cm) by plot. The most abundant tree species is White Cedar in all plots except for plot H (140–160) where Balsam Fir has the highest number of stems. When tagging and categorizing the tree species in plot H, there were many small Balsam Fir saplings with a DBH between 2 cm and 5 cm (Figure 18).
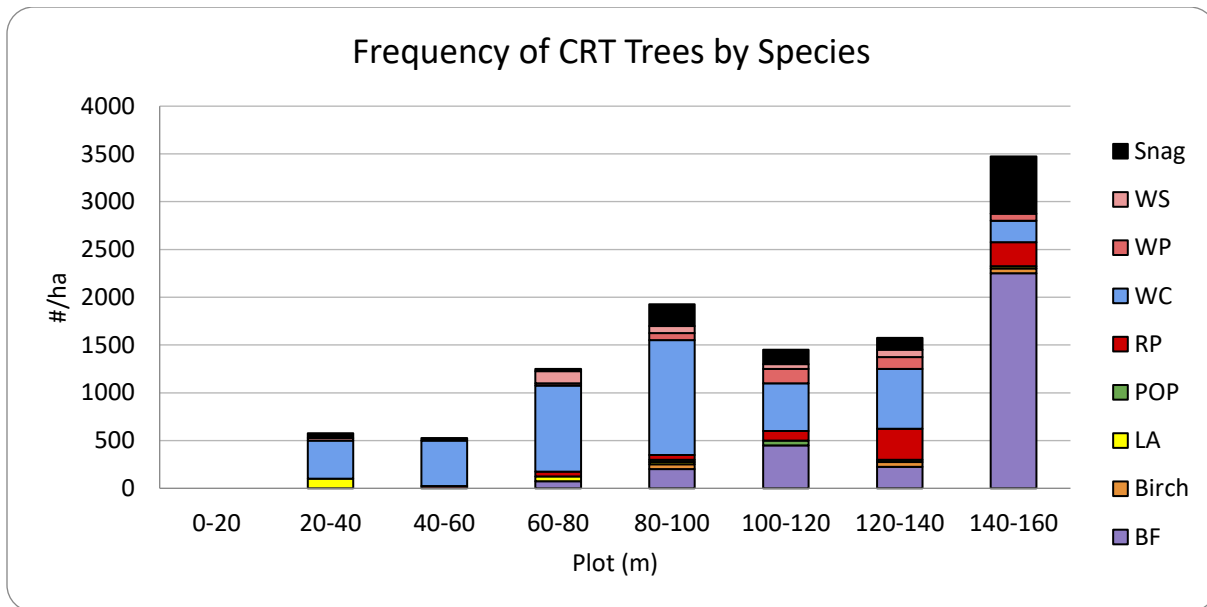
Figure 16: The frequency of each tree species per plot within the CRT study boundaries. Units are in # per hectare. Snag represents dead trees that have not fallen to the ground. Legend is as follows: WS White Spruce, WP White Pine, WC White Cedar, RP Red Pine, POP Trembling Aspen, LA Larch, Birch Paper Birch, BF Balsam Fir.

The majority of plot H tree biomass in Figure 17 is contained within Red Pine while the highest number of stems per hectare is Balsam Fir (Figure 16). White Cedar biomass declines from 94%–17% from plots B – H but remains the dominant species in terms of biomass. Snag (dead tree) biomass is the highest in plot E at 6.6% of total tree biomass while plot G and H snag biomass are 2.6% and 6.2% of total above-ground biomass.
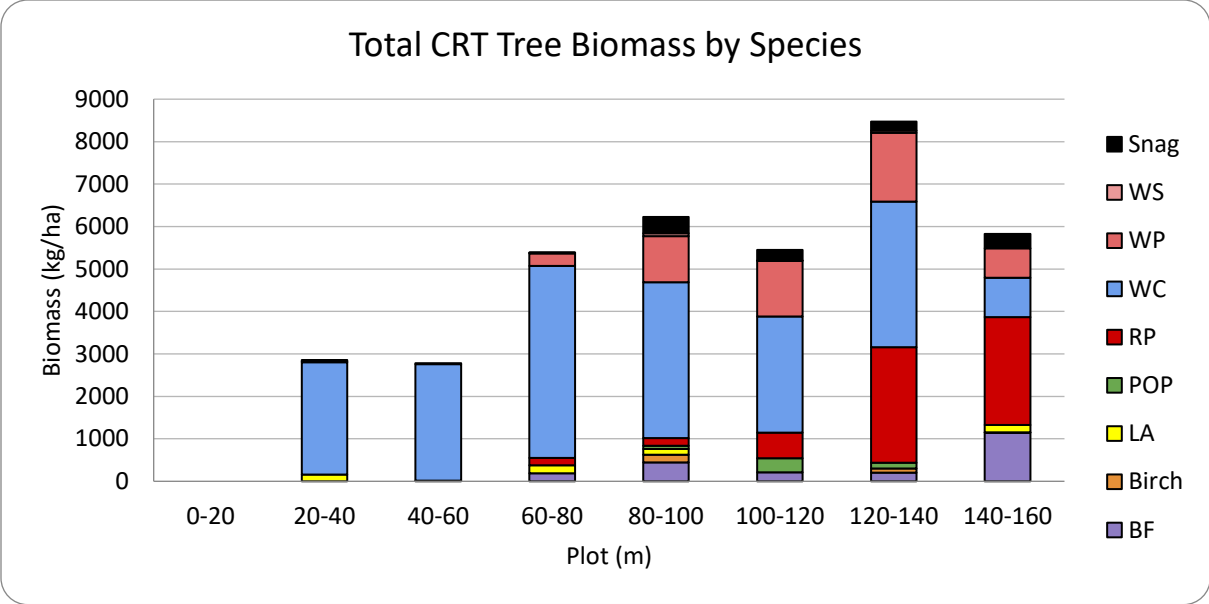
Figure 17: The biomass of each tree species per plot within the CRT study boundaries. Units are in kilograms per hectare. Snag represents dead trees that have not fallen to the ground. Legend is as follows: WS White Spruce, WP White Pine, WC White Cedar, RP Red Pine, POP Trembling Aspen, LA Larch, Birch Paper Birch, BF Balsam Fir.

Figure 18 shows the average tree diameter at breast height for the CRT. Plot H has the lowest average DBH due to the abundance of sapling Balsam Firs while plot B and C were comprised almost entirely of mature White Cedars.
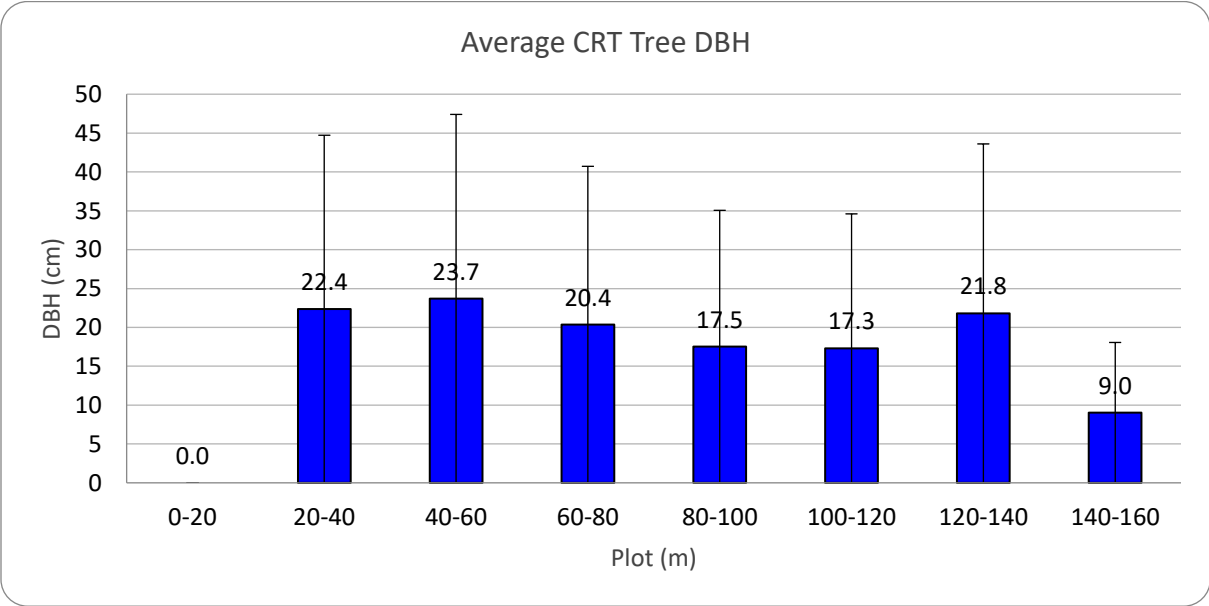
Figure 18: The average tree diameter (cm) at breast height (DBH) at CRT. Errors bars indicate ±1 standard deviation. Plot A is within the alvar.

Figure 19 shows mean litter biomass along the transect. The alvar possesses the lowest litter biomass with an increasing trend in litter on the ground beneath trees as one progresses inland along the transect. Again, Site H accumulates the least amount of litter on the forest floor consistent with the local minimum in above-ground biomass for that plot shown in Figure 15.

CRT Average Litter per Plot
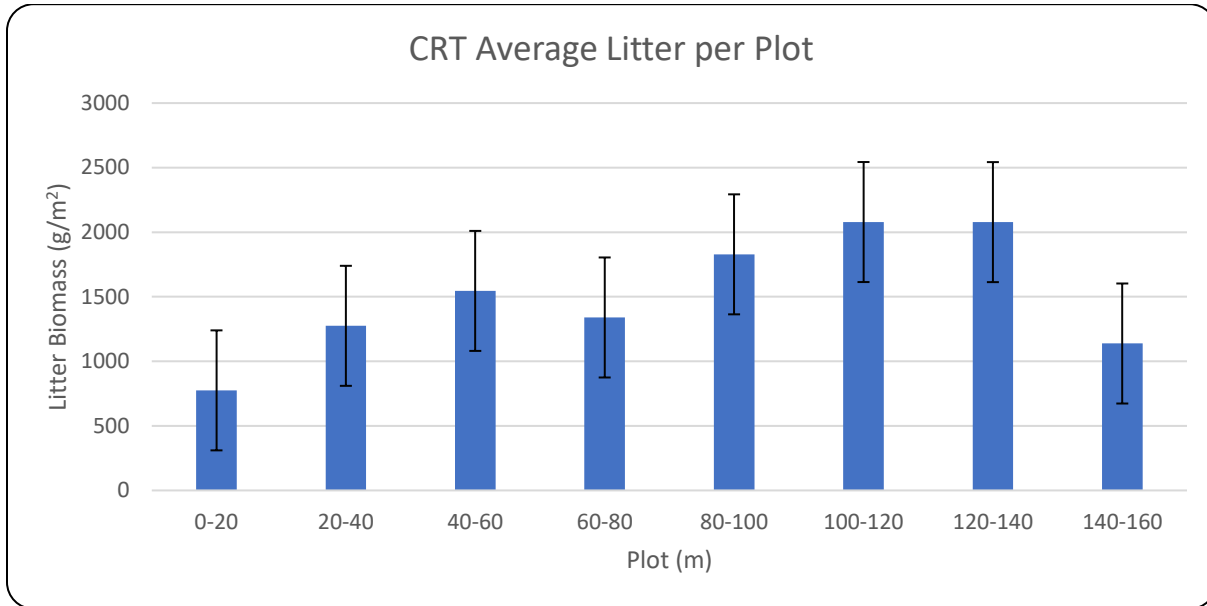
Figure 19: Average litter biomass (g/m^2) for all plots at CRT. Error bars represent ±1 standard deviation.

Figure 20 shows the correspondence between foliage biomass and litter on the ground across the entire study site.
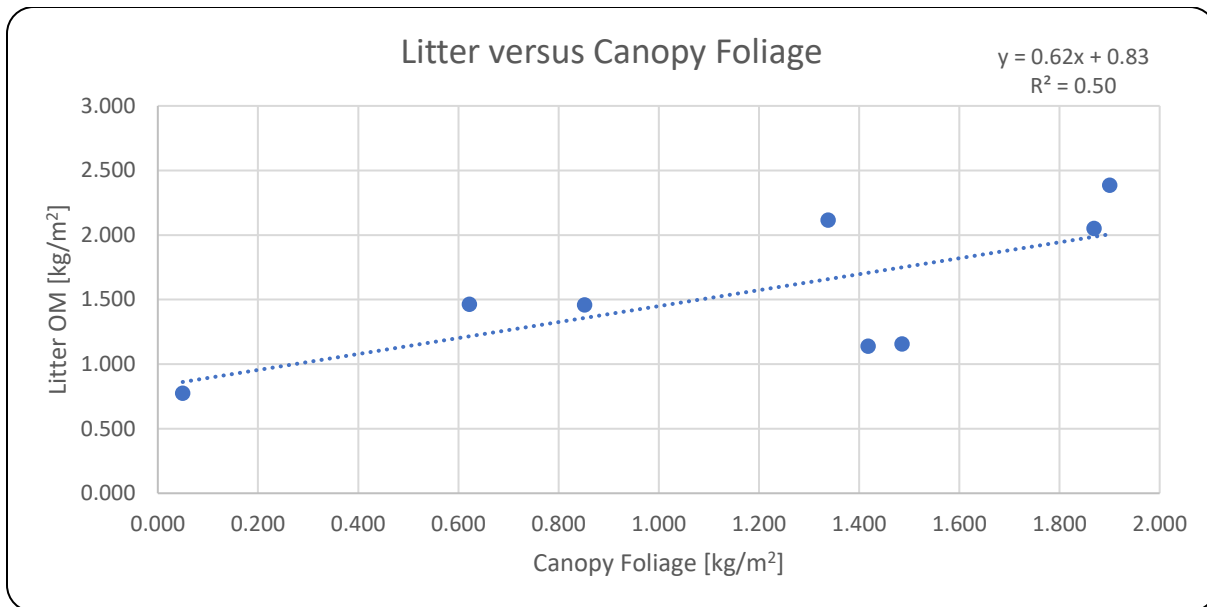
Figure 20: The relationship between the biomass of litter present on the forest floor and canopy foliage biomass for the CRT plots. The left most point corresponds to the deciduous alvar plot A where annual litterfall equals canopy foliage biomass.

Table 4 indicates the magnitude of the litter carbon pools with maxima at plot F and G. Alvar litter carbon pools are 48% of the forest carbon pools per unit area.

Table 4: The average amount of litter (kg[C]/ha) at CRT for each of the plots including plot A which is deciduous alvar. The rest of the plots are coniferous forest.

Plot Average CRT	Litter Biomass (kg[C]/ha)
A (0–20)	3796
B (20–40)	6247
C (40–60)	7572
D (60–80)	6564
E (80–100)	8960
F (100–120)	10186
G (120–140)	10183
H (140–160)	5576
Average Coniferous Forest	7898
Average Deciduous Alvar	3796

Figure 21 shows that forest deadwood biomass pool (2021) increases from plots B – F except for plot C which has the lowest deadwood biomass (plot A is deciduous alvar). Living tree biomass (Figure 15) does not suggest why the deadwood pool was so small at plot C. A random sampling issue is a

possible explanation.
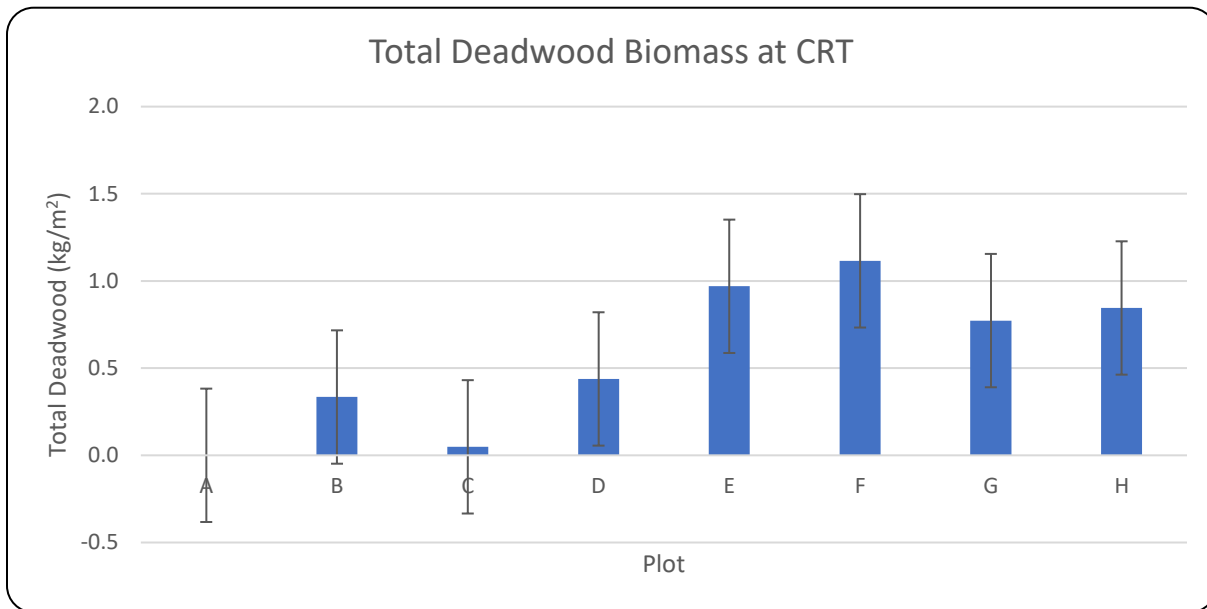
Figure 21: The total amount of deadwood biomass at the CRT site across plots A–H where plot A is deciduous alvar while plots E–H are coniferous forest. The average deadwood for the entire CRT site is 0.732 kg/m². The error bars represent ±1 standard deviation.

The Canadian Forest Carbon Model (Kurz and Apps, 1999) specifies 0.67% softwood of stems, 4% of branches and 2% of course roots contribute to the dead organic matter (DOM) pool annually. For the Crane River Tract these transfers from the living pool to the DOM pool are 494±181 kg/ha/y belowground and 1003±367 kg/ha/y aboveground. Presumably the belowground root contributions to the soil pool are direct and are included in soil core samples. If these proportions are valid for CRT, then the annual aboveground contributions of deadwood comprise 1003/7320 or 14% of the observable deadwood (Figure 21) on the forest floor. This suggests that it takes on average only 7.3 years for fallen deadwood to be incorporated into the soil pool by burial or decomposition. No measurements were taken to validate these rates. However subjectively it appears entirely possible that on this time scale while smaller twigs and branches would become part of the soil carbon pool, the fire-charred cedar logs would take much longer.

As Table 5 shows the amount of soil carbon in the coniferous alvar pool differs between the A and B horizons with A being consistently larger than B. CA3 horizons differ by 49%, CA2 horizons differ by 59% and CA1 differs by 79%. The average soil carbon is 23767 kg[C]/ha for both A and B horizons. The average soil carbon for A and B horizons are 34896 and 12638 kg[C]/ha, respectively. Figure 22 indicates

that Creeping Juniper has almost equal amounts of AGB and litter that comprises 51% of the total carbon pool while soil carbon pool comprises 49%. There are no estimates of root biomass.

Table 5: Soil carbon pool for coniferous alvar (Creeping Juniper) CA collar locations. *N* = 8

Coniferous Alvar	Horizon	Soil Carbon (kg[C]/ha	Depth (cm)	Organic Fraction	Bulk Density (g/cm^3)
CA3	B	12753	3.5	0.05	1.6
CA3	A	24871	7.5	0.2	0.4
CA2	A	41066	8.5	0.2	0.6
CA2	B	16975	4.5	0.05	1.6
CA1	A	38752	9.5	0.2	0.5
CA1	B	8186	1.5	0.05	2.4
Average		**23767**	**5.8**	**0.1**	**1.2**
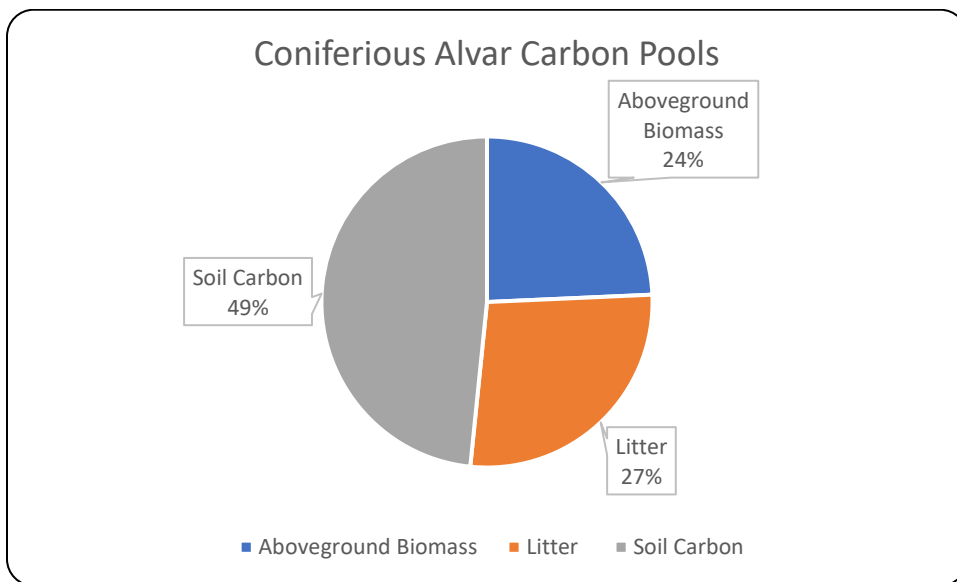
Figure 22: Coniferous alvar *(Juniperus horizontalis)* carbon pools summary.

Figure 22 shows the soil carbon is the main pool between the AGB, litter and soil carbon pools – a difference between the coniferous alvar and forest pool sizes and the deciduous pool sizes. The corresponding carbon pools aboveground biomass and litter pools are similar in size (Figure 22 and Table 6). Comparing Tables 6 and 7, the aboveground biomass pool is much smaller for the deciduous alvar. The deciduous alvar site only had grass and small shrubs with the occasional seedling spruce tree. The coniferous alvar soil pool is almost 3× smaller than the deciduous alvar soil pool and the coniferous forest soil pool.

Table 6: Coniferous alvar carbon pools for aboveground biomass and litter.

Coniferous Alvar Pools	Crane River Tract (kg[C]/ha)
Aboveground Biomass	11932
Litter	13422
Soil Carbon	23767

The deciduous alvar carbon pool (figure 23) is almost entirely made up of soil carbon.

Aboveground pool makes up 1% while litter makes up 5% of the total carbon pools.
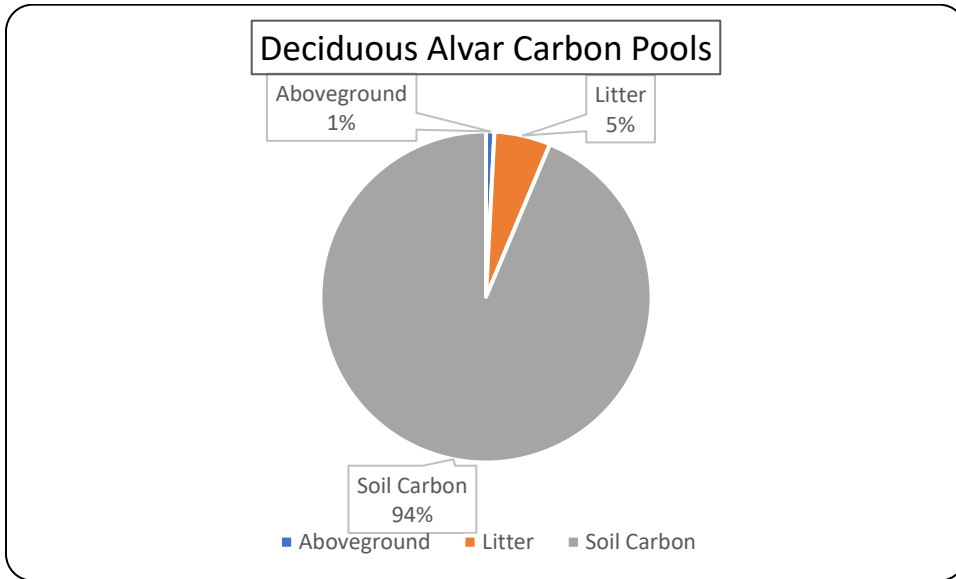
Figure 23: Deciduous alvar carbon pools summary

Table 7: Deciduous alvar pool sizes for litter, soil carbon and aboveground biomass (kg[C]/ha).

Deciduous Alvar Pool	Crane River Tract (kg[C]/ha)
Aboveground	565
Soil Carbon	65455
Litter	3796

Deciduous Alvar Aboveground Biomass
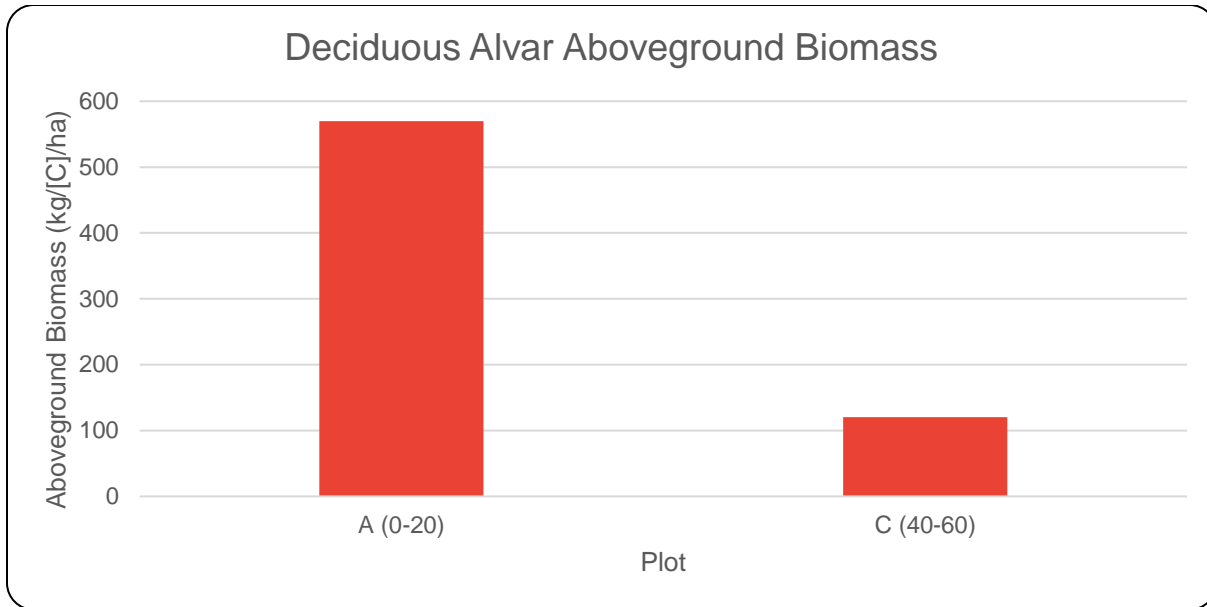
Figure 24: The deciduous alvar AGB averages at CRT per plot including the entirety of plot A (0–20) and alvar-only zones of 40–60 transitional zone (plot C).

Figure 24 shows that plot A had a higher AGB – almost five times higher than plot C. Plot A was fully deciduous alvar while plot C was a mixed transitional zone with specific areas designated as deciduous alvar. Transitional zones between forest and alvar have less AGB compared to pure deciduous alvar, possibly due to the litter fall from the trees inhibiting plant growth of the surrounding alvar. Table 8 shows more litter biomass in the deciduous alvar transitional zone C rather than A but more aboveground biomass in plot A compared to C.

Table 8: The aboveground biomass and litter biomass (kg[C]/ha) for deciduous alvar plot A and alvar portion of plot C. N = 23 for plot A. N = 3 for plot C.

Deciduous Alvar	Aboveground Biomass (kg[C]/ha)	Litter Biomass (kg[C]/ha)
A (0–20)	570	3796
C (40–60)	120	6131
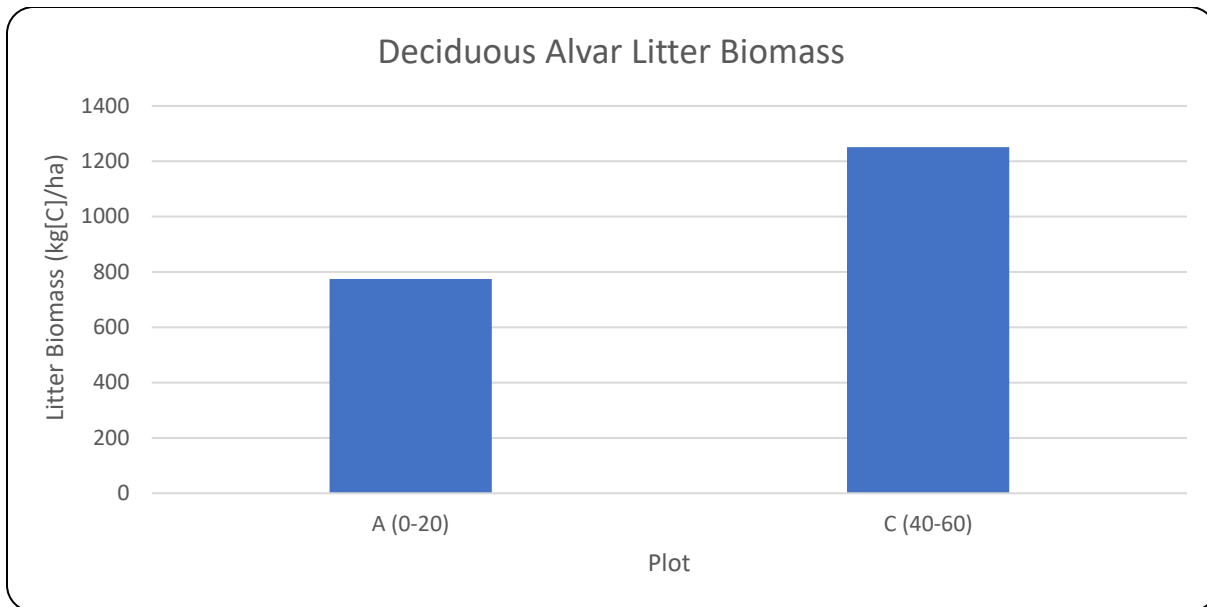
Figure 25: Average litter organic carbon (kg/m^2) for deciduous alvar plots at CRT. 40–60 are transitional zones between forest and alvar.

Litter biomass (kg[C]/ha) was higher in plot C than plot A due to the species composition. Plot A had no mature cedar trees while plot C had sections of deciduous alvar and was classified as a transitional zone with both trees and deciduous alvar at the perimeter peripherals. The litter fall from the cedar trees accumulated in plot C while the litter fall from the deciduous plot A contained no coniferous leaves, only deciduous leaves.

3.1.2 – Hay Bay Carbon Pools

Table 9 summarizes the White Cedar Forest carbon pool at Hay Bay with deadwood as the smallest pool while soil carbon is the largest pool. The root pool Is divided into structural (>2mm diameter) and fine (<2mm diameter) roots.

Table 9: Coniferous Forest pool summary including aboveground biomass, soil carbon, litter, deadwood and root pools, at Hay Bay.

Coniferous Forest Pools	Hay Bay (kg[C]/ha)
Aboveground	86523
Soil Carbon	90933
Litter	6889
Dead wood	4869
Structural Roots	21631
Fine Roots	1560

Figure 26 shows the two largest Hay Bay Forest carbon pools are within 2% of each other. Combined, they make up 86% of the carbon pools at HB. Deadwood makes up the smallest pool.
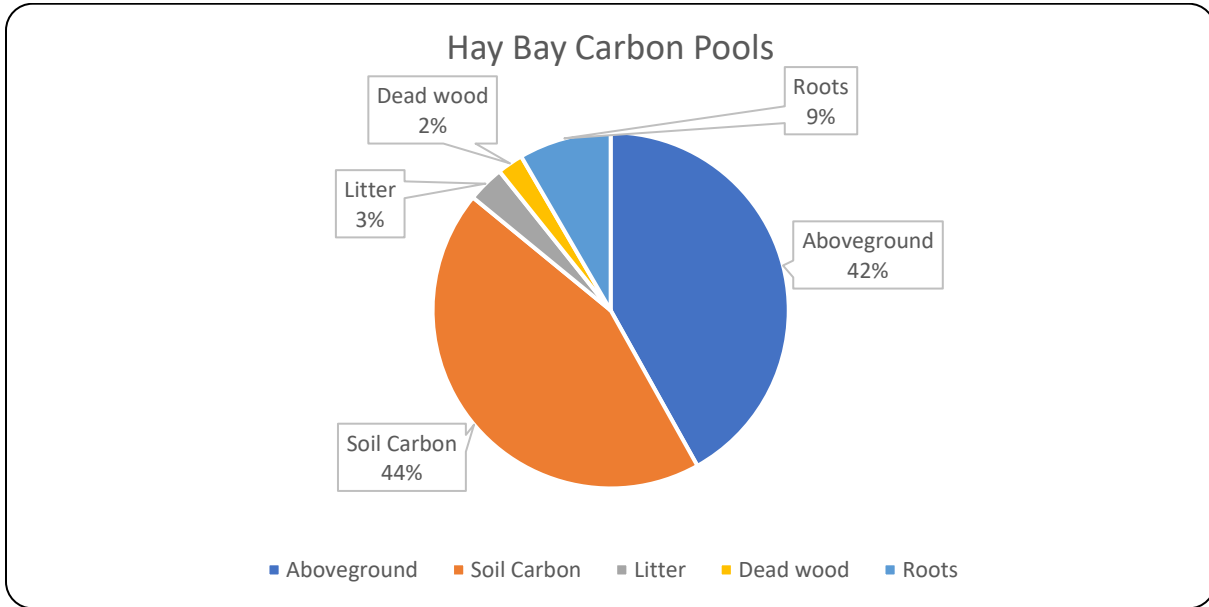
Figure 26: Hay Bay carbon pools (soil, aboveground, deadwood, roots and litter) expressed in percentages.

Table 10: Root biomass [kg/m^2] at the surface (0–10 cm soil layer) and the total biomass [kg/m^2] for deeper soil depths ranging from 11–30 cm, for fine roots (<2mm) and all roots (<2 mm and >2 mm) at Hay Bay.

ROOT BIOMASS (kg/m^2)	A	C&D	E	F	G	MEAN	SD
FINE ROOTS							
0_10	0.79	0.56	0.41	0.83	0.31	0.58	0.23
TOTAL	0.87	0.89	0.62	1.73	0.70	0.96	0.44
% SURFACE	89.96	63.22	66.94	47.86	44.30	60.28	
ALL ROOTS							
0_10	0.85	0.59	0.66	1.50	0.31	0.78	0.45
TOTAL	1.29	2.05	0.94	3.74	0.79	1.76	1.21
SOIL DEPTH [cm]	12	17	20	20	30	19.8	6.6

The fine roots (<2mm) make up an average of 60.3% of the roots at the surface across the five sites that had been cored and sorted. The largest number of fine roots at the surface were found in site A with almost 90% of the fine roots within the surface 0–10 cm layer. The smallest number of fine roots at the surface was at site G with 44.3% found in the surface layer.

Shallow soils typically have a higher percentage of fine roots in the surface layer. Locations E and F are both 20 cm deep, but site F almost has double the fine root biomass in the 0–10 cm layer. However, at Site F, the fine root biomass found in the 10–20 cm layer was larger than in the surface layer. The same applies for Site G. Site E, while maintaining the same soil depth as F, has almost 20% more fine roots at the surface which might be related to differences in canopy cover, litter understory, and the amount of buried wood. Site G had large amounts of buried wood from a partially decomposed tree when the soil collar contents were sorted. Site F also had a large amount of buried woody debris in the soil profile while Site A had almost no wood debris. Sites C, D and E had small amounts of woody debris. The distribution of fine roots extended deeper when the soil range was deeper but there are multiple factors that effect the distribution such as the soil contents and the displacement of roots via large woody debris.

Table 11: Soil, aboveground biomass, litter, and deadwood carbon pools at Hay Bay accounting for sites M1, M2, M3 and average between sites

HB Plot	Soil (kg[C]/ha)	Aboveground Biomass (kg[C]/ha)	Litter (kg[C]/ha)	Deadwood (kg[C]/ha)
M1	81238	71821	6328	3527
M2	124405	108787	7092	3679
M3	71112	78962	7247	7402
Average	90933	86523	6889	4869

M1, M2 and M3 are labels for the three 50 m^2 sampling plots within the 20 × 20 m medium site at Hay Bay where leaf-fall, and soil carbon were measured. Respiration measurements were confined to eight pairs of collars at M2. Table 11 shows that the highest Hay Bay Forest aboveground biomass was at M2 which was 1.4 and 1.5 times larger than that at sample locations M3, and M1, respectively. The highest litter carbon was found in M3 followed by M2, and M1. The highest deadwood biomass was found in M3 followed by M2 and M1.

3.2 – Carbon Dynamics

This section provides a concise overview of how the respiration results presented in the following sections were acquired and how they relate to the soil carbon balance questions under consideration. Operational details of the equipment and measurement methodology are contained in Chapter 2. Fluxes analysed here, were sampled using two protocols as either time series or surveys. Time series form a continuous record of the soil flux taken every fifteen minutes, over a period ranging from one day to two weeks at a single location. Time series show how emissions vary from a single collar in response to changes in environmental conditions. Surveys were conducted over the course of 3–4 hours on individual days, from all the plots, and used to provide a snapshot of the spatial variability in emissions under the prevailing ambient conditions on sampling days and the difference between R_h and R_a. An additional set of survey fluxes are presented which were measured from *litter pucks* containing subsamples of litter-only residing on the ground surface at each forest sampling site over the duration of the field program. These are also used to provide a snapshot of the spatial variability in heterotrophic litter respiration under the prevailing ambient conditions on sampling days. But also, these are used to explore what proportion of R_h may be emanating from the forest litter compared to the underlying soil column.

The flux results presented here span three years (2020, 2021, 2022) in two separate locations. Hay Bay contains R_t and R_h fluxes from 2020, 2021 and 2022 while Crane River Tract contains R_h fluxes

from 2022 and R_t fluxes from late 2021. For the 2022 study period, the flux readings focused on dead collars measuring R_h, hence the paucity of living collar (Ra) data. Ra data was collected at CRT in late 2021 from October 2021 to early January 2022.

3.2.1 – Crane River Tract Dynamics

Figure 27 shows that soil decomposition varies between forest locations from April to November 2022 with emissions at plot H approximately double those at plot D. The overall seasonal average heterotrophic respiration is 2.19 µmol/m^2/s. ANOVA test showed no significant difference among the plot locations. ($P > 0.05$)
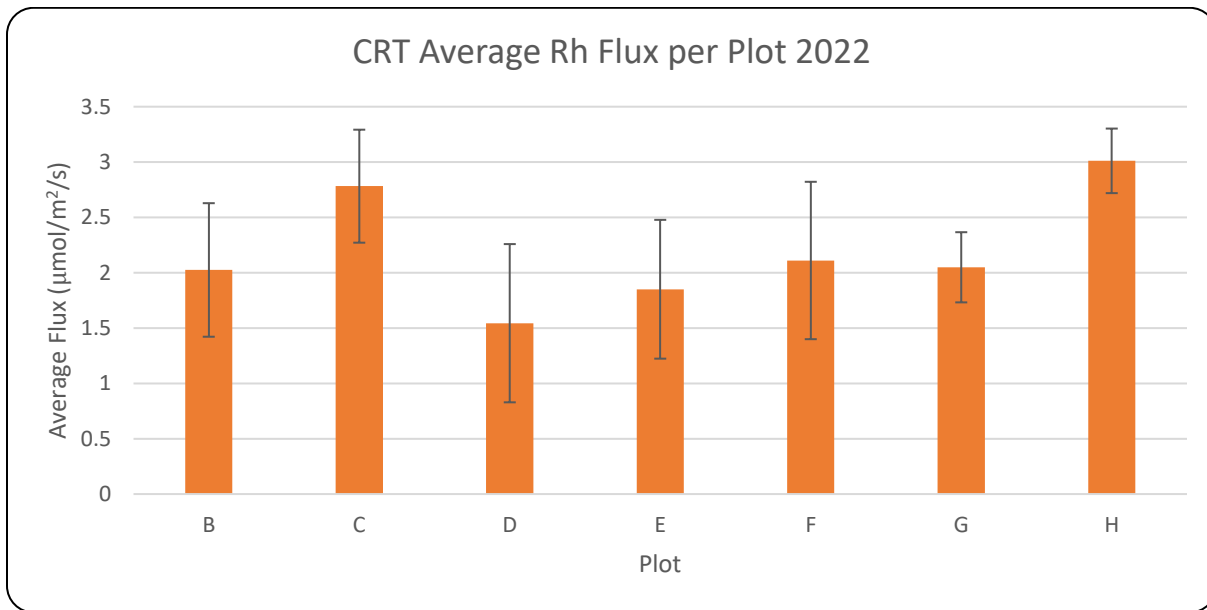
Figure 27: The average time series, heterotopic fluxes (µmol/m^2/s) for CRT 'dead root' collars Overall average is 2.19 (µmol/m^2/s). Flux data from April 10th, 2022 – November 28th, 2022. Error bars represent ±1 standard deviation. N = 10472.

Figure 28 illustrates how soil decomposition varies seasonally in 2022 with the maximum in August being approximately 2.75 times larger than that the April minimum. Flux variability is largest in the fall months.
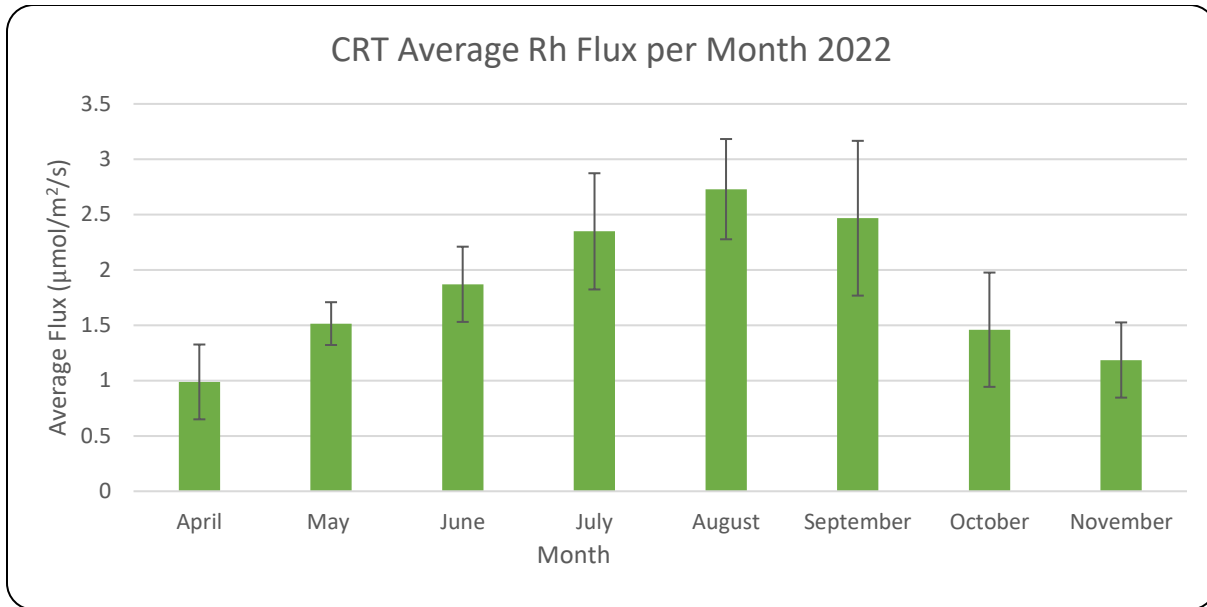
Figure 28: The monthly average time series, heterotrophic forest fluxes ($\mu mol/m^2/s$) for CRT 'dead root" collars. Total average 2.19 ($\mu mol/m^2/s$) per all measured months. Flux data from April 10th, 2022 – November 28th 2022. Error bars represent ±1 standard deviation (N = 10569).

Figure 29 shows the mean time series dead root collar (R_h) emissions from the alvar measured between June 8, 2022, and October 24, 2022. The D collars are situated in plot A which is representative of the shrubs, forbs and grasses in the alvar more generally where the mean R_h is 1.34 $\mu mol/m^2/s$. The A collars are located within the 15 m diameter patch of Creeping Juniper (coniferous) where the mean R_h is 1.21 $\mu mol/m^2/s$.
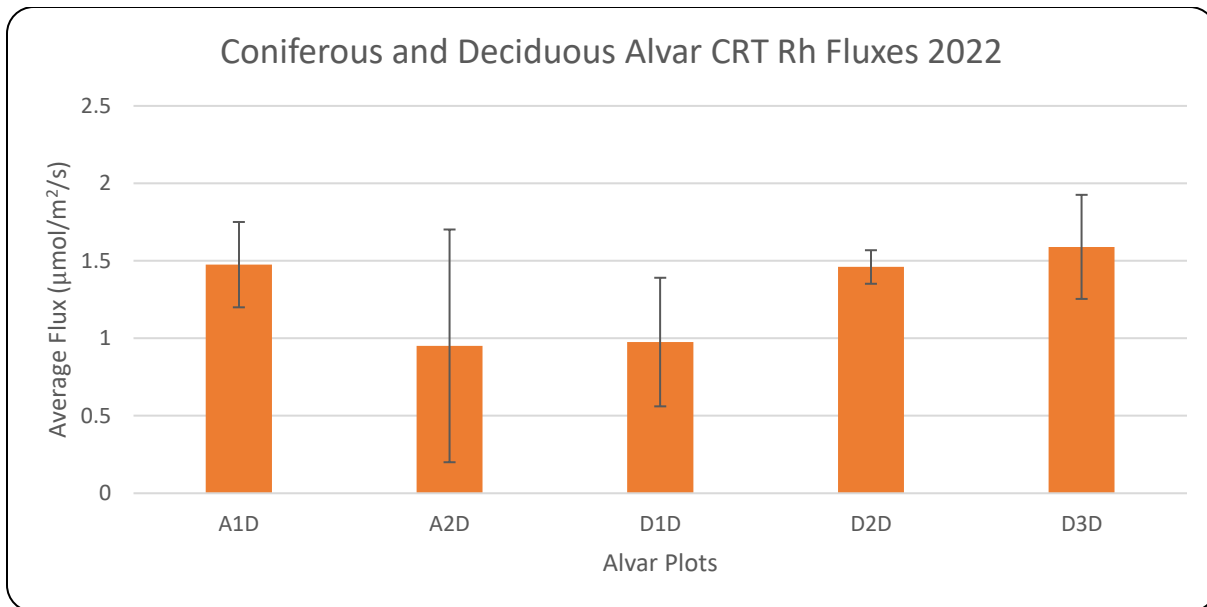
Figure 29: The average time series, heterotrophic fluxes ($\mu mol/m^2/s$) for CRT 'dead root' collars, measuring R_h at coniferous (A1D, A2D) and deciduous (D1D, D2D, D3D) alvar plots. *N* = 699. Error bars represent ±1 standard deviation.

Figure 30 shows the average R_t time series flux at CRT in 2021. R_t was only measured for six different intervals from October to January and does not include plots B,G,H. After the installation of flux collars at the Crane River Tract in September 2021, the fall period was set aside for measurement of the fluxes from only the living collars in the alvar and forest to allow for the senescence of recently severed roots in the *dead* collars. The total respiration R_t from the living collars in the alvar, Plot A and from four of the forest sites between October 2021 and January 2022 are shown in Figure 30. At this time the pV solar charging system for powering the LI8100 batteries had not been fully extended to all sites and hence data from plots B, G and H are not available. Within the forest, combined respiration from the soil and roots was the highest at plot C averaging 3.5 $\mu mol/m^2/s$ with plot E emitting only approximately 50% of the maximum. The alvar emitted approximately 42% of that from Plot C over that time period and approximately 88% of that from forest site E.
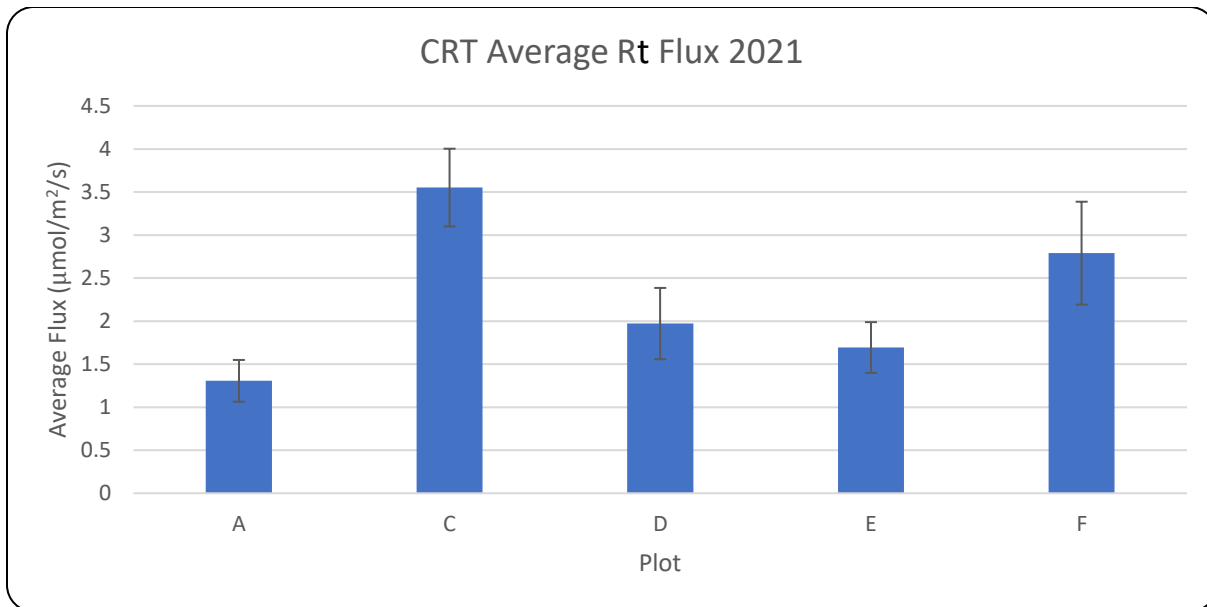
Figure 30: The average time series total respiration fluxes (μmol/m^2/s) for CRT 'living root' collars, measuring R_t per plot. Flux data from October 2021– January 2022. N = 4966. Error bars represent ±1 standard deviation.

Figure 31 and Table 12 compare the heterotrophic, autotrophic and total forest respiration from all the survey data. The results show that the soil decomposers and roots are making equal contributions of approximately 2.4 and 2.3 μmol/m^2/s, respectively to the combined CO_2 emissions from the forest floor at the CRT study site as a whole, under ambient moisture and temperature conditions.
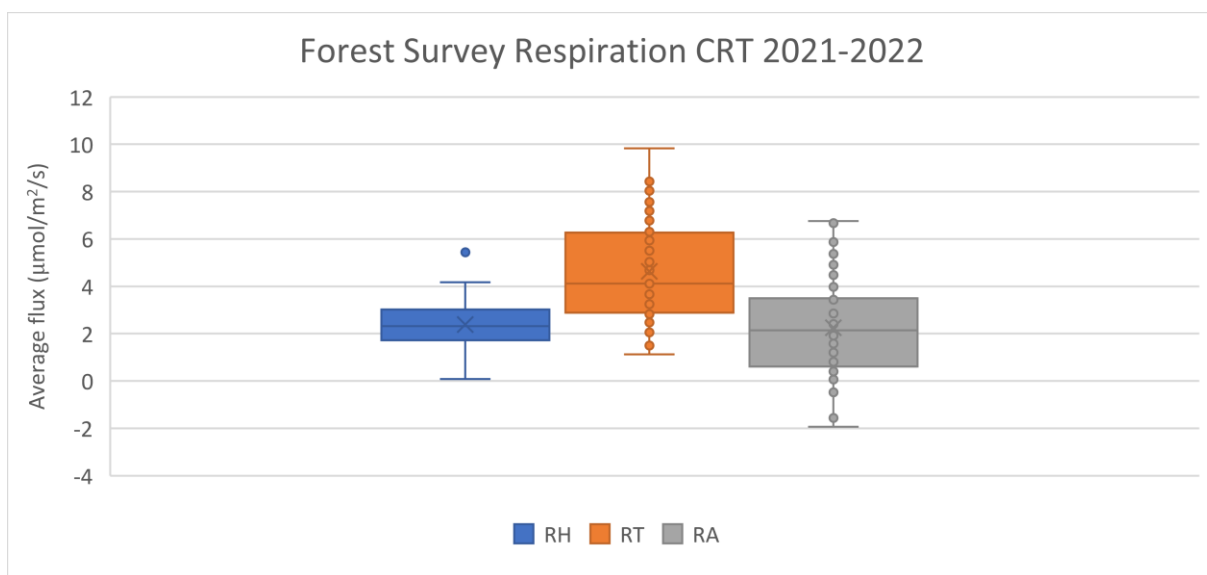
Figure 31: Coniferous Forest survey respiration fluxes (μmol/m^2/s) from CRT for 2021–2022. N = 67.

The R_h data is less dispersed than the R_a data and R_t data, suggesting that variations in forest respiration arise from variations in root growth and maintenance compared to variations in the activity of soil microorganisms While the box and whisker plot does show an outlier in R_h, when analyzing the raw data, the triplicate readings associated with that outlier were similar to each other.

Table 12: Statistical table of coniferous forest (CRT) regressions, statistical significance, average fluxes, average temperature, standard deviation, SD and coefficients of determination, R^2. The regression is flux (y) against temperature (x).

Forest Flux Temp Regression	Regression Equation	R^2	Statistical Significance	N	AVG Flux	SD	AVG Temp
Coniferous forest R_h	y = 0.0512x + 1.6731	0.14	***	67	2.38	0.97	13.81
Coniferous forest R_t	y = 0.1876x + 2.0345	0.40	***	67	4.63	2.12	13.81
Coniferous forest R_a	y = 0.1364x + 0.3613	0.21	***	67	2.25	2.09	13.81

The regression equations for CRT coniferous forest shows that when X (temperature) is 0°C, the flux (Y) is 1.67, 2.03 and 0.36 μmol/m^2/s for R_h, R_t and R_a respectively. R_a was calculated by subtracting R_h from R_t for each pair of readings at each site. The slopes represent the flux sensitivity to temperature and indicate that emissions from heterotrophs are about one-third as sensitive to changes in air temperature as that arising from root emissions. Consequently, the sensitivity of total forest floor emissions to temperature appears to be primarily driven by that of the living vegetation to temperature variations as opposed to that of decomposers.

Figure 32 and Table 13 show the corresponding R_h, R_a and R_t survey flux data for the alvar.
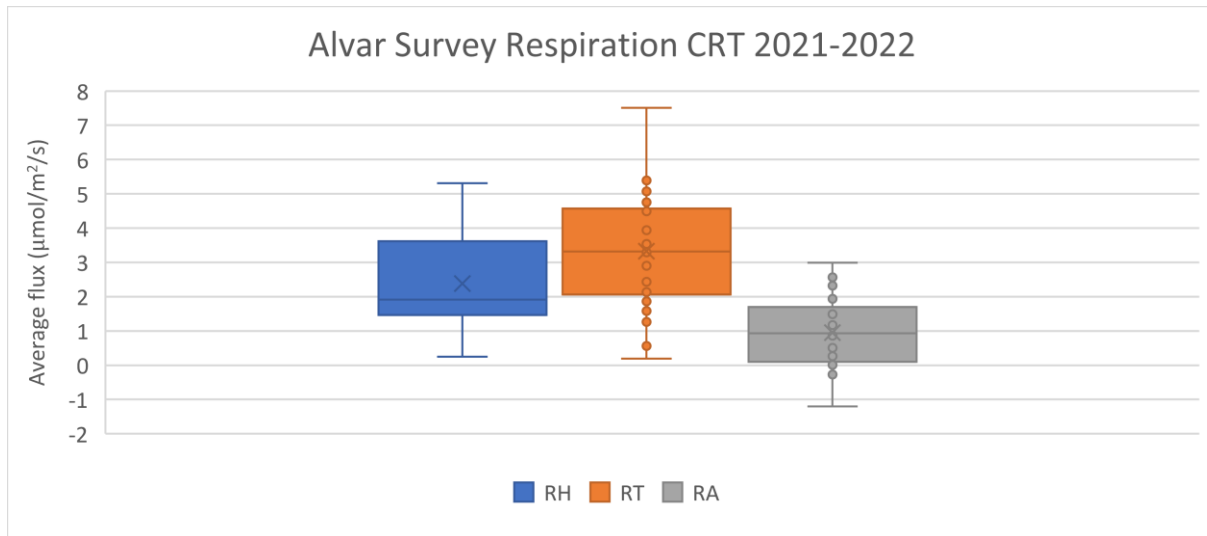
Figure 32: Alvar (coniferous and deciduous) survey respiration fluxes ($\mu mol/m^2/s$) from CRT for 2021–2022. $N = 30$. R_a is calculated as the difference between R_t and R_h for each collar pair and then averaged.

Since surveys were taken on the same day for all plots within the span of four hours, the assumption is that flux differences between each pair of collars are primarily driven by the presence/absence of roots. R_h is 2.5 times larger than R_a in the alvar but the ranges are similar. R_t has the largest range of average fluxes with overlaps of quartile 2 (Q2) and 3 (Q3) against R_h Q3. However, R_t Q2, Q3 has no overlap with R_a Q2 or Q3. ($P < 0.05$).

Table 13: Statistical table of alvar (CRT) regressions, statistical significance, average fluxes and standard deviations, SD average temperature, and R^2 values. The regression is flux in $\mu mol/m^2/s$ (y) against temperature in ^0C.

Alvar Flux Temp Regression	Regression Equation	R^2	Statistical Significance	N	AVG Flux	SD	AVG Temp
Alvar R_h and Temperature	y = 0.1129x - 0.0601	0.39	***	30	2.38	1.47	21.6
Alvar R_t and Temperature	y = 0.1615x - 0.158	0.67	***	30	3.33	1.60	21.6
Alvar R_a and Temperature	y = 0.0486x - 0.0978	0.15	*	30	0.95	1.01	21.6
Coniferous Alvar R_t and Temperature	y = 0.1623x - 0.0694	0.57	**	30	3.73	1.78	23.4
Deciduous Alvar R_h and Temperature	y = 0.1165x - 0.3042	0.52	***	30	2.05	1.29	20.2
Deciduous Alvar R_t and Temperature	y = 0.1564x - 0.1378	0.76	***	30	3.02	1.43	20.2

The P values in Table 13 are all less than 0.05. Coniferous alvar temperature was generally higher than the deciduous alvar temperature. The factors responsible for the coniferous alvar temperatures being warmer than in the deciduous alvar could be related to lower albedo or reduced latent heat flux since they were measured at the same time. Coniferous forest temperatures (Table 12) are generally cooler than alvar temperatures (Table 13) indicative of the cooling influence of the shade from the forest canopy.

Figure 33 indicates that from plots B–H, the percentage of total foliage biomass that comprises White Cedar, gradually decreases while the percentage of foliage comprising Red Pine, White Pine and Balsam Fir, increases. Therefore, the potential exists that the spatial pattern in leaf-fall is not only a function of foliage biomass but also interspecies differences in shedding rates.
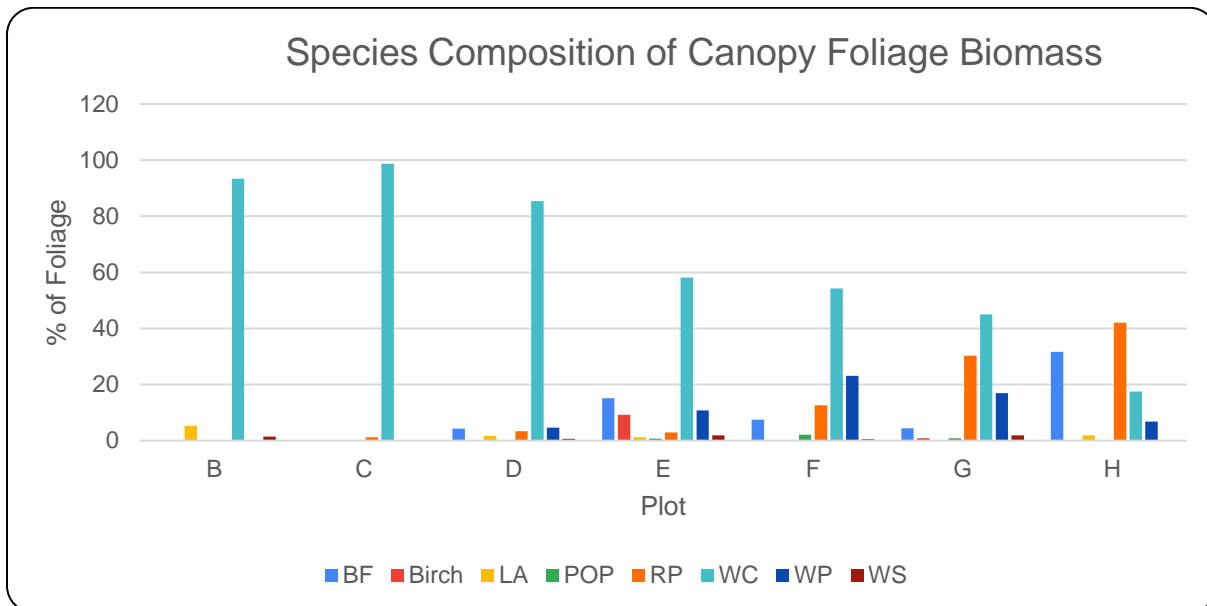
Figure 33: Foliage biomass for CRT expressed in percent (%) of total foliage biomass by species, for each plot. Legend abbreviations are the same as used earlier in figures 16 and 17.

Figure 34 shows the annual leaf-fall rate in 2021–2022 of 337.6 g/m^2/y was 78% larger than that in 2022–2023 of 189.4 g/m^2/y. The pattern of leaf-fall by plot remains relatively unchanged between the two years except for plot F which dropped the fewest leaves in Year II.
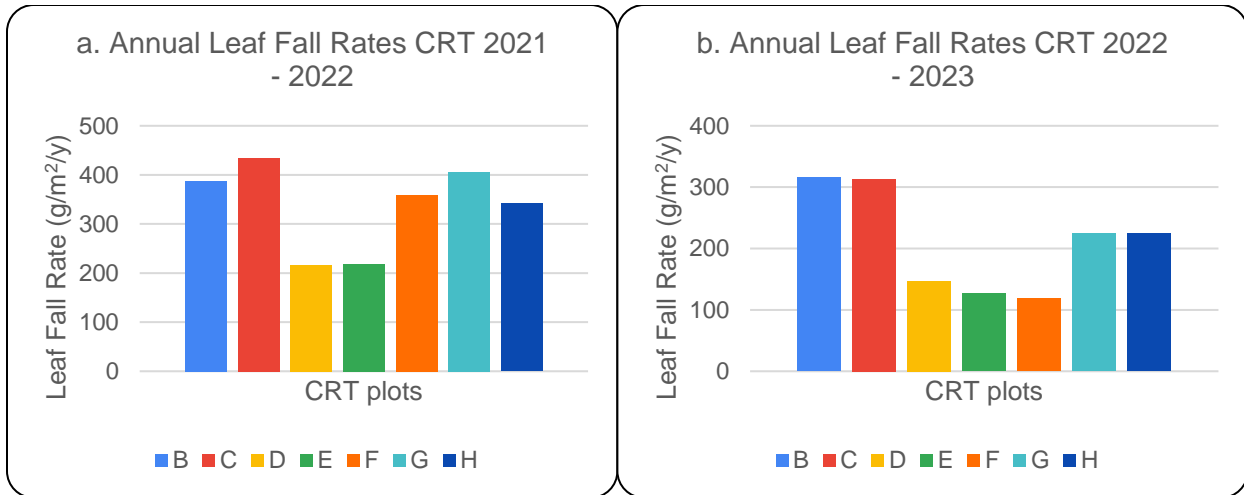
Figure 34 a, b: The annual leaf-fall biomass (g/m^2/y) at CRT for two collection years 2021–22 and 2022–23, respectively, using a combination of tarps and basket traps at each of the seven plot locations.

Figure 35 shows the regression of annual leaf-fall against litter biomass for the two study years. The graph seems to suggest that in a year with higher leaf-fall rates, plots with greater ground litter correspond to plots with higher measured leaf-fall rates. While in a year with lower leaf-fall rates the inverse is true. However, the *P*-values for both years were not significant, suggesting there is no relationship between annual leaf-fall and litter biomass. The blue correlation coefficient (r) is -0.44 with a negative slope while red correlation coefficient (r) has a positive slope of 0.1.

A separate regression between leaf-fall and canopy foliage biomass for 2021–22 and 2022–23 showed no significant relationships between the two. However, the R^2 values were higher at 0.24 (2021-22) and 0.5 (2022–23).

Overall, there is a good correlation between foliage biomass and litter biomass on the forest floor (Figure 20). It is therefore noteworthy that the mechanism connecting the two, leaf-fall, is not correlated with either. Given the variability in interannual leaf-fall over two years (Figure 34), it may take several years before the longer-term delivery of leaves released from the canopy and delivered to the forest floor is reflected in the two biomass pools.
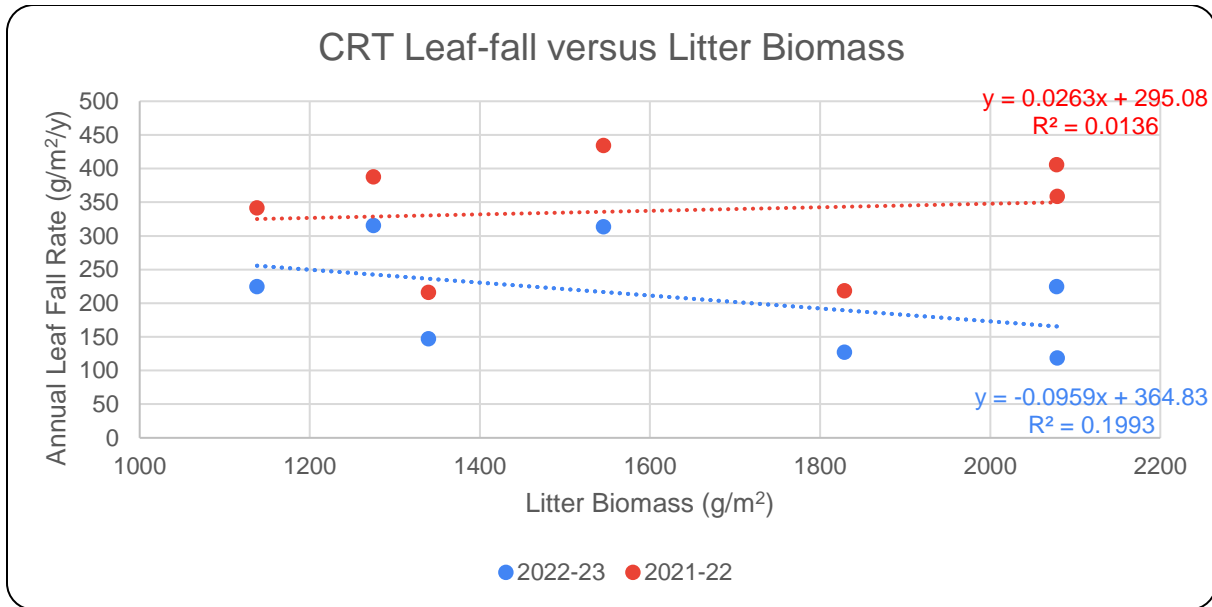
Figure 35: The regression between litter biomass and annual leaf-fall rate for CRT by plot in 2022–23 (red) and 2021–22 (blue). Litter biomass was measured in 2021.

Figure 36 shows leaf-fall rates in the conifer (Creeping Juniper) portion of the alvar. The interannual difference of 42.5 g/m^2/y represents a 63% *increase* between the two collection years. Error bars represent the maximum and minimum of the six samples collected.
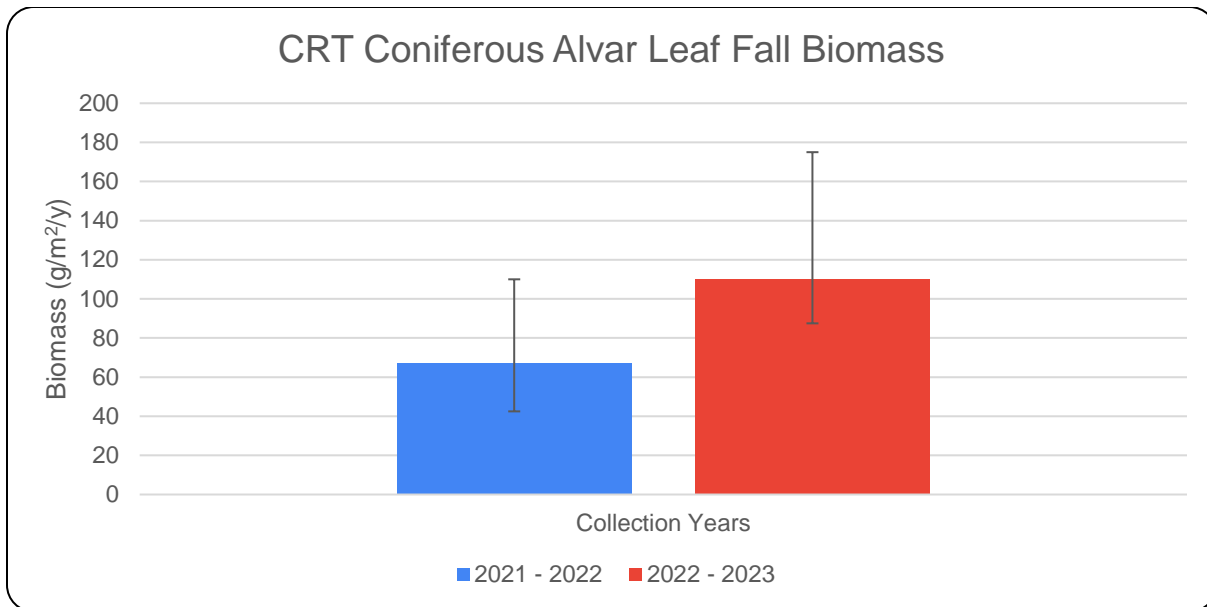
Figure 36: Annual coniferous leaf-fall rates (g/m^2/y) from CRT Alvar plot of Creeping Juniper over two full collection years. Leaf fall traps are described in methodology section.

Table 14 shows the variability of coniferous alvar leaf-fall from the two study years.

Table 14: Annual coniferous alvar (Creeping Juniper) leaf-fall for two years

Coniferous Alvar	Leaf Fall kg/ha/y
2021–2022	675
2022–2023	1100

It is also noteworthy that the factors that may be responsible for interannual variations in leaf-fall seem to differ between coniferous trees and the Creeping Juniper, given that they responded in opposite direction over the two years.

Field litter puck flux measurements were taken in triplicate and all three readings were used to formulate the figures and tables below. The reason for taking triplicate readings was reduce the likelihood that a single outlier would have an uninterpretable impact on the analysis. With three readings, distinguishing a false reading is made much easier by the internal consistency in values from the same sample taken in rapid succession.

The respiration from litter decomposition is shown in Figure 37. The average litter puck flux at CRT shows a gradual decrease by approximately 34% from plot B to E (Figure 37). Plots B and C represent transitional forest zone between the deciduous alvar and the coniferous forest. However, the litter sampled in plots B and C came from directly beneath the forest canopy portions of the plots. Within the transitional zones, the predominant tree species was Eastern White Cedar (Figure 16 &17).

Plots D through H were classified as completely forested plots and contain an increasing proportion of Red and White Pine and Balsam Fir (Figure 16 & 17). ANOVA test showed no significant differences in litter R_h between plots ($P > 0.05$).

Figure 37 shows the mean flux for all samples of litter was 1.1 µmol/m^2/s. The lowest average litter flux occurred at plot E while the highest average litter flux occurred at plot B. The one-way ANOVA showed no significant difference between litter R_h and plot. Simple regressions for flux (Y) against biomass (g/m^2), air temperature, H_2O range and GMC showed only temperature ($P < 0.001***$) having a significant effect on the CO_2 flux as $R_h = -0.034x + 1.72$ ($R^2 = 0.13$).
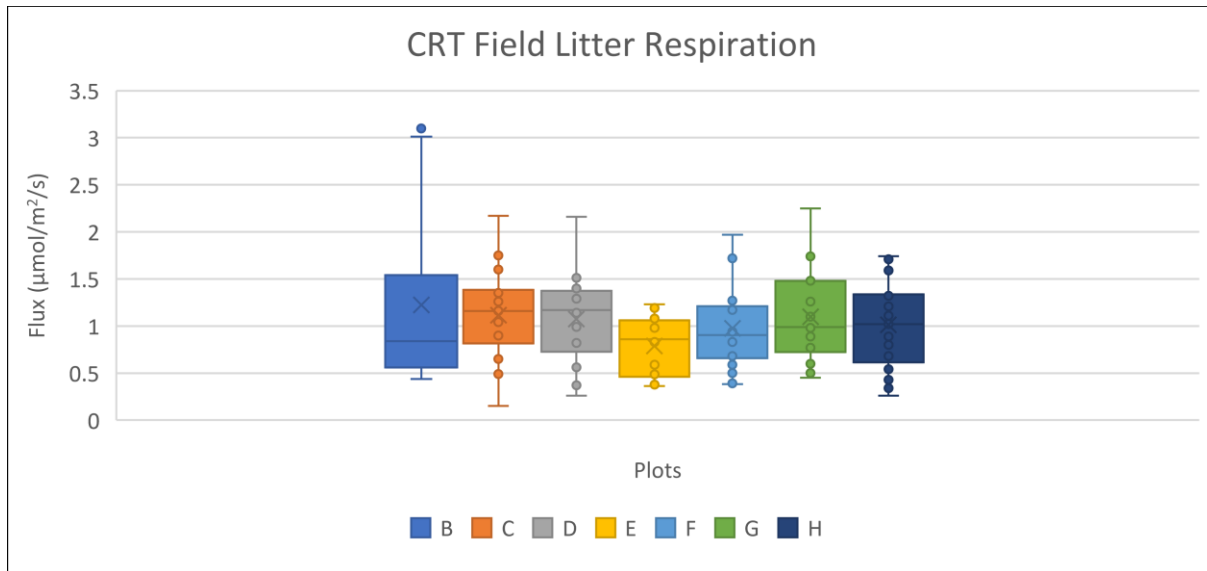
Figure 37: The total litter flux (µmol/m^2/s) values for field litter pucks at Crane River Tract from June 6, 2022, to October 14, 2022. Seven plots were measured at CRT each with $N = 18$.

The corresponding litter biomass and its decline over the summer while in the field is shown in Table 15. A regression was done to examine if the respiration rate was related to litter biomass within the sample at the start of the experiment and it showed a P-value > 0.05, indicating a lack of relationship between the independent variable of litter biomass and the dependant variable of respiration rate, at CRT. The R^2 for the regression was 0.001. The smallest and largest change in biomass occurred at plot C and H respectively with a difference of 637 g/m^2 biomass change between the two plots. The initial biomass was highest in plot H and lowest in plot G. There is a significant difference ($P < 0.05$) between the R_h fluxes for field litter pucks between HB and CRT.

Table 15: Biomass (g/m^2) for the in-field litter pucks at CRT from June 7, 2022, to November 28, 2022. The average initial and final biomass have a difference of 11%. Asterisks represent pucks with possible tears to the nylon fabric which possibly lost some biomass.

CRT Plot	Initial Biomass (g/m^2)	Final Biomass (g/m^2)	Change in Biomass (g/m^2)
B	3045	2599	- 446
C	2713	2650	- 64
D*	2904	2548	- 357
E	2471	2217	- 255
F	2764	2586	- 178
G	2255	2102	- 153
H*	3236	2535	- 701
AVERAGE	**2770**	**2462**	**- 308**

Table 15 show the average difference between the initial and final biomass is -11%. Plot C had the least amount of change in biomass with a -3% difference while plot H had the greatest decline in biomass at -21%.

Under controlled lab conditions, the effect of temperature and moisture on the litter respiration were examined. The samples collected from each plot used identical litter as that used for the field litter pucks and samples contained the same litter biomass. This experiment took place over 4 days within a 12–14h measurement period each day.

In this section on laboratory experiments, triplicate readings were taken but only the third reading was utilized due to a buildup of CO_2 within the samples while stored in sealed bags between sets of readings. This was detected as a systematic decline in the flux over three 60 second intervals after the readings commenced for all samples. Bags were to preserve as much moisture as possible between the sample run times in the growth chamber while temperatures were changing. This would control for the effects of variations in moisture due to drying out. This procedure did not anticipate the buildup and lack of natural ventilation for CO_2 resulting from decomposition within the bag. This had the effect of increasing the CO_2 gradient between internal and ambient concentrations which accelerated the rate of gas loss when first exposed to ambient conditions. The excess amount of CO_2 in the puck is released over the initial two 60 second ventilation periods, and equilibrium is assumed to be reestablished for the third reading.

Over the entire temperature range (5–25°C) the lowest CRT fluxes emerge from plot G while the highest fluxes emerge from plot E.

Figure 38 shows the litter respiration in the lab averaged 4.68 µmol/m^2/s which is approximately 4× larger than the field fluxes. Litter from plot E respires maximally while the lowest average litter flux occurs in plot G. Samples from E and C have large flux data distribution compared to other samples.
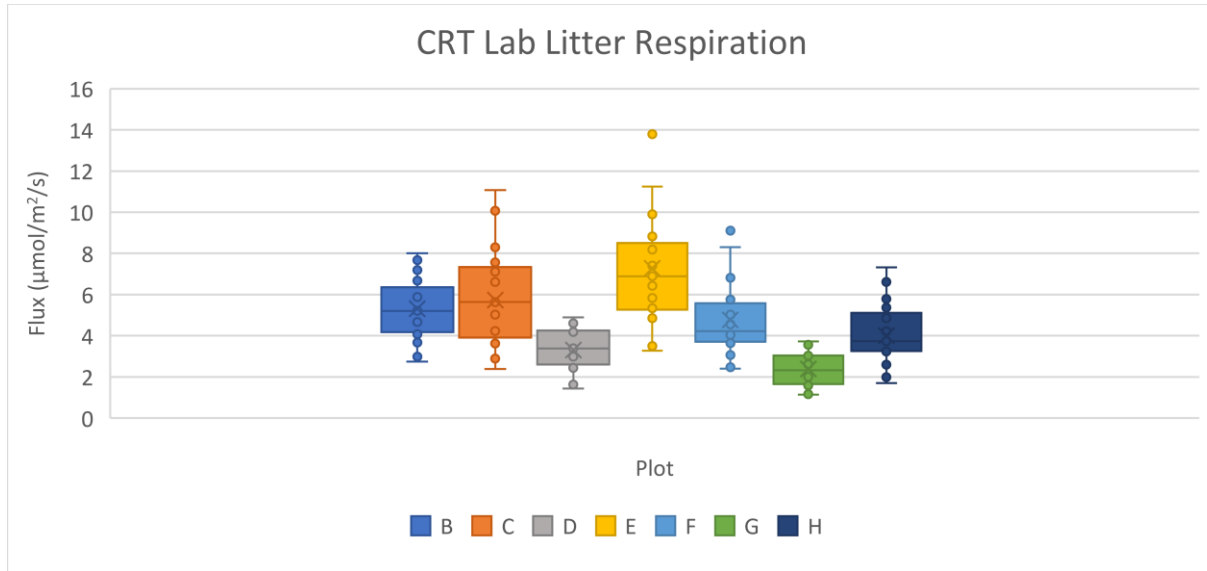
Figure 38: The litter flux (µmol/m^2/s) from growth chamber litter pucks from the Crane River Tract over the entire temperature range of 5°C to 25°C and moisture range of 0.5 to 2 GMC from June 6, 2022, to October 14, 2022.

Table 16 shows the simple regression equations. The result show none of the P values holding significance and extremely low R^2 values with the lowest P value and R^2 values belonging to sample biomass.

Table 16: Statistics for CRT lab litter respiration experiments including regression equations, R^2, *P*-value, N, and correlation coefficient (R). The simple regression is CO_2 flux against litter biomass, GMC, T chamber and H20 range.

Flux Simple Regression	Regression Equation	R^2	*P*-Value	N	Correlation Coefficient
Biomass (g/m^2)	y= 0.001x + 1.739	0.02	0.10	175	0.13
GMC	y= - 0.084x + 4.803	0.00	0.87	175	-0.01
T chamber(^{0}C)	y= - 0.030x + 5.221	0.01	0.25	175	-0.09
H20 Range (mmol)	y= - 0.017x + 4.802	0.00	0.69	175	-0.03

Table 17 shows Plot E has the highest average flux while plot G has the lowest average flux. However, while plot G does have the lowest biomass out of all the plots, plot E does not have the highest biomass. Plot E has the second lowest biomass. Plot D has the highest biomass.

Table 17: The average flux (μmol/m^2/s) and biomass (g/m^2) for the growth chamber litter pucks.

Plot	Average Flux (μmol/m^2/s)	Biomass (g/m^2)
B	5.32	2713
C	5.74	2738
D	3.31	2949
E	7.28	2499
F	4.77	2524
G	2.39	2098
H	4.00	2770

Figure 39 a,b,c,d,e, shows that at all temperatures, the litter from Plot E consistently has the highest flux while plot G is consistently the litter with the lowest flux. Although the flux differences between samples becomes exaggerated as temperatures increase, regressions show biomass was not significant in determining flux variability ($P > 0.05$).
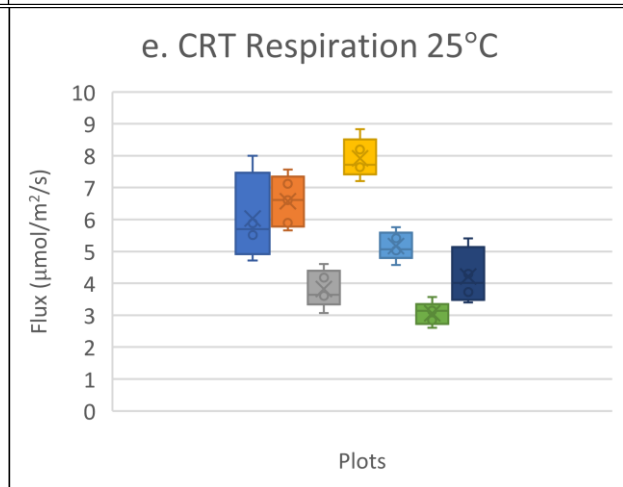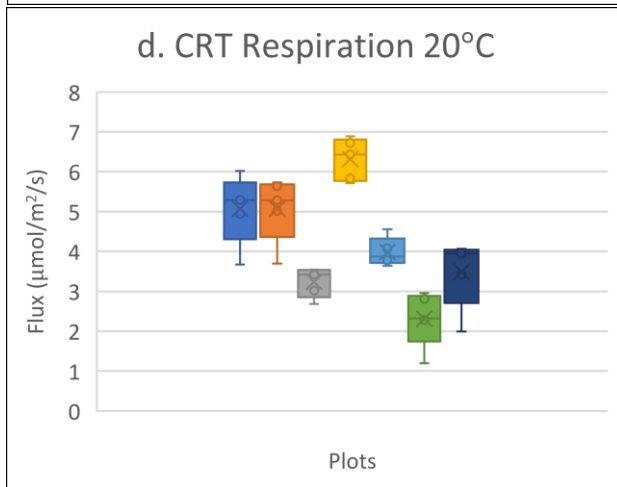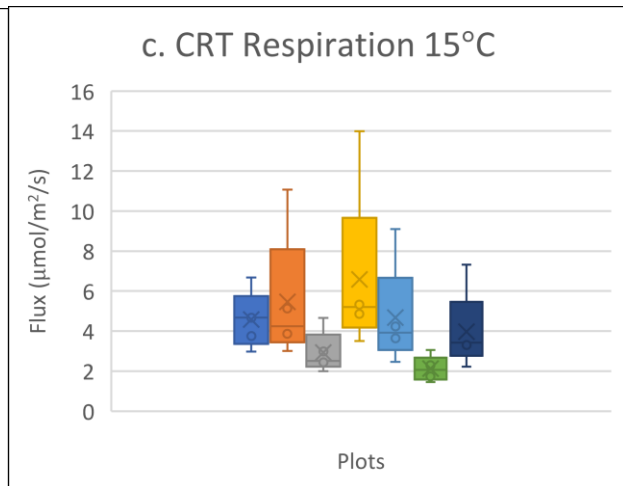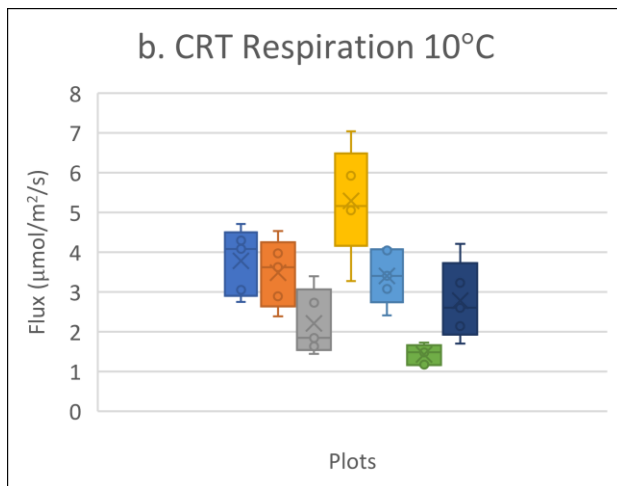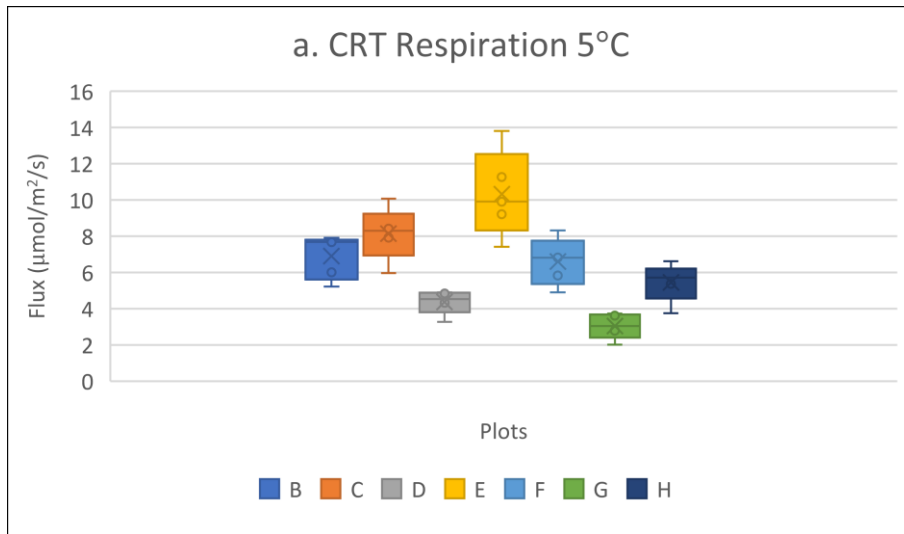
Figure 39 a,b,c,d,e: Mean growth chamber CRT litter respiration (μmol/m²/s) at 5, 10, 15, 20, 25°C, respectively over the entire moisture range.

Figure 40 a,b,c,d,e, shows how manipulating moisture content affected litter respiration. Plot E has the highest flux at each GMC measurement while plot G has the lowest respiration in each GMC measurement. The GMC values at which the experiment was conducted are mean (1.10), maximum (1.52), minimum (0.25), median (0.75) and mode (0.84). These values were derived by taking the average GMC per plot B–H from the field litter pucks over the growing season and calculating the total GMC mean, median, mode, max and min from plots B–H. It appears that the flux differences between samples are reduced at the highest moisture levels experienced in the field and become exaggerated at the driest moisture levels experienced in the field. But again, regressions between the fluxes and sample biomass did not yield significant relationships.
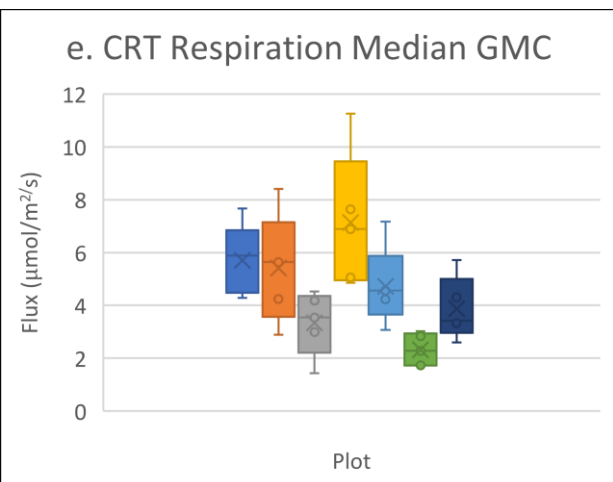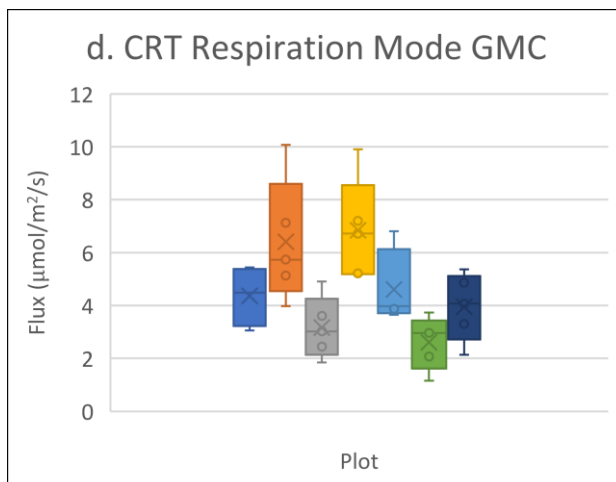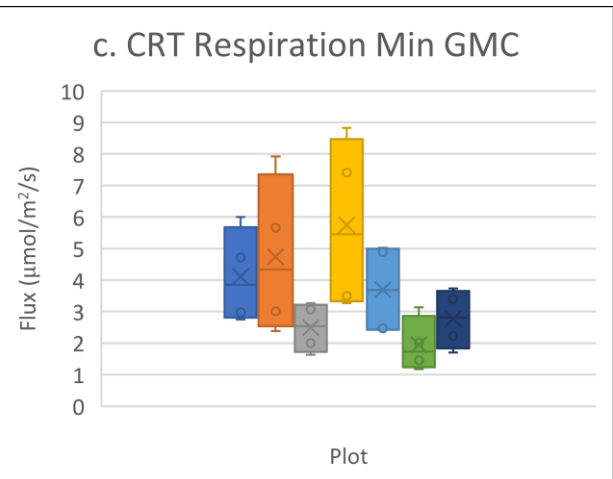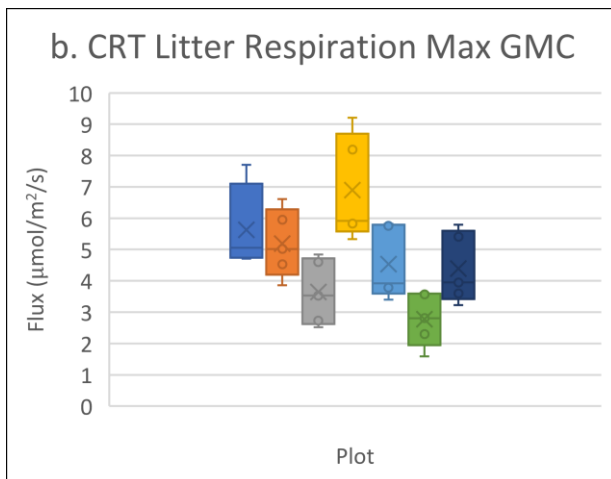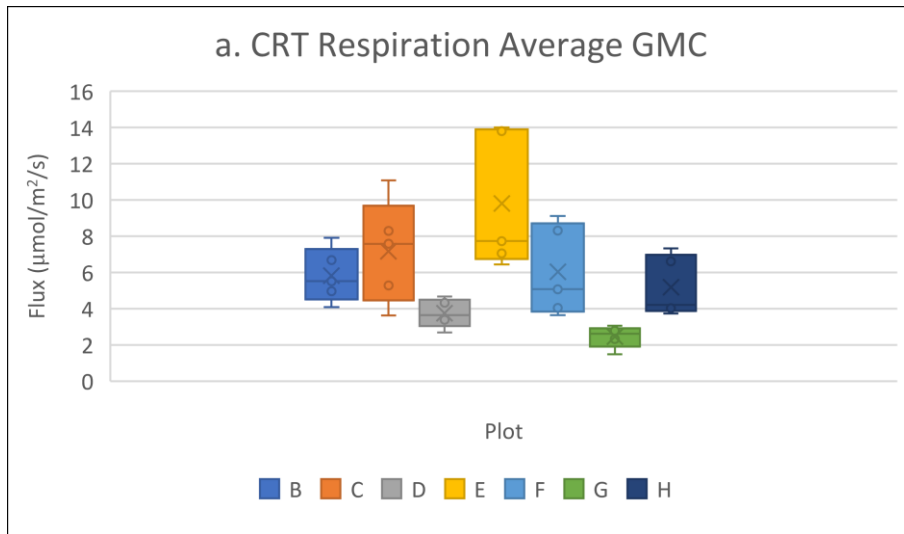
Figure 40 a,b,c,d,e: Growth chamber CRT litter respiration (µmol/m²/s) at Average, Maximum, Minimum, Mode and Median GMC, respectively, averaged over the entire temperature range.

Figure 41 shows four large peaks of soil C% and N% at (35,10)A, (60,10)A, (115,10)A and (140,10)A. The N% is typically higher than the C% at CRT for the same coordinates.
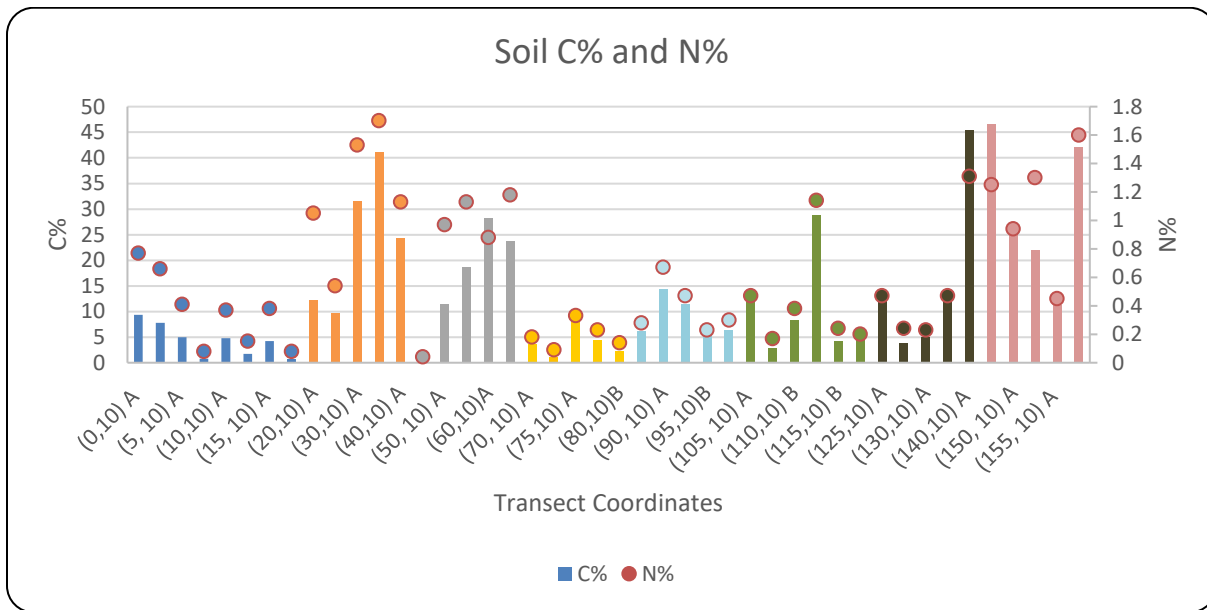
Figure 41: Sample soil carbon (C% - bars) and nitrogen (N% - circles) percentages that are present at CRT from (0,10) to (0,160). Samples were extracted at 5m intervals and include both A and B horizons. Each color represents a different plot with dark blue representing the deciduous alvar plot, orange plot B, grey plot C, yellow plot D, light blue plot E, green plot F, black plot G and pink plot H.

Figure 42 shows the soil C% and N% averages per plot at CRT with the lowest percentage of carbon found in the deciduous alvar and the highest amount in plot H which contained an abundance of Balsam Fir and dead snags. Plot B and H have the highest N%.

Table 18 shows the N%, C% and CN ratio across three difference landscape environments along with the standard deviation and coefficient of variation. T-tests between deciduous alvar and coniferous alvar show no significant difference between the two sets of CN ratio data. Coniferous alvar and coniferous forest show no significant difference ($P > 0.05$) between the two sets of CN ratio data. Deciduous alvar and coniferous forest, show a highly significant difference ($P < 0.05$) between the two sets of CN ratio data.
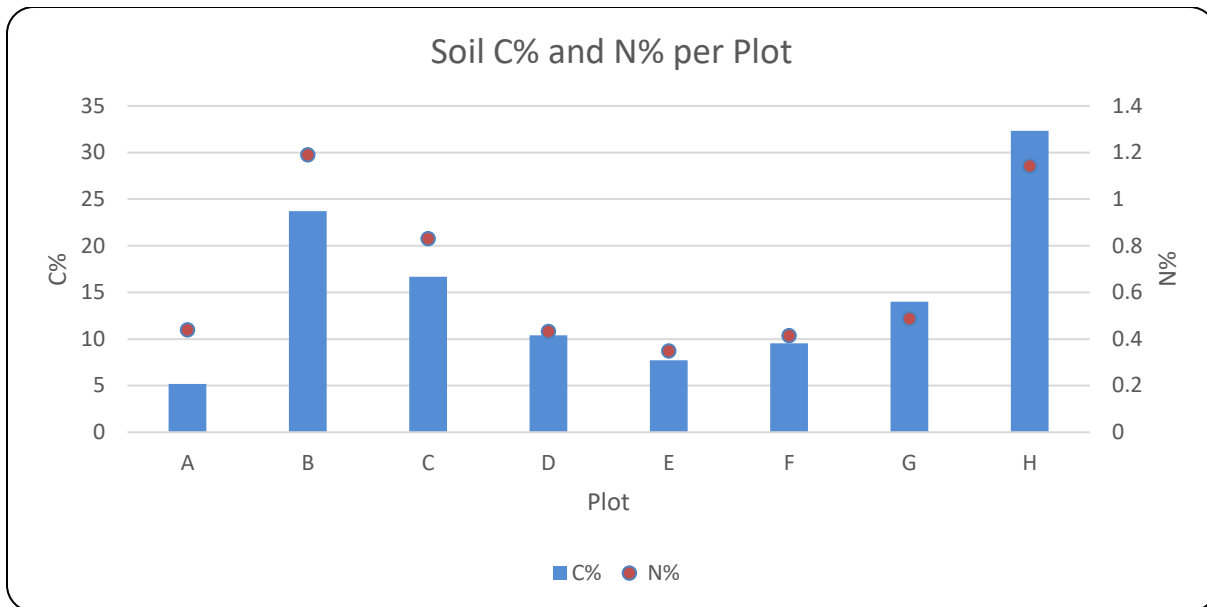
Figure 42: The average soil carbon C% and nitrogen N% for each of the CRT plots. Plot A represents deciduous alvar while B–H represents coniferous forest.

Table 18: The average, standard deviation and coefficient of variation for soil N%, C% and CN ratio for deciduous/coniferous alvar and coniferous forest at CRT. Only coniferous forest and deciduous alvar differed significantly for C% (P < 0.01) and CN ratio (P < 0.001).

	Deciduous Alvar			Coniferous Alvar			Coniferous Forest		
	N %	C %	CN ratio	N %	C %	CN ratio	N %	C %	CN ratio
Mean	0.58	6.47	13.42	0.64	9.35	18.50	0.66	15.41	23.50
SD	0.58	5.97	1.87	0.57	7.2	11.90	0.49	13.25	7.94
CV	1	0.92	0.14	0.89	0.77	0.64	0.74	0.86	0.34

Figure 43 shows the regression between C% and N%. Most forest points are clustered towards the bottom left-hand corner with lower C% and N%. The forest values are equally distributed about the best-fit line, the alvar values are consistently distributed below the best-fit line.

The CN ratio shows (Figure 44) a gradual increase from alvar to transitional zones through to fully forested plots. Average CN ratios for plot A are 13.3, plot B 22.3, plot C 23.9, plot D 24.4, plot E 25.1, plot F 24.9, plot G 29.1, and plot H 32.7. There are large peaks in the CN ratios (Figure 41) at (60,10)A, (75,10)A, and (145,10)A. The deciduous alvar plot ranges from (0, 10) to (20, 10) and the CN values are approximately 48% smaller than coniferous forest CN values. The average CN ratio for CRT coniferous forest is 23.5. For deciduous alvar, 13.4. Figures 43 shows a significant difference ($P < 0.05$)

between the CN ratio of the deciduous alvar plot A and the coniferous forest plots B–H. It shows general trend of increasing CN ratio from plots B–H.
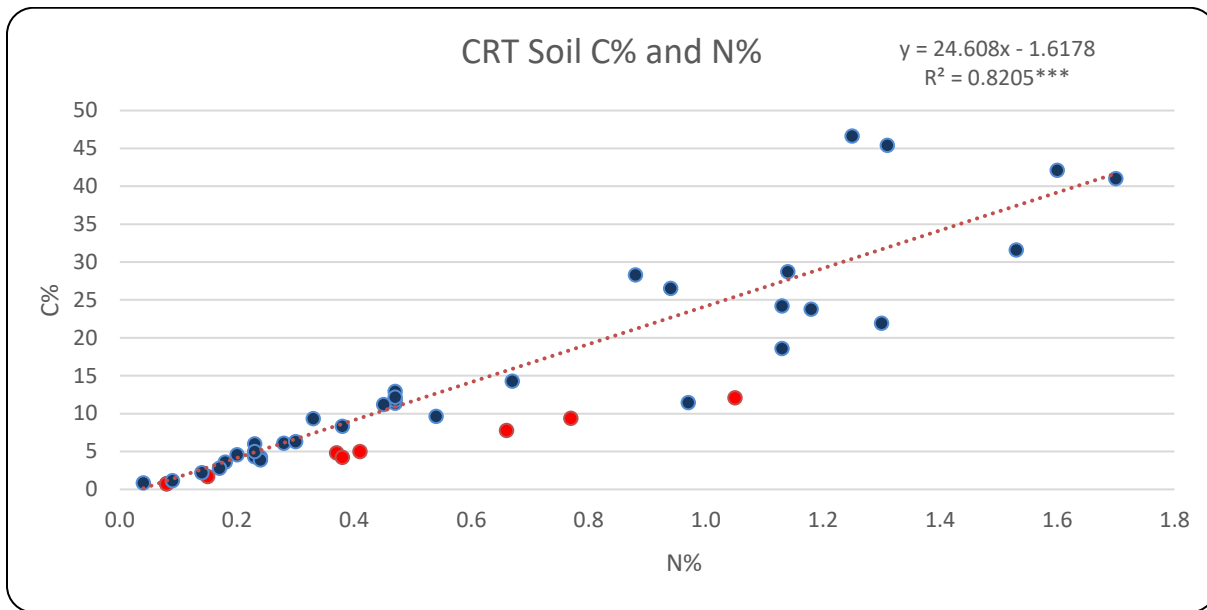
Figure 43: Regression of carbon (%) to nitrogen (%) across the center of the study transects from (20,10) to (0,160) with measurements at 5m intervals. The coniferous forest values are black while deciduous alvar values are red. R^2 value applies to all the data and not just the forest values.
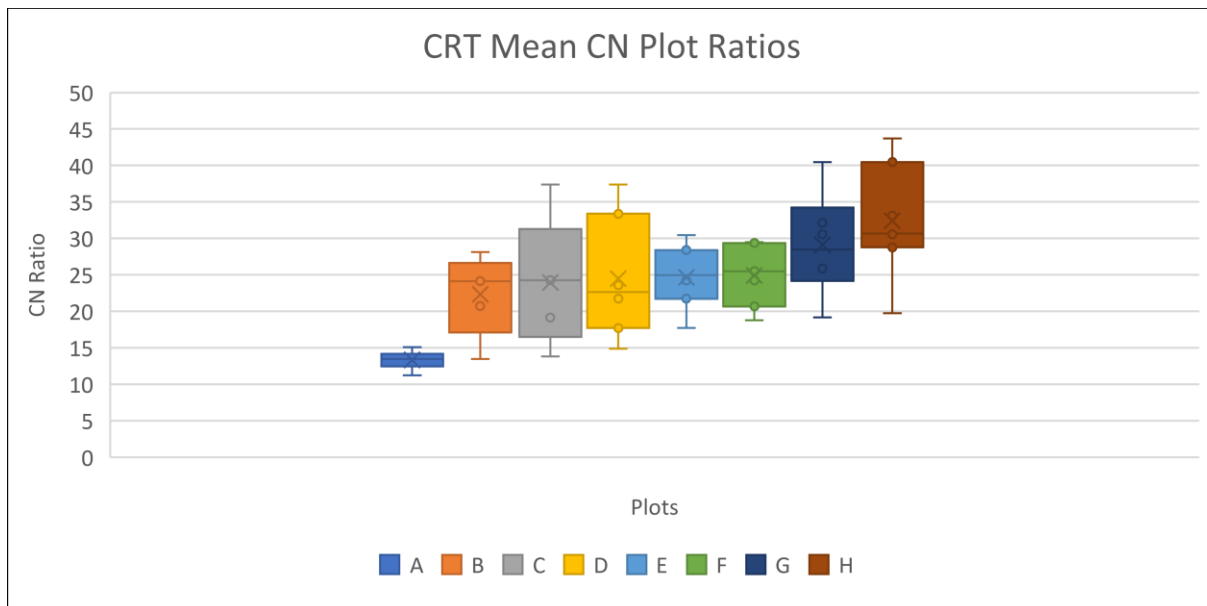
Figure 44: Box and whisker diagram showing the CN ratio at each of the CRT plots. Plot A is deciduous alvar while plots B–H are coniferous forest.

Within the coniferous alvar, Figure 45 shows there is a general increase in C% with N% ($P < 0.05$) with one outlier. The slope of the regression equation suggests the Creeping Juniper CN ratio averages approximately 10.18. By comparison in Figure 46, the mean CN ratio in the deciduous alvar is 10.92.

C and N Concentrations in Coniferious Alvar

$y = 10.921x + 2.3238$
$R^2 = 0.751*$
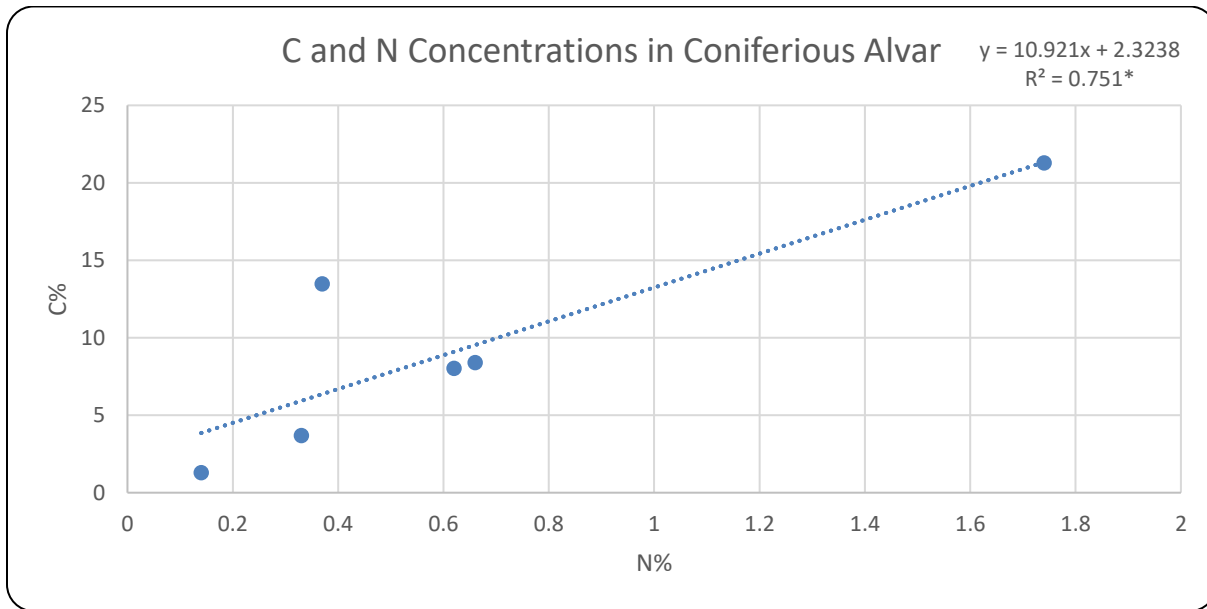
Figure 45: C and N concentrations of soil in the coniferous alvar plot for A and B horizons.

Figure 46 shows that the changes in soil C% are strongly correlated with the changes in soil N% in the deciduous alvar. The average CN ratio for CRT deciduous alvar is 13.4. There is no significant difference between CN ratios in coniferous and deciduous alvar.
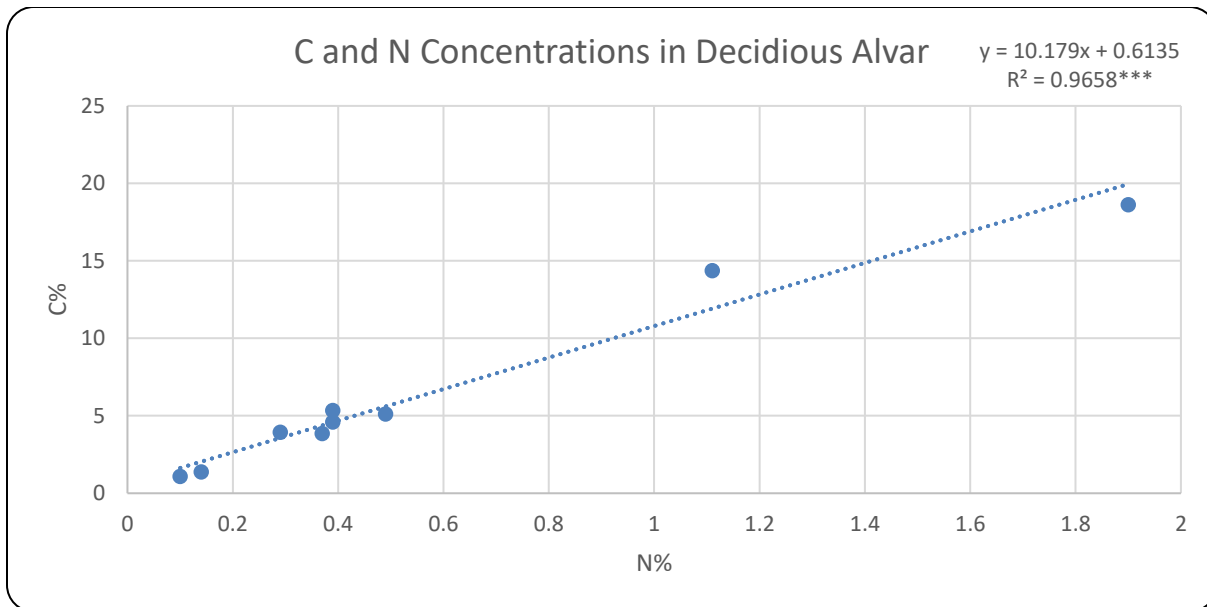
Figure 46: CN ratios of soil in the deciduous alvar plot for A and B horizons.
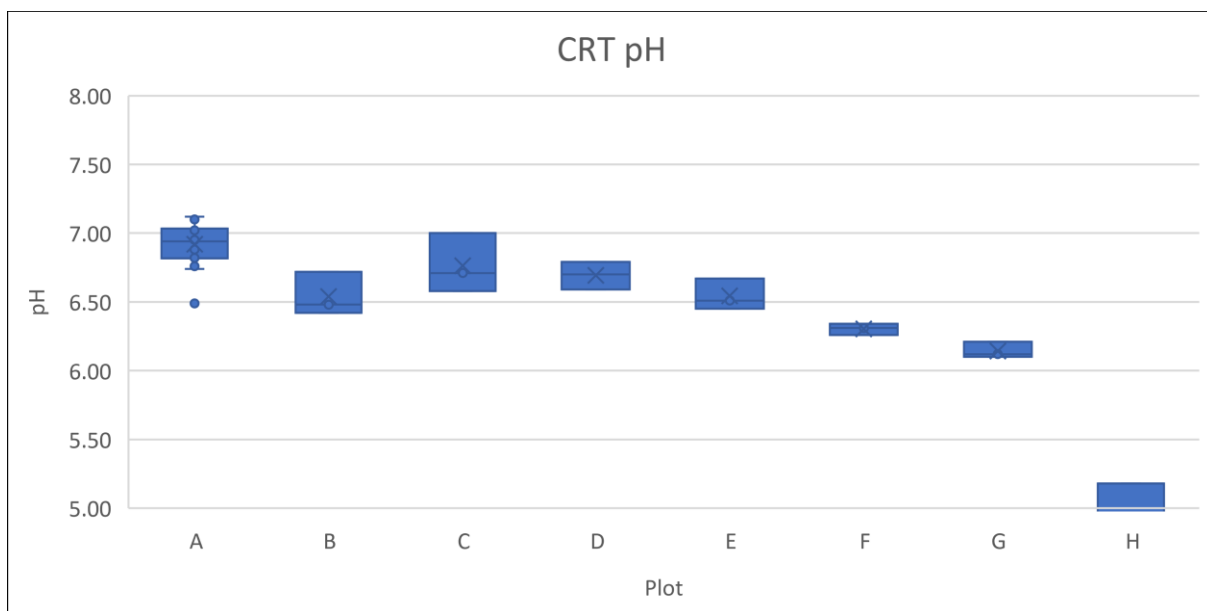
Figure 47: pH for all eight plots at CRT measured from the top 5 cm of soil.

The pH patterns at CRT show a steady decrease from plots A through G and a sudden drop in pH at plot H.

3.2.2 – Hay Bay Dynamics

Figure 48 shows the heterotrophic respiration flux at Hay Bay during 2022. The overall R_h average is 2.07 (µmol/m^2/s). R_a was not measured in 2022. Figure 49 shows the Hay Bay fluxes during 2021 when R_a was measured.
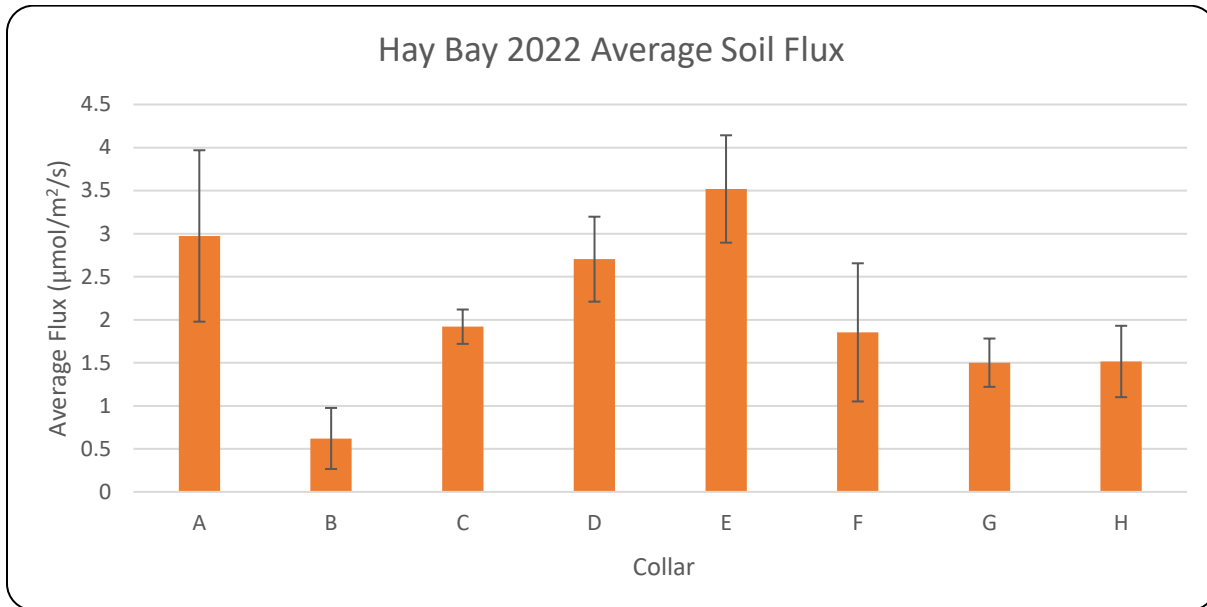
Figure 48: Average time series fluxes (µmol/m^2/s) for Hay Bay dead-root collars measuring R_h. Flux data from April 10th, 2022 – November 28th, 2022 (N = 14619). Error bars represent ±1 standard deviation.
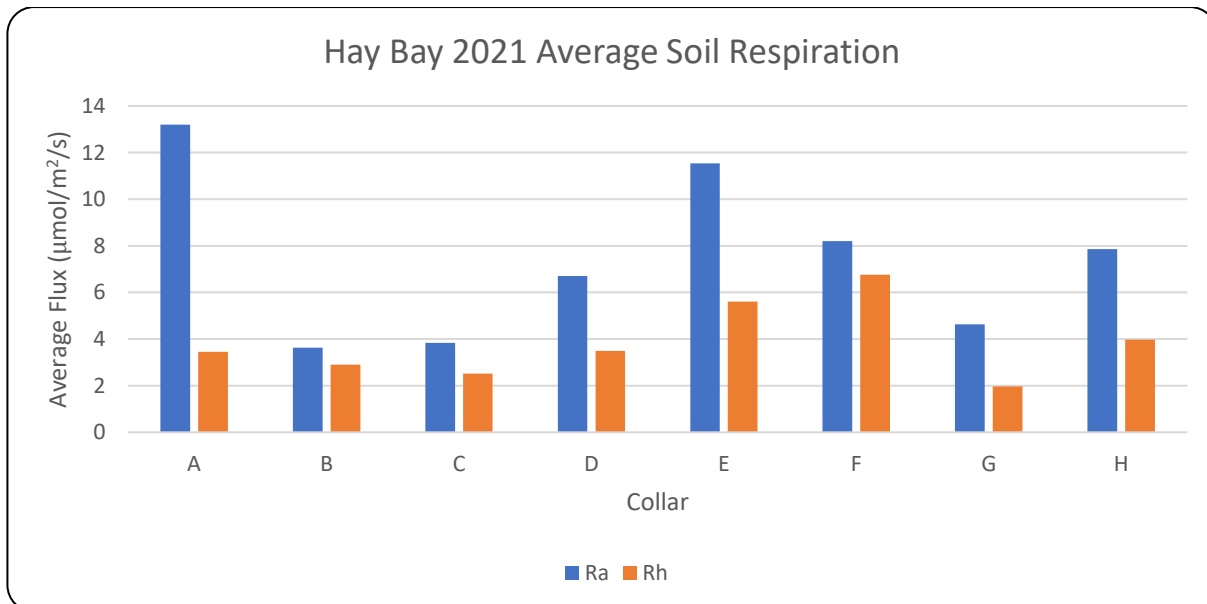
Figure 49: Average time series fluxes (µmol/m^2/s) for Hay Bay living collars (Rt) and dead collars (R_h) in 2021. Total soil flux average is 7.5 (µmol/m^2/s) for all eight locations. Total heterotrophic average is 3.8 (µmol/m^2/s). Flux data from June 1st, 2021 – October 12th, 2021.

Interesting to note that in Figure 48 and Figure 49, HB 2021 (R_t) and HB 2022 (R_h) fluxes show similar patterns in which collar A has the highest (or second highest) flux, followed by an oscillating pattern of gradually increasing fluxes up to collar E, and a gradual decrease in flux until collar H.

Figure 50 shows the averages for the time series fluxes for R_a and R_h at Hay Bay in 2020. Most of the fluxes remain between 4 and 6 μmol/m²/s with the notable exceptions of collar E, and collar G, which are locations where root respiration dominates over microbial respiration. In the case of E, it appears this is due to an unusually large R_a whereas at G this appears to be due to an unusually small R_h.
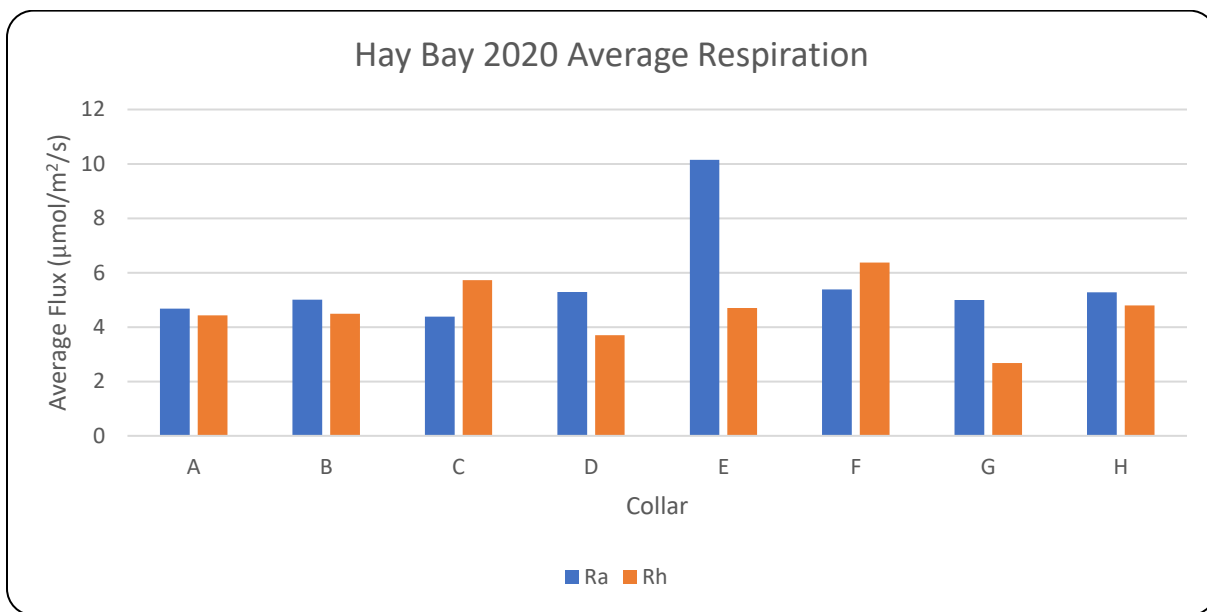
Figure 50: Average time series fluxes (μmol/m²/s) for Hay Bay living collars (R_t) and dead collars (R_h) in 2020. Overall living (R_t) average is 5.6 μmol/m²/s and R_h (dead-root) average is 4.61 μmol/m²/s).

Figure 51 shows the annual leaf-fall at Hay Bay over the course of three years. On average, 2022–23 had the lowest leaf-fall while 2021–22 had the highest. Leaf fall also varies with location.
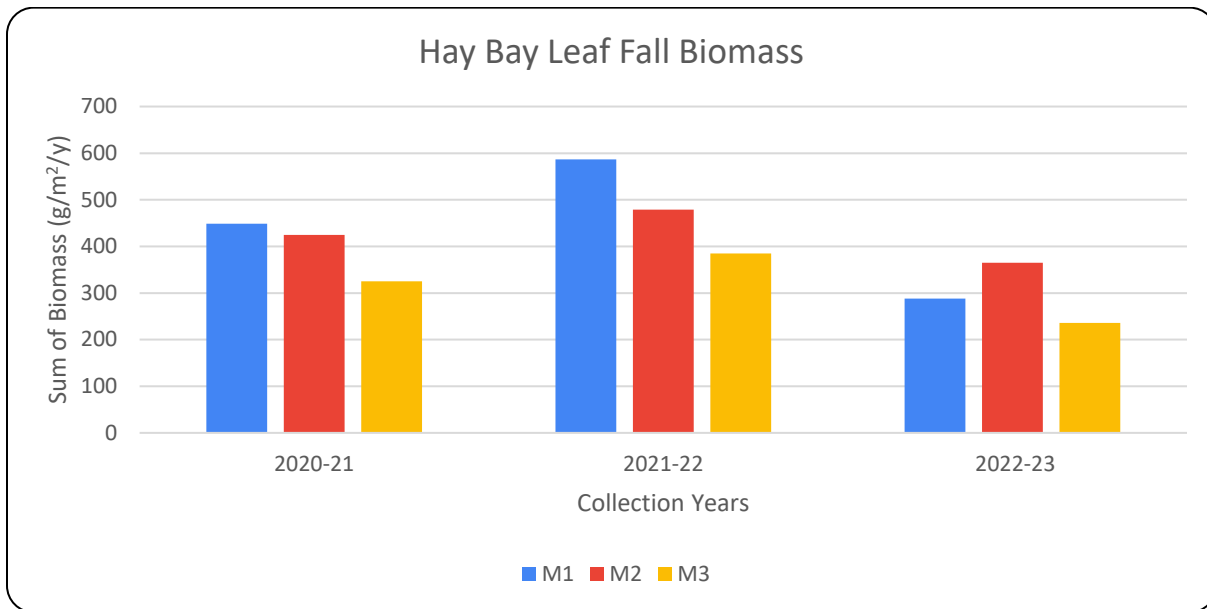
Figure 51: Sum of annual leaf-fall biomass ($g/m^2/y$) at Hay Bay over the course of three full collection years at sub-sites M1, M2, M3.

Table 19 shows there is large year to year leaf-fall variability in leaf-fall between the collection years. The difference between the average leaf-fall for 2021–22 (highest) and 2022–23(lowest) represents a 34.7% difference.

Table 19: Hay Bay leaf-fall at M1, M2, M3 sites for three years.

Hay Bay Leaf Fall	2020–21 (g/m^2)	2021–22 (g/m^2)	2022–23 (g/m^2)
M1	449	587	305
M2	425	479	393
M3	325	385	250
Average	400	484	316

Figure 52 shows the average in situ R_h litter flux is highest at collar D, followed by collar G. The arithmetic average field litter flux for the entire Hay Bay site over the 2022 sampling period is 0.81 $\mu mol/m^2/s$. Collar H has the lowest average flux. The mean overall flux is 0.81 $\mu mol/m^2/s$. ANOVA test does not show a significant difference between the collar means ($P > 0.05$). Simple regressions for flux (Y) against biomass (g/m^2), temperature, evaporation (mmol/s) and GMC showed only biomass ($P < 0.05*$) and temperature ($P < 0.05***$) having a significant effect on flux rates.
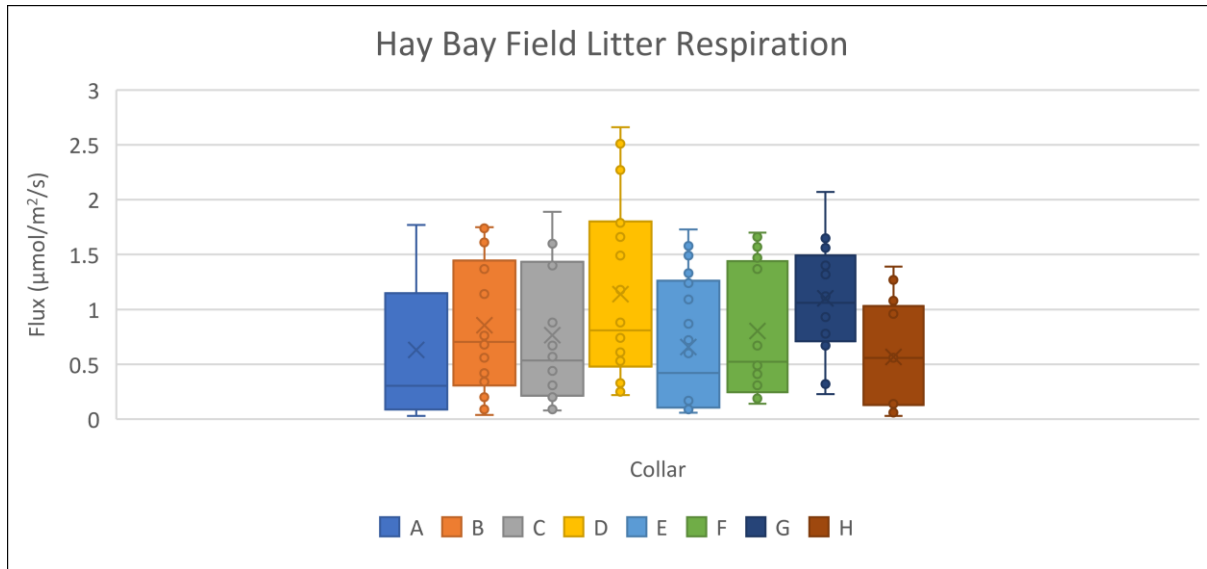
Figure 52: The measured litter flux (N = 21, $\mu mol/m^2/s$) from in situ field litter pucks at Hay Bay from June 6, 2022, to August 15, 2022. Eight sample locations were measured at Hay Bay within a 7×7m sub-plot, M2.

Table 20 shows the average decline in litter biomass at Hay Bay is -11.4% from June 7th, 2022, to November 28th ,2022. The collar with the smallest change in biomass is collar F (less than 1%) while the largest change in biomass comes from collar A with -44.5% difference between initial and final biomass. Collar A values are suspect since some parts of the nylon stocking were damaged, which could have resulted in loss of litter biomass. With this anomaly removed, the average decline of litter biomass in the field was 107 g/m^2 or -8%.

Table 20: Biomass (g/m^2) for the in-situ litter pucks at HB from June 7, 2022, to November 28, 2022. The average initial and final biomass show a difference of 11.4%. Asterisks represent pucks with possible tears to the nylon fabric that possibly lost some biomass.

HB Collar	Initial Biomass (g/m^2)	Final Biomass (g/m^2)	Change in Biomass (g/m^2)
A*	1057	586	- 471
B	1083	981	- 102
C	1146	1057	- 89
D	1873	1732	- 140
E	1045	879	- 166
F	1618	1605	- 13
G	1783	1694	- 89
H	1121	968	- 153
AVERAGE	1341	1188	- 153

At HB, the lowest fluxes emerge from collar A while the highest fluxes emerge from collar G, averaged over all of temperature treatments. Figure 53 shows the flux pattern gradually increases from collar B–G and decreases dramatically at collar H. There was no alvar at HB and all of the litter pucks and flux collars were in a single 20×20 m plot.
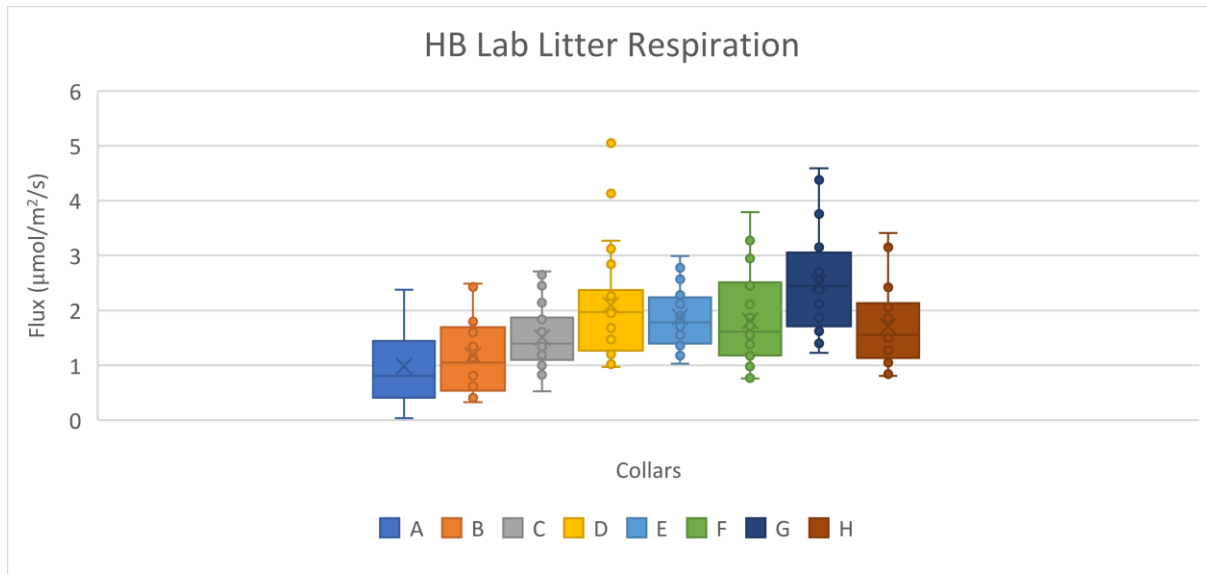
Figure 53: The total litter R_h flux ($\mu mol/m^2/s$) values for growth chamber litter pucks at Hay Bay from January 12–18, 2023. Eight collars were situated within a single 20×20 m plot at Hay Bay.

In contrast to the lab litter experiments from Crane River Tract, Table 21 for the Hay Bay lab litter experiments show all four factors having a significant effect on R_h flux with biomass and GMC being the most significant and temperature being the least significant.

Table 21: Statistical analysis showing the regression of R_h litter flux against biomass, GMC, Tchamber and H20 range at HB.

Flux Simple Regression	Regression Equation	R^2	Statistical Significance	N	Correlation Coefficient
Biomass (g/m²)	y=0.001x + 0.675	0.25	***	200	0.50
GMC	y= 0.991x + 0.659	0.25	***	200	0.50
Tchamber	y= 0.032x + 1.141	0.06	***	200	0.25
H20 Range	y= 0.101x + 1.051	0.21	***	200	0.46

Table 22: The average R_h flux (μmol/m²/s) and biomass (g/m²) for the growth chamber litter pucks at HB from January 12–18 2023.

Collar	Average Flux (μmol/m²/s)	Biomass (g/m²)
A	0.98	898
B	1.18	1114
C	1.51	1091
D	2.10	1754
E	1.88	1015
F	1.81	1563
G	2.50	1614
H	1.72	1133

The average flux as shown in Table 22, is highest at collar G while the average biomass is highest at collar D – followed closely by collar G. The total average flux for all collars is 1.71 μmol/m²/s. The lowest flux and biomass occur at collar A. Figure 54 (a,b,c,d,e) show D as the collar with the largest flux range while G has the highest average flux. The lowest average flux comes from collar A. Generally, fluxes are higher from all locations as temperatures increase.

The differences in the fluxes under different moisture treatments are shown in Figure 55 (a,b,c,d,e). Again, the lowest litter moisture contents appear to exaggerate the flux differences with location compared to when the samples are the wettest.
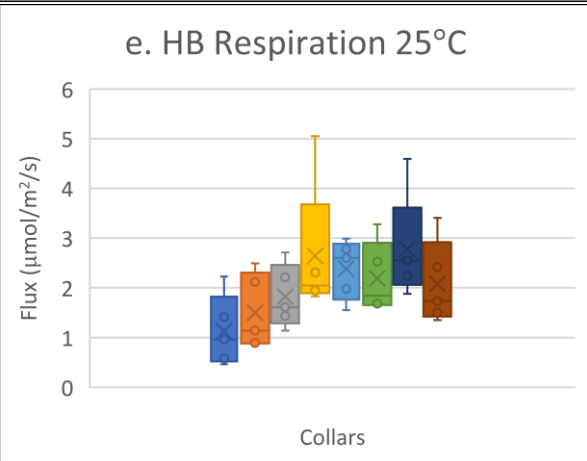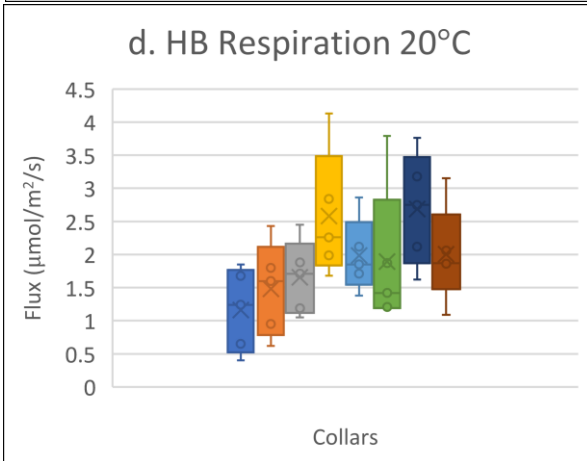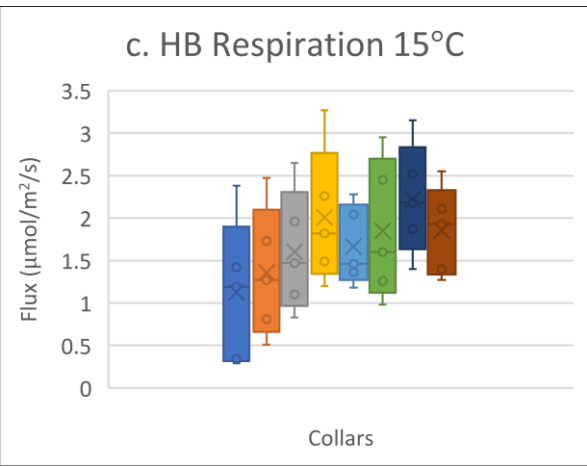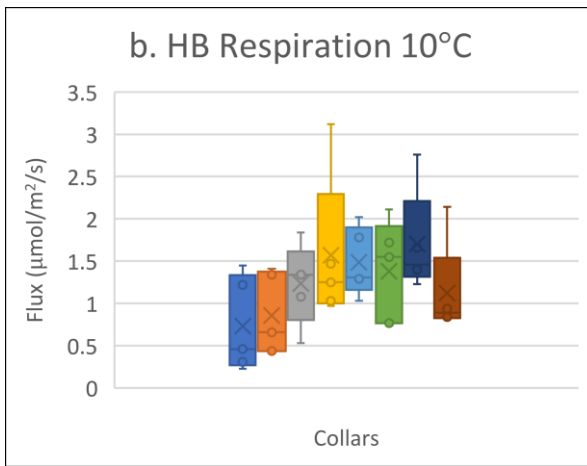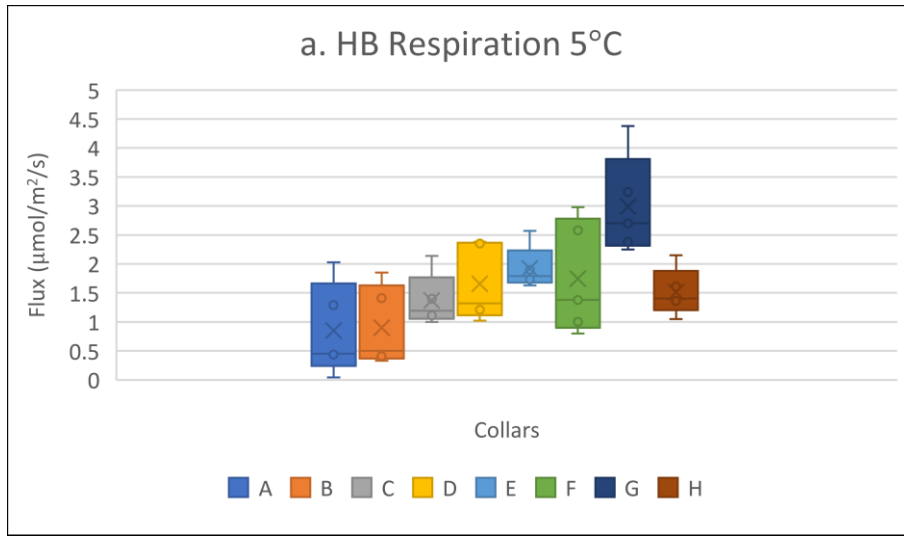
Figure 54 a, b, c, d, e: Growth chamber HB litter respiration ($\mu mol/m^2/s$) at 5, 10, 15, 20, 25°C, respectively.
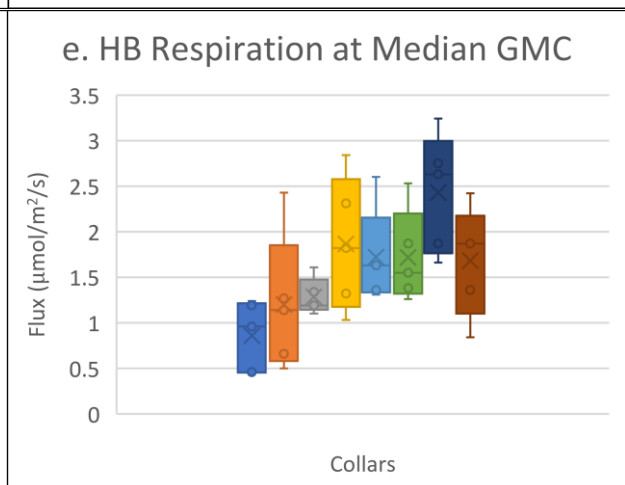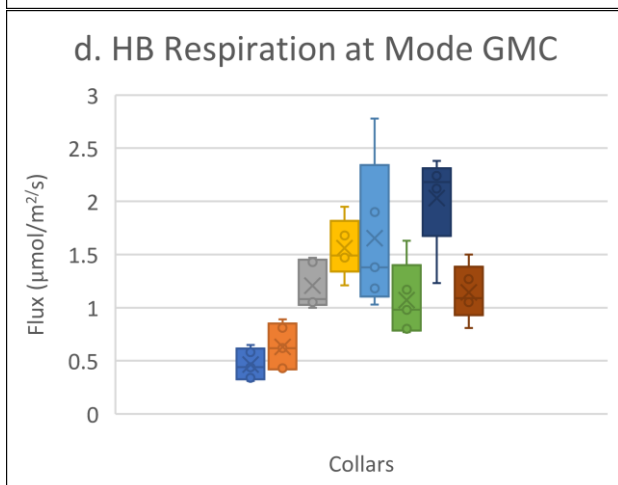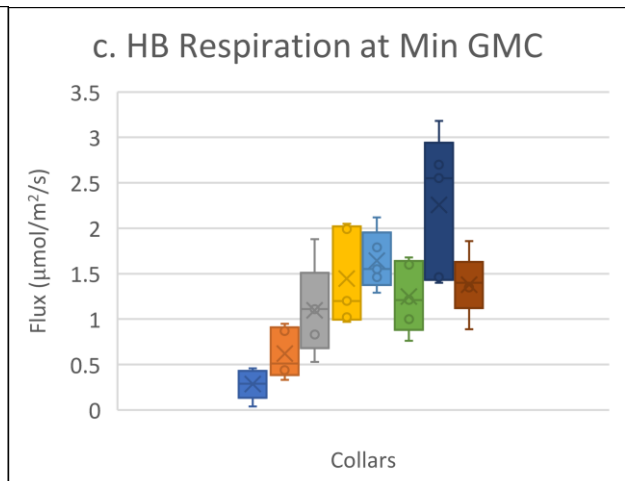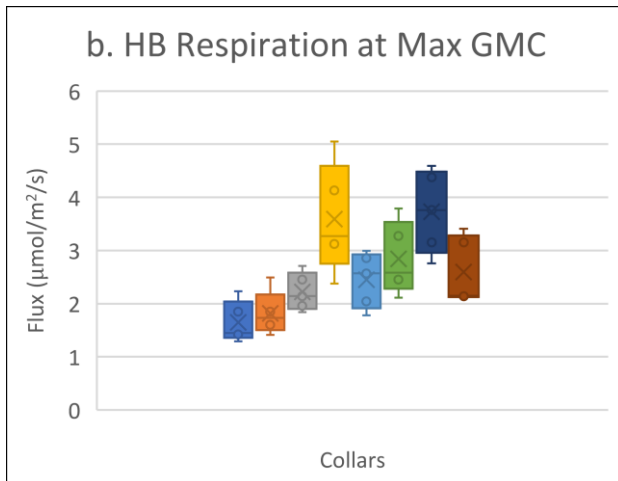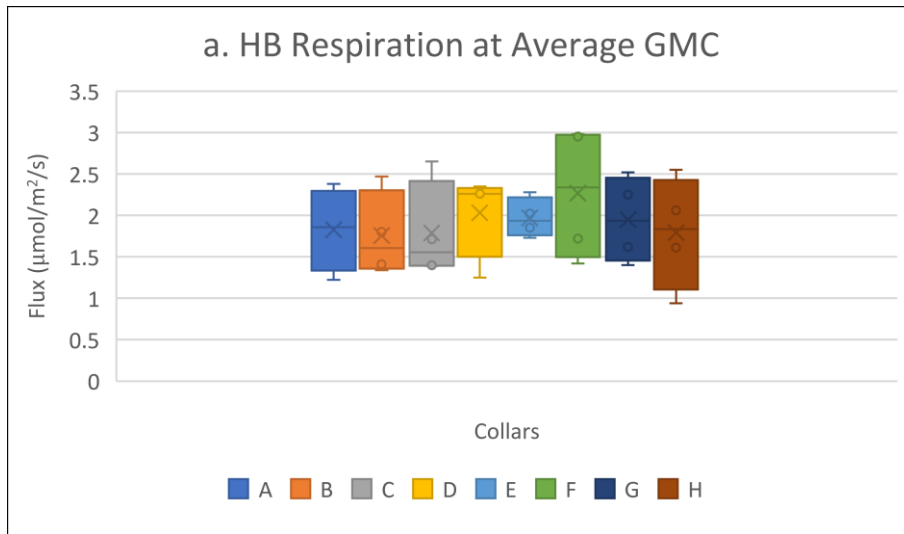
Figure 55 a,b,c,d,e: Growth chamber HB litter respiration flux ($\mu mol/m^2/s$) at Average, Maximum, Minimum, Mode and Median moisture contents, respectively.

3.3 – Carbon Budget

The soil carbon budget is described in equation (1). The annual inputs are leaf-fall and root growth and the incorporation of deadwood into the soil profile. The output is soil respiration via heterotrophic decomposition. The change in storage $\Delta C/\Delta t$ kg[C]/m²/y is positive when the soil is accumulating carbon and negative when the soil is losing carbon. When gains balance losses and the change in storage is zero the soil is in a steady state. The residence time for soil carbon is how many years a carbon atom spends in the soil reservoir before moving to a different pool and can be inferred from the size of a carbon pool relative to the inputs or outputs under conditions of steady state, inputs would equal outputs.

Table 23 summarizes the magnitude of the carbon pools, and Table 24 summarizes the component annual carbon fluxes and the carbon budget for the soil and ecosystems examined in this thesis. An explanation of how each of the values were obtained then follows.

Table 23: Carbon pool summary table of CRT forest, HB forest, CRT deciduous alvar and CRT coniferous alvar.

Summary of Carbon Pools (kg[C]/m²)				
	CRT Forest	HB Forest	CRT Deciduous Alvar	CRT Coniferous Alvar
Foliage	0.92	1.22	0.06	0.51
Branches	1.33	1.56		
Bark	0.74	0.79		
Stems	5.26	5.17	0.06	0.70
Roots (structural)	2.06	2.18		
Roots(fine)	0.15	0.29		
Total Living Biomass	10.47	11.22	0.12	1.21
Litter	0.79	0.69	0.38	1.34
Deadwood	0.36	0.49		
Soil	6.47	9.09	6.55	2.38

For both the forest at Crane River Tract and at Hay Bay, the allometric equations of Lambert et al. (2005) were applied to each tree and then expressed per unit area of the plot they were growing in and averaged for each location. The foliage estimates and stem estimates for the alvars at CRT were based on

assays of foliage stripped from the aboveground plants and averaged. The structural root biomass in the forests was based on allometric estimates based on total living biomass (assumed 80% aboveground and 20% belowground). Fine root biomass was based on the empirical relationships of Chen et al. (2004) for Pine and Fir (which differed little) utilizing the mean basal tree diameter in each plot, stem density for each plot and mean annual temperature. Litter biomass is based on assays of forest litter collected from each plot in alvar and forest, then averaged. Deadwood biomass is based on assays of deadwood biomass on the forest floor within each plot combined with deadwood biomass of all snags within each plot, then averaged. The carbon fraction of all vegetation biomass is 0.5. Soil carbon is based on soil core assays for each layer using Equation (2). Carbon fractions were assumed to be 50% for the soil organic fractions determined by loss-on-ignition for each horizon of each soil core.

Table 24: Annual carbon flux summary table of CRT forest, HB forest, CRT deciduous alvar and CRT coniferous alvar. Green is soil carbon gains; orange is below-ground carbon loss, brown is annual change in storage of the soil, vegetation and ecosystem. Terms in italics are dependent on modeled satellite determinations of photosynthesis (GPP). BGDOM and AGDOM represent the contributions to the soil pool of belowground dead organic matter and aboveground dead organic matter, respectively.

Table 24 Summary of Annual Soil Carbon Fluxes (kg[C]/m^2/y)				
Carbon Fluxes (kg[C]/m^2/y)	CRT Forest	HB Forest	CRT Deciduous Alvar	CRT Coniferous Alvar
Leaf-fall	0.10	0.19	0.07	0.04
BGDOM	0.04	0.04		
AGDOM	0.07	0.07		
Root Turnover Inputs (fine)	0.10	0.13		
Total Soil C Inputs	0.30	0.43		
Heterotrophic Soil Respiration (Rh)	0.58	0.50	0.40	0.35
Soil Carbon Budget (ΔC)	**-0.28**	**-0.07**		
Root Respiration (Ra)	0.54	0.47		
Total Soil Respiration (Rt)	1.12	0.97	0.40	0.35
Gross Vegetation C Uptake (GPP)	*1.29*	*1.29*		
Gross Ecosystem C Uptake (GEP)	*1.29*	*1.29*		
Net Ecosystem CO2 Uptake (NEP)	*0.33*	*0.54*		
Ecosystem Respiration (RE)	*0.68*	*0.68*		
Net Vegetation C Uptake (NPP)	*0.61*	*0.61*		

The inputs to the soil carbon budget in Table 24 are shown in green. Leaf-fall was based on two-year average leaf-fall collected at CRT and three-year leaf-fall collected at HB. Inputs of belowground dead organic matter (BGDOM) follow Kurz and Apps (1999) scaled to 2% of the belowground structural root biomass. Inputs of aboveground dead organic matter (AGDOM) was scaled to 0.68% of aboveground stems and 2% of aboveground bark (Kurz and Apps, 1999), with the assumption that deadwood biomass is presently in steady state. Structural annual root growth was assumed to remain at 20% of total tree growth, NPP (He at al., 2018; Murphy & Moore, 2010). Total tree growth for CRT was obtained from 20-year average GPP obtained by Achidago (2023) for a 5×5 km plot of 90% coniferous forest adjacent to the experimental site using satellite-based chlorophyl fluorescence Light Use Efficiency (LUE) models (1.29 kg[C]/m^2/y). GPP was multiplied by 0.47 (Waring et al., 1998) to obtain forest NPP (0.61 kg[C]/m^2/y}. Achidago's analysis showed that forest productivity had not changed significantly between 2000 and 2020 and therefore would apply to the study period. There were no data from Achidago (2023) for GPP at Hay Bay, so the same annual GPP and NPP values were applied to the coniferous forest there. The annual inputs of fine root carbon follow Chen et al. (2004) based on estimated fine root biomass (from Table 23) and empirical relationships for annual fine root turnover rates employing annual temperature and stand age.

The annual soil carbon respiratory losses, R_h (Table 24; orange) were calculated by binning all the measured time series R_h fluxes at 5^{0}C intervals between temperatures of 0, 5, 10, 15, 20, 25 and 30°C, to create a regression equation where X was the mean temperature and Y was the flux at the median temperature. Monthly mean fluxes were generated using mean monthly temperatures from the Tobermory RCS weather station and then combined to produce annual fluxes. Binning the fluxes within temperature intervals has the advantage of reducing noise in the data and of making it easier to manage and more cohesive to analyze for annual averages given that February and March were months when very little data was collected from any of the habitats while in other months some habitats are overrepresented by field measurements relative to others.

Table 25: The regression equations used to estimate monthly R_h for the two forests and two alvars using monthly mean air temperatures. *N* = 31804.

BINNED SITE 2022–23	REGRESSION EQUATION	R^2
HB Coniferous Forest	y=0.1173x + 0.5778	0.97
CRT Coniferous Forest	y=0.0653x + 1.1146	0.96
CRT Coniferous Alvar	y=0.0591x + 0.5398	0.78
CRT Deciduous Alvar	y=0.0357x + 0.8338	0.96

From Table 25, the CRT coniferous forest has the highest flux (1.11 μmol/m^2/s) when air temperatures are at the freezing point, when X=0. When X=10, the largest flux is still CRT coniferous forest. However, at air temperatures of 20^{0}C, the Hay Bay coniferous forest has the largest flux because it shows the highest sensitivity to temperature (0.1173 μmol/m^2/s/^{0}C) which is 80% greater than its CRT counterpart.

On an annual basis, by employing all the inputs and outputs to the soil carbon budget in Table 24, it is estimated that the soil at CRT remains in a negative annual balance with -0.28 kg[C]/m^2/y and the soil at Hay Bay has a slightly negative annual balance of -0.07 kg[C]/m^2/y.

For forests where there is no understory, GPP equals gross productivity of the trees, and 47% of this is retained and 53% is released as autotrophic respiration. NPP is equivalent to 0.61 kg[C]/m^2/y (Table 24). When combined with ΔC in the soil of -0.28 kg[C]/m^2/y, the CRT ecosystem as a whole is sequestering carbon annually at a rate of 0.61 - 0.28 = 0.33 kg[C]/m^2/y, the gross ecosystem productivity, GEP. At HB the corresponding vegetation and soil C budgets sum to 0.54 kg[C]/m^2/y.

Unfortunately, there is little research on alvar roots and proportional make up of total alvar SOC and Achidago's work examined GPP of forests over 20 years, not alvars. Therefore, the effects of adding roots to the leaf-fall input for both coniferous and deciduous alvar carbon budgets at the CRT were not available. There is a lack of research done on alvar roots and alvar GPP.

4.0 – Discussion

This chapter will focus on the interpretation and comparison of the results to other studies done in the scientific community. A 2×2 matrix comparing the Hay Bay coniferous forest, CRT coniferous forest, CRT coniferous alvar and CRT deciduous alvar, is used in this discussion.

Table 26: The 2×2 matrix comparing Hay Bay coniferous forest, Crane River Tract coniferous forest, CRT coniferous alvar and CRT deciduous alvar for organizing the Discussion chapter.

HB Coniferous Forest	CRT Coniferous Forest
CRT Coniferous Alvar	CRT Deciduous Alvar

4.1 – Carbon Pools

Comparing the forest (HB and CRT) carbon pools in Figure 13 & 26, they are very similar. The litter pool is slightly larger at CRT (5%) compared to HB (3%). Lower amounts of litter can occur even when AGB is higher in HB than CRT, suggesting a faster litter turnover rate in HB compared to CRT.

There is an absence of an understory pool at both CRT and HB (Figure 11) due to the large canopy preventing sunlight from reaching the forest floor and the thick layer of needle litter biomass covering the ground – both factors inhibit understory growth. The total living biomass at CRT is highest in plots D–H as those plots are forested plots while A is alvar, B and C are transitional zones between forest and alvar. While most of the CRT plots have an almost 50:50 ratio of soil to aboveground biomass pool size, plot A and G are unique. The size of plot A aboveground biomass is almost non-existent when compared to the rest of the plots due to the lack of trees in the alvar. Plot G has a soil to above ground biomass ratio of 40:60, suggesting it has the greatest amount of aboveground biomass across all of the plots (Figure 12, Figure 15). In the alvars, the sizes of carbon pools vary between the coniferous and deciduous alvars with soil carbon comprising 49% and 94% of coniferous and deciduous alvar total pool size, respectively. Much of the deciduous alvar aboveground biomass senesces on an annual basis and deciduous leaves decompose faster than coniferous leaves. The carbon held in the AGB and litter is transported to the deciduous alvar soil carbon pool at a faster rate than the coniferous alvar. The coniferous alvar have similar total pool percentage sizes in terms of litter and AGB at 27% and 24% respectively, and the carbon pools are of similar sizes compared to the deciduous alvar pools due to the phenological differences between deciduous species and coniferous species, including but not limited to, a higher surface area to volume ratio in leaves, the time and percentage of foliage senescence, the waxy compounds and higher lignin content present in coniferous species. All these factors, alongside abiotic factors such as temperature and moisture regimes, can inhibit speed of decomposition and the transference of carbon from one pool to the next.

4.1.1 – Aboveground Biomass Pool

The average aboveground biomass (AGB) pool at CRT Coniferous Forest and HB Coniferous Forest are 61762 and 86523 kg[C]/ha, respectively. There is a 29% difference between the study sites. With the inclusion of coarse root biomass these values increase to 77203 and 108154 kg[C]/ha of living tree carbon. The Puric-Mladenovic estimates (Figure 4) for living carbon, which also include coarse roots, at the two sites are 190000–220000 kg[C]/ha and 29000–140000 kg[C]/ha respectively. These are 2.46–2.85 times larger than those measured at Crane River Tract and 27%–129% of those measured at Hay Bay, respectively. There are several differences in methodology that might contribute to these

differences. The field studies are stand specific whereas the remote sensing-based estimates are for larger tiles which invariably include non-forest surface cover. The calibration of the algorithms converting reflectance to living biomass were developed in forests elsewhere in southern Ontario and applied to the Northern Bruce Peninsula. But oddly the map suggests the forests at Hay Bay and Crane River Tract occupy the extremes in living carbon storage in the Northern Bruce Peninsula whereas the allometric formulas used for this study suggest that the biomass of both forests is rather similar, and somewhere in between the extremes shown in Figure 4.

The species composition varies between the two sites with HB comprised of Eastern White Cedar and CRT comprised of Eastern White Cedar, Red Pine, Balsam Fir, White Pine, White Spruce, Larch, Birch, and Poplar. Studies have shown differences in carbon content per tree species with average tree C content for hybrid Poplar (239 kg[C]), Red Oak (139 kg[C]), Black Walnut (132 kg[C]), Norway Spruce (114 kg[C]), and Eastern White Cedar (146 kg[C]) (Wotherspoon et al., 2014). The annual carbon assimilation rate of Eastern White Cedar is 0.65 t[C]/ha/year – approximately 650 kg[C]/ha/year – while hybrid Poplar has an annual carbon assimilation rate of 1.06 t[C]/ha/year (1060 kg[C]/ha/year) (Wotherspoon et al., 2014). This shows the difference of carbon assimilation and average carbon content per tree, between different tree species with fast growing, deciduous species sequestering almost twice the amount of carbon compared to slower growing coniferous species. The amount of carbon stored in the tree itself varies between species as well. Comparing plots B and H of CRT, the amount of AGB at plot B is higher than H even though plot H had more stems/hectare (Figure 12 & 16). The Balsam Firs make up approximately 2500 stems/ha at plot H but have the lowest average biomass for wood biomass, branch, bark and foliage biomass for all CRT plots, due to the age of the tree. Most Balsam Firs were 2–4 meters tall and there were a lot of standing dead snags. Plot H had the highest number of dead snags per hectare (Figure 16, Figure 17). Balsam Firs are shade tolerant; when a tree falls, sunlight can penetrate the canopy and hit closer to the forest floor where all the Balsam Fir saplings reside. The canopy gap benefits Balsam Firs and allows them to take advantage of it by increasing growth, causing a large proportion of stem frequency at plot H to be small Balsam Firs. Average tree diameter shows plot H, where all the Balsam Firs are, with a DBH of 9 cm while other plots range from 17.3–23.7 cm DBH (Figure 18).

Even though the Balsam Firs were the most numerous, they did not contain the highest biomass in plot H. Red Pines contained over half the tree biomass at plot H while the predominant tree biomass at other plots were Eastern White Cedar. The shift from Cedar to Red Pine could be a result of growing

conditions as Red Pine does not tolerate flooding while White Cedars are flood tolerant. The alvar region floods from winter meltwater in the spring and the waters reach up to plot D. The occurrence of Red Pine, both species frequency and biomass, starts to increase from plot E–H, suggesting that these plots are not waterlogged during some months of the year. White Spruce, another species that prefer well drained soils, start increasing biomass and stem frequency from plot D–H. There is a variation of aboveground biomass from plots B–H at CRT with plot G (120–140 m) containing the largest AGB while plot C (40–60m) contains the smallest AGB. The majority of AGB in each of the seven forest plots at CRT is stored within the woody stem followed by branches, bark and foliage. Woody biomass at plot G is greater than the woody biomass in the rest of the plots. While plot G has the greatest AGB, plot H has the highest stem density with approximately 3500 stems per hectare when scaled up: over twice that of the rest of the CRT plots. However, most of the stems at plot H were comprised of small Balsam Firs with a diameter at breast height (DBH) of <10 cm. Smaller trees in higher frequency of occurrence yields a lower biomass than large trees with a lower occurrence frequency. The species distribution at CRT varies based on plot while the HB is almost entirely comprised of Eastern White Cedar. Over half of the tree species at plot H are Balsam Fir and Cedars only make up 14% of the tree species distribution compared to a 65% Cedar species composition at plot E which had the second highest AGB after plot G.

In a coniferous Scots pine forest, the total aboveground biomass was 152.1 Mg/ha (76050 kg[C]/ha) and the leaf biomass was 7.0 Mg/ha (3500 kg[C]/ha) (Santa Regina, 2001). The AGB falls within the CRT and HB AGB pools. The average aboveground biomass pool at CRT Coniferous alvar and CRT Deciduous alvar are 11932 and 565 kg[C]/ha, respectively. One of the reasons for this large difference is the presence of woody biomass at the coniferous alvar and the lack of it in the deciduous alvar. Wood biomass is, proportionally, the largest contributor to AGB, in comparison to branches, bark and leaves. The predominant species at the coniferous alvar is Creeping Juniper which has a woody stem and branches containing high amounts of lignin, compared to the predominance of grasses at the deciduous alvar site that contain no woody biomass and very little lignin. Grass foliage dies on an annual basis and cannot store AGB over a period of multiple years. Deciduous AGB has an annual maximum while coniferous AGB has no annual maximum and can continue to accumulate AGB on a yearly basis. Both coniferous and deciduous alvars are much smaller than the CRT coniferous forest AGB which is smaller than the HB coniferous forest AGB. The HB site had three subsites (M1, M2, M3) with M2 having the largest AGB at 108787 kg[C]/ha – a 37% increase compared to M1 and M3 (Table 11). All of the soil flux collars and data collection were located in M2. The large difference of AGB in M2 could indicate the plot as having more stems per hectare or a greater amount of wood and leaf biomass.

AGB at CRT did not comprise only fully forested plots. There was a finger of forest that branched out into the alvar and low lying, grassy rock formation around the finger did not contain any trees. Plot B and C contained some areas of the transitional zone between alvar and forest. There was 50% less living aboveground biomass (kg/ha) at plots B and C in comparison to plots D–H. When compared to the amount of AGB at HB, the transitional zones at CRT brought down the average AGB. Age also plays a factor in the amount of AGB produced. A younger stand would have less AGB than an older stand with stands <2 years containing 1.4 t/ha AGB (700 kg[C]/ha) and stands >75 years containing 202 t/ha AGB (101000 kg[C]/ha) (Wang et al., 1996). Increased stand age correlates to an increase in biomass allocation to the woody stem tissue while the majority of nutrients (N, Ca, K, Mg, P) accumulated in leaves. Nutrients in AGB are generally allocated to the following areas in descending order: leaf > branch > stem branch > stem wood (Wang et al., 1996).

4.1.2 – Litter and Deadwood Pool

The litter pool is the repository of all of the litter that has fallen and has not yet decomposed. Mean CRT Forest litter averages 7898 kg[C]/ha which is 12.7% larger than the HB forest litter at 6889 kg[C]/ha. One of the reasons for this is that the aboveground biomass pool at HB is larger than the AGB at CRT by 28.6%. Since the main input to the litter pool is AGB biomass, the higher values of AGB at HB allows for a larger mass of litter fall to occur. There is a strong correlation (R^2=0.5) between litter and the foliage canopy at CRT (Figure 20). A study in 2006 suggested that litter, rather than decomposition, controlled the litter pool dynamics due to R^2=0.77 between litter and canopy foliage (Hall et al., 2006). The regression between litter and canopy foliage at CRT shows 50% of the variation of the litter pool can be explained by canopy biomass. The other 50% of the variation in litter pools could be due to decomposition. Heterotrophic litter decomposition is affected by temperature, moisture, decomposer species composition and litter chemistry (Adair et al., 2008). Short term – in lab incubation for 77 days – increased temperature leads to increased rates of respiration and decomposition to a certain point – with temperatures at 10°C having the greatest amount of respiration while temperatures of 30°C having the lowest respiration rate (Bradford et al., 2010). But my results for CRT show the opposite while HB supports Bradford et al. (2010). For the CRT lab litter, temperatures of 5°C had the highest average respiration rate while temperatures of 10°C had the lowest average respiration rate. HB lab litter experiments showed the opposite of CRT with temperatures of 25°C had the greatest amount of respiration while temperatures of 5°C had the lowest respiration rate. Through the entire lab experiment, the CRT respiration fluxes exhibited strange patterns of flux oscillations that did not make sense. The lab flux values were 3–4× larger than the field flux values, possibly due to the lack of

ventilation and flux buildup within the sealed bags. More experiments should be conducted to get a better understanding of the lab flux patterns.

My results show how low soil moisture will inhibit the heterotrophs to undergo aerobic respiration. For the CRT litter, average GMC had the highest respiration while minimum GMC had the lowest respiration rate. This suggests that the litter microorganisms are less flood tolerant and require more aeration compared to HB. For HB litter, maximum GMC had the highest amount of respiration while modal GMC had the lowest respiration rate. With HB showing maximum GMC corresponding to the highest respiration rates suggest that the litter microorganisms at the site are better adapted to wetter conditions considering the HB site is located beside a large body of water.

The species composition of heterotrophs has different rates of decomposition between heterotrophs that have evolved to be hot temperature tolerant and cold temperature tolerant (Bradford et al., 2010). If the litter chemistry includes a high amount of nitrogen to carbon, the heterotrophs would have a higher rate of decomposition due to N not being a limiting factor (Hobbie et al., 2000). Unfortunately, the CN analysis of litter components was not done in this thesis due to the lack of a specific litter standard for the EA analyzer to compare the litter samples to. Another factor effecting the size of the litter pool would be litter quality. In a coniferous forest stand with closed canopy, the litterfall is fairly homogenous all other factors being equal but when the forest thins or there is an open forest, a decrease of litter production follows (Millar, 2012).

Within the CRT forest, the litter biomass is highest at plot G followed by plot F and the lowest at plot H. Plot A was deciduous alvar and alvars have less litter biomass compared to forests (Van Der Maarel et al., 1989). Plot H had the highest number of stems per hectare but over half of them were small balsam fir with a diameter of less than 10 cm. Balsam Fir has a lower amount of leaf-fall compared to cedars of the same age with 8±28 kg/ha/year and 13±92 kg/ha/year, for Balsam Fir and Cedar respectively (Ferrari, 1999). At CRT, the Balsam Fir at plot H were much younger than any of the Eastern White Cedars. Younger trees shed less biomass compared to older trees. At Plot H there was also a high percentage of dead trees (Figure 20). Higher quality litter comprised of multiple species, decomposes slower than lower quality litter comprised of a single species. Coniferous leaves have a lower pH than deciduous leaves suggesting the coniferous forest plots would have a lower pH in comparison to deciduous alvar (Masuda et al., 2022). Soil pH values for CRT indicate the soils becoming more acidic from plot A – H with plot H having a pH of 5.1 while plots A–G pH range between 6.92 and 6.14. Plot H is

especially acidic compared to the rest of the CRT, possibly due to the high numbers of Balsam Fir saplings and snags.

The litter pool at CRT coniferous alvar (13422 kg[C]/ha) is 3.5× the size of the CRT deciduous alvar (3796 kg[C]/ha). Generally, deciduous species decompose at a faster rate than coniferous species due to deciduous leaves having greater amounts of potassium and phosphorus while having lower levels of lignin and ether – soluble compounds (Krishna et al., 2017) (Gao et al., 2014). The leaf litter is the portion of the litter that decomposes the fastest followed by small twigs and branches. Litter that is exposed to sunlight has a slower rate of decomposition due to desiccation compared to shaded litter (Krishna et al., 2017). The majority of the AGB at the deciduous alvar were grasses and all of the deciduous plot grasses died on an annual basis and contributed to the litter pool. Annual grasses decompose faster than coniferous needles which might be one of the reasons why the deciduous alvar litter pool is 3.5× smaller than the coniferous alvar.

Another reason for the alvar pool size difference is the composition of flora. Landscapes with higher species composition tend to have higher litter quality compared to landscapes with a single species growing on it. This is due to increased aeration and movement of oxygen through the layer as different leaf shape and sizes fall – a heterogeneous texture that allows greater circulation of moisture, permeability, surface area and nutrient dynamics (Krishna et al., 2017). While the deciduous alvar has a large assortment of species, the coniferous alvar only had one dominant species, Dwarf Juniper. The dominance of a single species in the coniferous alvar coupled with the slower decomposition rates in coniferous species, indicate that the litter layer is decomposing at a slower rate compared to the deciduous alvar. Between fungi and bacterial litter decomposition, fungi have a 75% greater capability to decrease litter organic matter compared to other microorganisms (Krishna et al., 2017). Bacterial biomass accounts for 25–30% of total soil microbe biomass (Krishna et al., 2017). Under nutrient enriched conditions such as the first frost that ruptures plant cell walls, rapid decomposition occurs via both fungi and bacteria. As temperature increases, moisture levels must increase as well as to not be the limiting factor for heterotrophic decomposers. The litter bacteria and fungi vary based on coniferous and deciduous landscapes and impact the rate of respiration based on species composition.

The coniferous alvar annually differed by 39% with lower leaf fall biomass in 2021–22 compared to 2022–23. This could be due to the annual variability of leaf fall in accordance with temperature and moisture regimes. Juniper species show a high mortality rate following dry spells with shrub and creeping juniper being more affected by drought than tree counterparts due to a shallow root system

(Camarero et al., 2020). These juniper species are more affected by drier spring-winter conditions and show a slower growing season with faster onset of growth compared to tree junipers (Camarero et al., 2020). Creeping juniper is intolerant to flooding with a ratio of 11:1 male to female creeping junipers post-waterlogging compared to a 1:1 ratio un-waterlogged (Thomas et al., 2007). Leaf mineral composition in Creeping Juniper includes Fe (0.055 mg/g), Mg (1.8 mg/g), Ca (12 mg/g), Mn (0.8 mg/g), K (3.5 mg/g), S (0.7 mg/g), and Al (0.036 mg/g) (Thomas et al., 2007). Comparing the coniferous alvar leaf-fall years to that in the CRT coniferous forest, the two years do not match up with the alvar having a larger leaf-fall in 2022–23 while the forest had a lower leaf-fall in the same year. The deadwood pool at CRT is 0.732 kg/m^2 (3660 kg[C]/ha). Compared to other coniferous deadwood pools from the literature, the CRT deadwood pool is smaller. The deadwood pool is poorly defined in literature due to the nature of identifying decayed wood based on species. The Canadian Forest Carbon Model fixes deadwood annual contributions to the DOM pool as proportions of standing live biomass. To get a comprehensive respiration flux and pool size, the volume of every single piece of deadwood – standing, aboveground and belowground – must be identified to tree species in order to get the wood density to calculate pool size and decay rate. Deadwood rates of decay are classified qualitatively and based on the observer for decay classes 1 – 5 with 1 being the least decayed and 5 being the most decayed. The decay rates for woody tissue varies on the environment. If the wood is not in contact with the ground, white and brown rot fungi (basidiomycete) dominate the decomposition process (Moroni et al., 2015). If the wood is partially buried, increased moisture levels lead to anerobic decomposition. A post fire study in Ontario Canada showed standing deadwood pools in Jack Pine forests to be 70 m^3/ha (13160 kg[C]/ha) while the unburied deadwood pool was 170 m^3/ha (31960 kg[C]/ha) (Moroni et al., 2015). Older forests (>100 years) have more buried deadwood with the Jack Pine forest having approximately 100 m^3/ha (18800 kg[C]/ha) of buried deadwood, 30 m^3/ha (5640 kg[C]/ha) standing deadwood and 90 m^3/ha (16920 kg[C]/ha) aboveground deadwood (Moroni et al., 2015). The CRT deadwood was all aboveground deadwood as it is nearly impossible to collect all buried deadwood within a single plot. Comparing the CRT aboveground deadwood to Moroni (2015), the CRT deadwood is 4.6× smaller.

Each of the CRT plots have different amounts of deadwood with the lowest at Plot A (deciduous alvar) which has no trees, thereby no access to deadwood. Plot C has 0.05 kg/m^2 (250 kg[C]/ha) of deadwood which corresponds to the partial transitional zone between alvar environment fully forested environment. Plot F had the highest amount of deadwood with 1.1 kg/m^2 (5500 kg[C]/ha) followed closely by plot E at 0.95 kg/m^2 (4750 kg[C]/ha). The large amount of deadwood also correlates to plot F with the greatest amount of litter and highest SOC found in this plot. The presence of deadwood

increased the soil organic carbon by an average of 57% in the first twelve centimeters of soil, by increasing the amount of microbial biomass for carbon (80%) and nitrogen (115%) (Nazari et al., 2023). It is possible the large amount of deadwood is one of the reasons why the SOC at plot F is higher compared to the rest of the plots. Plot E had the second largest SOC and third largest litter biomass following plot F and G respectively. Plot E had the deepest average depth across all of the plots, suggesting increased possibility of buried deadwood. Another reason plot E had a large amount of deadwood is an anecdotal piece of evidence. Near the borders of plot E, there was a collection of logs pointed in the same direction that had evidence of water weathering – driftwood logs. During the spring melt, parts of the study site were flooded with a water depth of up to 50 cm in the alvar regions. There is a possibility that annual floodwaters deposit deadwood logs at plot E which contributes to the second highest deadwood pool at CRT.

4.1.3 – Soil Carbon Pool

The coniferous forest soil carbon pool at CRT and HB are 64879 and 90933 kg[C]/ha, respectively. They differ by 28% even though both are coniferous forests. However, HB was almost entirely populated by Eastern White Cedars (*Thuja occidentalis*) with one or two Birch and Poplar while CRT was predominantly Eastern White Cedar but had various other species like Red Pines, White Pines, Balsam Fir, White Spruce, Poplar, Birch, and Larch as well. Devi, (2021), showed SOC being the highest under mixed coniferous stands, but the CRT and HB data show the opposite where HB SOC pool is 28% higher than CRT. Average peatland SOC pools of *Thuja occidentalis* is 769000 kg[C]/ha while cedar forests SOC pools range from 67000–88000 kg[C]/ha (Ott et al., 2016). This shows the large range of SOC pool for the same species. Both HB and CRT SOC pool values are slightly out of this range by 3000 kg[C]/ha but considering the predominant species at both sites are the same, it can be assumed that the size discrepancy between SOC pools is a normal factor. SOC pools are highly variable temporally and spatially with an emphasis on topographical features and soil properties (Zhang et al., 2018).

Comparing the soil carbon accumulation between the deciduous and coniferous alvar of CRT, the deciduous alvar has the higher SOC pool, almost twice the size of the coniferous alvar. This can be attributed to the growth and senescence patterns of deciduous vs coniferous species with 100% of aboveground deciduous grasses contributing to the soil carbon pool annually, compared to the 1/5th– 1/8th annual leaf-fall ratios of coniferous species contributing to the SOC pool. A study in Alberta Canada shows the SOC of deciduous (57800 kg[C]/ha) and coniferous forests 43700 kg[C]/ha) (Nickels & Prescott, 2021). The study showed that deciduous forest had the highest rate of soil organic matter

accumulation from leaf-fall. Grass sites followed the deciduous forest in SOM accumulation and the coniferous forest had the slowest rate of SOM accumulation (Nickels & Prescott, 2021). Due to the characteristics of deciduous forest – broadleaf, faster rate of decomposition compared to coniferous needles, thereby releasing carbon, nitrogen, soluble compounds, and calcium for greater rates of heterotrophic decomposition – the amount of soil organic matter accumulation was greater in the deciduous forest compared to the coniferous forest (Nickels & Prescott, 2021). Comparing Nickels & Prescott, (2021) coniferous forest soil pool (43700 kg[C]/ha) to the CRT coniferous forest soil pool (64879 kg[C]/ha), the CRT soil carbon pool is 32% greater while the HB soil carbon pool is 51.9% greater. This further pushes the idea of temporally differing soil carbon pools. While soil carbon pools have a wide range between sites, fire plays an important role in regulating soil carbon pools. The soil carbon pool at CRT and HB (Figure 13, Figure 26) shows the percentage of carbon in each of the pools as almost 50/50 for AGB and soil carbon. Both are coniferous forest sites but the soil carbon pool at HB is nearly 1/3rd larger than CRT. The fire of 1908 burned through the CRT but not HB. HB was used as a logging site; the trees clearcut but soil unburned. The initial assumption for this thesis was both sites had their pool sizes reset to zero after the fire and logging event over 100 years ago, but studies have shown little impact of logging on forest soils with carbon loss of 10–15% across varying forest types (Kreutzweiser et al., 2008). Hay Bay soil carbon pool might not have been reset to zero and had more soil carbon to start – one of the reasons why the SOC pools between the two study sites are different.

The SOC within a Red Cedar (*Juniperus virginiana*) and Scotch Pine (*Pinus sylvestris*) shelterbelt from a depth of 0–15 cm, was 3994 g/m^2 (19970 kg[C]/ha) (Sauer et al., 2007). A study in Ontario Canada shows mature coniferous forest comprised of Eastern White Cedar (*Thuja occidentalis*) and White Pine (*Pinus strobus*) to have a SOC of (100,000 kg[C]/ha) (Vijayakumar et al., 2020). A third study shows the SOC of a coniferous forest stand in Australia to be decreasing by (1490 kg[C]/ha/year) (Palosuo et al., 2012). *Pinus ponderosa* forest contain (106000 kg[C]/ha) of SOC (Conant et al., 1998). Comparing the CRT and HB SOC pool values to these studies, there is a large variation between the pool sizes and a general trend of decreasing SOC per year. The soil is losing more carbon to the atmosphere via respiration than it gains via leaf and biomass fall into the system, when the contributions of root growth are ignored.

There is a large range for SOC even within CRT at each of the eight plots. The SOC at CRT was three times larger in plot F (118867 kg[C]/ha) than plot B (39881 kg[C]/ha) (Table 3) (Figure 14). This could be due to the difference in forest composition at the two plots. Plot B is the closest forest plot to

the alvar and is situated on a 'finger' of forested land that is elevated and surrounded by rocky outcrop and grassy depressions. The trees in plot B were almost exclusively Eastern White Cedar except for a few Larch trees. Plot F was deeper in the fully forested region away from the 'finger' and had a larger range of species variability with Eastern White Cedar, Balsam Firs, White Pine, Red Pine, White Spruce and snags. When scaled up, the number of tree stems per hectare is almost 3× larger at plot F compared to plot B which could explain the large amount of SOC variation between the two plots. Plot F contains the large spike in SOC at coordinates 110, 10 meters which is over 5× the SOC at the rest of CRT (Figure 14, Table 3). The spike in SOC was due to a deep soil core sample and the high organic fraction in the B horizon. Even within the CRT plots, the SOC is highly variable per plot. This is true for HB sites where M2– contained 124405 kg[C]/ha SOC while M3 contained 71112 kg[C]/ha SOC. M2 also had the largest aboveground biomass at 108787 kg[C]/ha which would influence the SOC.

Factors that effect SOC include temperature, moisture, topography, soil properties (chemical and physical) and human activity (Zhang et al., 2018). Temperature changes via climate activity will change plant productivity inputs and soil heterotrophic respiration outputs (Sun et al., 2019). Topsoil is the most sensitive to temperature changes due to its proximity to alternating weather patterns and high lability (Lyu et al., 2021). The quality and quantity of vegetation input effects the microbial composition and by extension, the decomposition rate (Sun et al., 2019). Vegetation can alter the soil characteristics. Structural factors such as bulk density, pH, soil type/texture, elevation, terrain and groundwater levels accounted for 62.50% of total SOC variation (Zhang et al., 2018). The bulk density of CRT forest soil averaged 0.6 g/cm^3 while the deciduous alvar averaged 1.1 g/cm^3. The deciduous alvar bulk density is almost twice the density of forest, suggesting higher porosity and increased air and water flow between the pores of the soil in the forest, possibly increasing the rate of respiration and decomposition (Table 3). The coniferous alvar bulk density was higher than the deciduous alvar BD, at 1.2 g/cm^3. The two alvars had similar BD despite the deciduous and coniferous difference between the two. This could be caused by the lack of tree cover and tree roots in the alvars. The root system of deciduous grasses is not thick or strong and the roots of Creeping Juniper are shallow and near the soil surface. There is no churning or loosening of soil via deep roots, which feeds into a positive feedback cycle where soil compaction restricts root growth and prevents tree species with large root systems from taking over and loosening the soil. Within the 0–10 cm soil depth, bulk densities are lower in temperate forests (0.66 g/cm^3) compared to boreal forests (0.85 g/cm^3) and a lower bulk density correlate to greater pore space, allowing oxygenation of the soil and increased SOC (Wei et al., 2013). One of the main differences of

topography between the two study sites is the presence of water at HB. HB is a coastal site situated on Lake Huron and the research site was <5m from the coast while CRT was inland. SOC content increased with higher elevation due to the decrease of temperature and higher moisture levels which slows down decomposition (Liu et al., 2015). A mean annual temperature increase of 1°C causes the SOC to decrease by 1.87% per year (Sun et al., 2019). In cool temperate deciduous forests, 23 – 33% of soil respiration can be attributed to SOC decomposition (Sha et al., 2021).

Soil organic carbon pool can be divided into two categories: Particulate organic carbon (POC) pool and Mineral associated organic carbon pool (MAOC) (Cotrufo et al., 2019). The POC pool is predominantly comprised of decomposing plant biomass with low nitrogen while the MAOC pool is comprised of microbial products that have a high nitrogen content and chemically bonds to minerals in the soil. Coniferous forest tends to store carbon in the POC pool while deciduous forests store soil carbon in the MAOC pool (Cotrufo et al., 2019). Mixed forest stands have the greatest amount of SOC followed by coniferous and deciduous forest stands (Devi, 2021). Mixed forest stands can store 46.8% more SOM than monostands (Devi, 2021). However, when comparing the CRT forest to HB forest, the CRT (mixed forest stand with multiple species of coniferous trees), had a lower SOC than HB (almost pure cedar stand). One explanation is the 1908 fire. There is evidence at the CRT of burned and charred stumps. At HB, there is no evidence – anecdotal or physical – that states the 1908 fire touched that site. HB had a heavy logging industry in the late 1800s and early 1900s. The nature of logging is discriminate unlike fire which burns through everything in its path. Any tree that was too small would not be cut down for timber and the tree canopies would have been useless to the logging company and thereby left behind in the logged forest stand. It is assumed that the 1908 fire of CRT, reset accumulating surface litter biomass and organic soil layer to zero however, there is grounds to believe this assumption is not the case at HB (Kreutzweiser et al., 2008). So, the differences in soil depth and SOC at the two sites may have more to do with antecedent conditions (logging versus fire) than the present-day vegetation communities.

The deciduous alvar plot has fluctuations in SOC from (0,0) to (20,20) with variations of SOC from 2–14 kg[C]/m^2. Differences of plant inputs, litter quality, and soil pH effect SOC. Comparing the deciduous and coniferous alvar sites, (Figure 22, Figure 23), the soil carbon pool is, proportionally, much larger in the deciduous alvar (which is 94% soil carbon pool) compared to the coniferous alvar (49% soil carbon pool) due to the annual dieback of all deciduous plant matter contributing to the large proportion of soil carbon pool compared to the AGB and litter pools. The SOC pool size itself is 3× larger

in the deciduous alvar (65500 kg[C]/ha) compared to the coniferous alvar (23767 kg[C]/ha), owing to the differences between deciduous and coniferous species. According to the IPCC, the sizes of aboveground and belowground carbon pools varies based on the environment type. The CRT falls within the cool temperate moist environment which has the second largest belowground biomass after boreal moist environment. There is a lack of dark subsoil (B horizon) at CRT presumably due to the young age of the forest unable to build up the subsoil layer in the short 114 years since the fire.

These two factors combined increased the amount of organic carbon in the forest soil compared to alvar. The average soil carbon pool at CRT Coniferous alvar and CRT Deciduous alvar are 23767 and 73185 kg[C]/ha, respectively. The coniferous alvar pool is 67% smaller than the deciduous alvar pool of the same size. One of the reasons for this difference is the plant matter that grows at each alvar. The coniferous alvar was predominantly comprised of *Juniperus communis* (Dwarf Juniper) while the deciduous alvar was comprised of various grass, forb and shrub species. It is assumed that the turnover rate for deciduous grasses as an input to the litter biomass, would be 100% annually since all of the grasses senesce and die during the fall.

In coniferous species however, not all of the foliage input senesces on an annual basis. At CRT, the leaf-fall varied per year with 2021–22 showing a $1/5^{th}$ foliage turnover rate while 2022–23 had $1/8^{th}$ foliage turnover rate, suggesting annual variability in foliage turnover that is dependant on temperature and moisture regimes. At Hay Bay the foliage turnover was 16.4% in 2020–21, 19.8% in 2021–22 and 12.9% in 2022–23. All of the HB foliage turnover rates are within the $1/5^{th}$ (20%) – $1/8^{th}$ (12.5%) turnover rates seen at the CRT, suggesting that the leaf-fall values are within the normal range for Eastern White Cedar and, the leaf-fall is highly variable from year to year. One-fifth of Eastern White Cedar foliage in a central Minnesota cedar swamp, senesces per year (Reiner, 1974). Approximately 7% of canopy leaf-fall occurred per year in a coniferous (*Pinus sylvestris L.*) Scots pine forest (Bealde et al., 1982) while the Canadian Forest Carbon Model (Kurz and Apps, 1999) assumes canopy leaf-fall to be 15% ($1/7^{th}$) for the conifers in the Cool Temperate Ecoregion.

The collected 2023 root biomass data from CRT was 1.01 kg/m^2 (5050 kg[C]/ha) total roots, 0.66 kg/m^2 (3300 kg[C]/ha) fine roots and 0.35 kg/m^2 (1750 kg[C]/ha) coarse roots. The total roots made up 2% of the total carbon pools at CRT. One of the reasons why the measured root pool is so small could be due to sampling processes. Only one root core was taken at each plot and the root drill was not able to cut through very thick roots larger that a few centimetres. The root samples could, by chance, have been taken at low root density areas, thereby contributing to the low root biomass samples. It is unlikely

that trees live and grow with so little root biomass considering the belowground to aboveground biomass ratio in the literature is 20:80 (Murphy & Moore, 2010) (Vogt et al., 1995). Since roots form a consistent proportion of aboveground biomass, then increasing AGB will increase root biomass by the 20% proportionality coefficient. The field structural root pools values were scaled up to 20% accordingly.

Fine root biomass pool derived from Chen et al. (2004) show fine root biomass at CRT and HB to be 0.15 and 0.29 kgC/m^2 or 1.5% and 2.6% of aboveground biomass, respectively (Table 23). Fine root biomass (<2mm) sampled at seven locations at CRT in October 2023 yielded an estimate of 0.33 (± 0.12) $kg[C]/m^2$ or approximately twice a large as model estimate although no distinction was made between living and dead fine roots. Fine root biomass depends on where the sample was taken. Samples taken directly under the canopy of a tree would have more coarse, thick roots but few fine roots. Conversely, a root sample taken past the drip line would have more fine roots. To get a better understanding of root biomass in future studies, it is recommended to take a greater number of root samples per plot with randomized locations within the plot. But Vogt et al (1998) indicate there are problems with time of sampling as well as the sample size. The root: shoot ratio – the proportion of root biomass allocation compared to aboveground biomass allocation varies with tree characteristics (age, basal area, density), understory layer and soil depth. Soil depth was much shallower at CRT compared to HB, suggesting less rooted soil area and less roots in the soil profile in general. As root biomass and foliage biomass decreases, the amount of biomass allocated to the stem increases (Riech et al., 2014).

Structural root biomass was scaled to 20% of total living biomass at each site and therefore comparisons between sites are identical to living biomass comparisons with HB being 7% larger.

4.2 – Carbon Dynamics

Carbon dynamics is described as the movement of carbon between the pools resulting from factors such as decomposition, respiration and accumulation. Carbon moves from the AGB to the soil pool via decomposition of leaf and litter fall. The carbon will remain in the soil pool for months or years depending on how labile the carbon is. High lability carbon will remain in the soil pool for a shorter period of time compared to low lability carbon. Decomposition via heterotrophs release soil and litter carbon in the form of CO_2 into the atmosphere where the AGB absorbed carbon dioxide via photosynthesis and use it for growth and maintenance.

4.2.1 – Time Series CO_2 Flux

The IRGA was programmed to take time series flux readings every fifteen minutes for 96 values per day. Seasonal and daily sinusoidal patterns emerge. Seasonally, the average flux per month increases

from April to August, peaks in August, and decreases from August to December. The factor most responsible for this pattern is temperature (Dilustro et al., 2005). As temperature increases, both photosynthesis and metabolic processes increase. This is true for soil microorganisms and root respiration. The average heterotrophic flux throughout the 2022–23 study period at CRT was 2.19 $\mu mol/m^2/s$ (829 g[C]/m^2/year) while HB averaged at 2.07 $\mu mol/m^2/s$ (784 g[C]/m^2/year) – a 5.4% difference between the two sites. Both CRT and HB average fluxes are withing the normal annual flux for global temperate forests which have a mean annual flux of 769±338 g[C]/m^2/y (Sha et al., 2021). A study on *Chamaecyparis thyoides* (Atlantic white cedar) showed annual modeled soil flux to be 1.15±0.5 μg $CO_2/m^2/hr$ (860 g[C]/m^2/year) which is very close to the 2022–23 CRT R_h flux (Xu et al., 2020). CRT 2022–23 flux per plot was highest in plot H, averaging approximately 3 $\mu mol/m^2/s$ followed by plot C averaging at 2.75 $\mu mol/m^2/s$. The lowest flux occurred at plot D with 1.5 $\mu mol/m^2/s$. Factors that affect the soil carbon flux includes temperature, moisture, and soil characteristics. A study of mixed pine forest showed the lowest soil carbon flux occurring in February 2022 (0.78 $\mu mol/m^2/s$) and the highest flux (6.99 $\mu mol/m^2/s$) in May 2022 (Dilustro et al., 2005). The maximum threshold of soil moisture is 18% volumetric moisture content (VMC) while the minimum threshold is 6% VMC. Soil moisture higher than 18% VMC or lower than 6% VMC will negatively impact heterotrophic respiration by producing an anerobic environment and drought environment respectively (Dilustro et al., 2005). Under dry conditions, the diffusion rate of enzymes and soluble carbon becomes limited to the microorganisms while under wet conditions, there is a lack of gas exchange and soil oxygen levels decrease due to the difficulty of oxygen diffusing into waterlogged soil pores (Sha et al., 2021). As long as soil moisture is non-limiting it should be temperature that influences respiration (Dilustro et al., 2005).

Soil characteristics such as texture influence the soil carbon flux (Stielstra et al., 2015). Comparing sand dominant soil vs clay dominant soils, the former has a higher soil porosity compared to the latter and contains a higher surface area to volume ratio which allows for increased microbes to colonize and live on the surface of each particle (Stielstra et al., 2015). Soil comprised of larger organic and inorganic particles have better drainage capabilities compared to soils with very small, fine particles or denser vegetation (Stielstra et al., 2015). HB average soil flux in 2022 had the greatest average flux in plot E followed by plot A and the smallest flux at plot B. HB soil respiration collars were contained within a single 20×20m quadrant but each set of collars were placed differently. For instance, Plot F was placed in between two cedar trees while plot E was placed with 60 cm of plot F. Interestingly, the soil flux in 2020 show plot E with the largest average soil respiration rate for R_a, 2021 second largest respiration for R_a (after plot A) but 2022 show plot E with the largest respiration for R_h at HB. 2021 and 2020 have plot F

as the largest R_h contributor at HB. This shows soil fluxes fluctuating spatially and temporally at the same study site but with differences in temperature and moisture regimes throughout the study years. Litter/leaf-fall quality and quantity could also play a factor with the 2021–22 leaf-fall being 34.7% greater than 2022–23 leaf-fall. The leaf-fall would accumulate more in landscape depressions and with litter contributing to 35% of soil respiration, soil flux would be higher in areas and years with greater leaf/litter fall (Han et al., 2015).

The CRT average heterotrophic flux for 2022–23 in the alvar was 1.21 µmol/m²/s (425 g[C]/m²/year) and 1.34 µmol/m²/s (471 g[C]/m²/year) for coniferous and deciduous alvars respectively. The reason for the deciduous alvar having a 9.7% higher flux than the coniferous alvar could be due to the growth patterns of deciduous species and characteristics of coniferous species. Coniferous litter is more acidic (pH 4.4) than deciduous litter (pH 4.7) and certain heterotrophs cannot respire in coniferous forest litter due to higher acidity (Burgess-Conforti et al., 2019). A study showed the average soil respiration flux per year as 4.8 Mg[C]ha/year (4.8×10¹⁰ g[C]/m²/year), in a coniferous forest comprised of *Pinus sylvestris* and 8.8 Mg[C]ha/year (8.8×10¹⁰ g[C]/m²/year), in a deciduous forests comprised of *Quercus robur* (Yuste et al., 2005). Deciduous species show a larger increase in soil respiration during the growing season compared to coniferous forests while winter soil flux is approximately the same between both types of forest (Yuste et al., 2005). Annual soil respiration for mature and old growth *Populus tremuloides* (trembling aspen) forest stands were 690, and 571 g[C]/m²/year, respectively in 2005 (Tang et al., 2009).

The average CRT autotrophic flux for 2021–22 – while not a complete study year – lends credence to the some of the 2022–23 average flux plots. For instance, R_a at plot C in 2021–22 was 3.5 µmol/m²/s – the highest flux per all CRT plots. Comparing Plot C R_a to plot C R_h, R_a had the highest average flux while R_h had the second highest R_h flux after plot H, suggesting Plot C is continuously one of the highest flux producing plots and gives the notion that soil carbon flux varies based on plot at CRT.

4.2.2 – Litter/ Leaf Fall

Annual leaf-fall refers to the tree leaves that falls per year while annual litterfall encompasses the tree leaves and combines it with any seed cones, bark, branches, woody tissue and other biological tree tissue that falls from the tree. Annually, the amount of leaf-fall varies per year with deciduous species producing a greater amount of litter fall annually compared to coniferous species (Gao et al., 2014). The annual variation can be due to a variety of factors such as the year being unseasonably warm

or cold, the annual precipitation being higher than normal or lower than normal and abnormal, high windstorms.

The foliage biomass at CRT varies by species composition. In plot B, 93% of foliage was comprised of Eastern White Cedar while plot H foliage composition contained 42% Red Pine, 32% Balsam Fir, and less than 20% Eastern White Cedar. The decrease of predominant Eastern White Cedar foliage from plots B–H show the gradual species composition change with distance from the forest edge. Comparing the foliage of CRT to HB, where the species composition is almost 100% Eastern White Cedar, differences of foliage leaf-fall can occur. The amount of foliage, type of foliage and rate of foliage decomposition vary with species specific traits. Between two deciduous species, *Fagus sylvatica* and *Quercus petraea*, the amount of annual leaf-fall decreases following a hot summer in the former while the latter remained unaffected (Bou et al., 2015). Needle like leaves from *Pinus, Abies* and *Picea* species have a lower surface area to volume ratio compared to flattened leaves found in *Thujia* and *Cupressus* species (Millar, 2012). The waxy cuticle that covers the leaves to prevent gas exchange, vary in composition within and between species with older leaves having a worn-down cuticle which can increase its susceptibility to fungal infection (Millar, 2012). As leaves of different species age, the chemical composition changes. Leaf nutrient content vary depending on species with the calcium content of *Thujia occidentalis* comprising 2% of oven dry weight while many pine species such as *Picea sitchensis* have less than 1% leaf calcium content (Millar, 2012). Leaf longevity varies per species with averages of *Quercus rubra* (Northern Red Oak), *Larix decidua* (European Larch), *Pinus strobus* (Eastern White Pine), *Pinus resinosa* (Red Pine) and *Picea abies* (Norway Spruce) as 5, 6, 36, 46 and 66 months, respectively (Gower et al., 1993). This translates to an annual yearly foliage turnover of $1/3^{rd}$, $1/4^{th}$ and $1/5^{th}$ for White Pine, Red Pine and Norway Spruce, respectively. Red Pine and White Pine were both found at CRT with Red Pine foliage being the most common in plot H. There is variability in the annual foliage turnover rate with 2021–22 being $1/5^{th}$ and 2022–23 having a turnover rate $1/8^{th}$ at both CRT and HB.

At CRT, the annual leaf-fall for 2022–23 was 189 g/m^2/year which is 43% less leaf-fall than 2021–22 (337 g/m^2/year). Leaf fall has a high level of annual variability due to changes in annual temperature and moisture regimes. Temperature effects the timing of leaf emergence and senescence, two major factors in determining the net ecosystem productivity (NEP) (Barr et al., 2004). The timing of leaf emergence and death also effects energy balance between latent and sensible heat flux of the climate (Barr et al., 2004). Increased temperatures in early spring combined with late fall senescence, increases

the carbon uptake period in comparison to cold temperatures in spring and early fall senescence. Climatic variability effects the NEP which can cause a decrease the leaf area index (LAI) after a drought or stress year (Barr et al., 2004). HB shows a year-to-year variability in the amount of leaf-fall with 2021–22 leaf-fall being larger than 2022–23 leaf-fall by 35%.

The plots with the largest leaf-fall for both study years are plots B and C. This could be due to the older age of the trees present since the average DBH at CRT correspond to plots B and C. The largest amount of foliage biomass is present at plot C as well. Older and larger trees have increased biomass per tree contributing to the annual leaf litter fall at plot B and C. The annual litterfall varied based on species with hybrid poplar trees (379 g/m^2/year (1980 kg[C]/ha/year)), Black Walnut (348 g/m^2/year (1740 kg[C]/ha/year)), Norway Spruce (297 g/m^2/year (1485 (kg[C]/ha/year)), Red Oak (250 g/m^2/year (1250 kg[C]/ha/year)) and White Cedar (45 g/m^2/ year (225 kg[C]/ha/year)) – ranked highest to lowest (Wotherspoon et al., 2014). The amount of Eastern White Cedar foliage per plot at CRT gradually declines from plot B to H. Average leaf-fall biomass was 337.6 g/m^2/year (2021–22), and 189.41 g/m^2/year (2022–23) for CRT and 400 g/m^2/year (2020–21), 484 g/m^2/year (2021–22), and 316 g/m^2/year (2022–23) for HB. HB M2 site where the soil collars were installed, consistently had high annual litter/leaf-fall. Comparing CRT and HB cedar litterfall value to Wotherspoon's, (2014), cedar values, the CRT and HB both have greater amounts of litterfall. Comparing the CRT annual leaf litter fall to an evergreen, broadleaved species *Quercus ilex*, 4.34 Mg/ha/year (434 g/m^2/year), the CRT values are on the lower end of the litter fall range (Bou et al., 2015). Another comparison, annual total litter fall in a Scots Pine forest was 5791 kg/ha/year while annual leaf-fall was 2917 kg/ha/year (Santa Regina, 2001). The annual amount of carbon and nitrogen that return to soil from the leaf-fall is 1419 kg[C]/ha, and 12.9 kg[N]/ha for carbon and nitrogen respectively (Santa Regina, 2001). In Scots Pine forest, the loss of dry litter during the decomposition process was 43% annually (Santa Regina, 2001). The average annual litter fall in pine forests is 356 g/m^2/year (1780 kg[C]/ha) (Han et al., 2015). In a coniferous forest (*Cryptomeria japonica)* the leaf/litter decomposition rate was 0.79–0.92 kg/year while deciduous forest (*Cornus controversa*) leaf litter decomposition rate was 2.83–3.15 kg/year – approximately 3.5× greater than the coniferous forest decomposition rates (Masuda et al., 2022). The number of coniferous leaves that senesce on an annual basis is 1/5th of the total canopy foliage for *Cryptomeria japonica* (Masuda et al., 2022).

A study in 1974 on the litterfall patterns of Eastern White Cedar show the amount of litterfall for 1971–72 (422 + 34 g/m^2) 1965–66 (563 + 20 g/m^2), and 1966–67 (488 + 13 g/m^2) (Reiners, 1974).

Reiners (1974) state that the foliage turnover per year for Eastern White Cedar is 21% or, approximately 1/5th of the foliage. The rate of foliage turnover reported for other coniferous species is 26% (*Abies balsamea*), 35% (*Picea glauca*), 45% (*Pinus rigida*) and 50% (*Pinus echinate*), per year (Reiners, 1974). A study in Korea showed coniferous forest litter fall averaged 556 g/m^2/year in 2011 and 434 g/m^2/year in 2012 (An et al., 2017). Deciduous forest litter fall averaged 435 g/m^2/year in 2011 and 573 g/m^2/year in 2012 (An et al., 2017). Annual leaf litter fall is highly variable on an annual basis between and amongst species.

Figure 35 shows the lack of a significant relationship between the annual leaf-fall rate and litter biomass. Perplexing is that Figure 20 shows a significant correlation between litter on the forest floor and canopy foliage. In Figure 35, there is a factor of two difference between the lower litter biomass sites and the higher litter biomass sites while leaf-fall varied by a factor of four. This can be explained by the fact that plots with the most litter on the ground are not places where the leaf-fall is the largest. Plot F and G (Figure 19, Figure 34) had the highest amounts of litter biomass but did not have the highest annual leaf-fall rates for either 2021–22 or 2020–23. The highest leaf-fall occurred in plot B and C for both years. Plots F and G have greater amounts of litter than the other plots. Leaf-fall throughout the forest could be carried by wind, snow, water, and the deposition of litter is shaped by topography. Figure 20 begs the question, if litter biomass is correlated with canopy foliage, why isn't it correlated with leaf-fall? One reason is that both foliage biomass and litter develop incrementally as they represent accumulation over several years, while leaf-fall is highly variable from year to year.

The evidence for varying rates of decomposition occurs in the litter pucks and CN ratios. The field litter pucks show the highest R_h occurs in plot B while the lowest flux occurs in plot E. There is a gradual decrease of R_h from plot B – E and then from plot E – H, the flux gradually increases. The CN ratio follows a similar pattern, gradually decreases from plot A – E, and then gradually increases from E – H, suggesting less labile carbon becomes available deeper in the heavily forested area and in the finger of old, Eastern White Cedars comprising plot B and C. The reason why plot D and E have lower CN ratios compared to the rest of the forest could be due to the plethora of surface deadwood that seemed to have been relocated to those plots via water. The deposition of surface deadwood at those two sites could increase the amount of nitrogen available to the microorganisms and lower the CN ratio. This suggests litter accumulation has as much to do with litter decomposition as leaf-fall since the leaf-fall isn't that well correlated with the litter on the ground. It is possible that decomposition is responsible for the litter on the ground. The regression for leaf-fall and canopy foliage showed no significant relationship

between the two but had a high R^2 of 0.24 (2021–22) and 0.5 (2022–23). This suggests two possibilities: either too small a sample size or too large a variation between the samples. The sample size for the leaf-fall baskets were N = 45 across the entirety of the CRT forest. The pattern of leaf-fall could have been obscured by the average amount of foliage per plot and the amount of canopy fall or, the likelihood of litter on the ground and canopy are connected for the lifetime of the litter turnover rate. This connection is based on the leaf-fall which varies highly from year to year. There was a large amount of variation in leaf-fall between the two study years with 2021–22 seeing 1/5th of the canopy foliage fall while 2022–23 saw 1/8th of the canopy foliage fall at CRT. HB leaf-fall varies from 1/6th in 2020–21, 1/5th in 2021–22, and 1/8th in 2022–23, of canopy foliage. This shows the large variability of leaf-fall from year to year at both sites dominated by Eastern White Cedar. Based on my data and Reiner (1974), the upper and lower ranges of leaf-fall for Eastern White Cedar could be 1/5th and 1/8th of canopy foliage, respectively.

4.2.3 – Survey Fluxes

Survey fluxes were taken in triplicate at both living and dead collars per plot, within a three-hour time frame. The purpose of this was to isolate the fluxes per plot without fluctuations in temperature or precipitation to see if the fluxes varied per plot all else being equal. HB did not have any measured survey fluxes in 2022–23, only CRT was measured in the study year. CRT coniferous forest respiration was measured for heterotrophic respiration (R_h) and total respiration (R_t) and autotrophic respiration (R_a) was calculated by subtracting R_h from R_t. The median line of R_t is outside R_h box, there is a significant difference between R_h and R_t, which is confirmed by $P < 0.05$. Average R_h was 6% larger than R_a but had a lower R^2 value (0.14 vs 0.21). The regression equations for CRT forest show R_t having the largest soil flux when temperature is zero, followed by R_h. When the temperature is 10°C, regression equations show R_h, R_t and R_a to be 2.2, 3.9 and 1.7 $\mu mol/m^2/s$, respectively. When the temperature reached 20°C, the R_h, R_t and R_a are 2.7, 5.8 and 3.1 $\mu mol/m^2/s$, respectively. R_h is higher than R_a when temperatures are 10°C but when temperatures reach 20°C, R_a is higher. This suggests R_h is more sensitive to higher temperatures compared to R_a, possibly due to higher temperatures correlating to higher rates of evaporation and lower soil moisture. At lower temperatures, the flux is more dependant on R_h but at higher temperatures, the majority of the flux arises from R_a. The assumption of R_h and R_a was both collars were the same with the exception that one collar had dead roots and the other had living roots – the living and dead collars were within 10 cm of each other. The only difference between them were roots. But when measured, it could be that the R_h collar had lot more roots compared to the living collar which had little or no roots to begin with. There could have been a greater amount of litter or higher lability at R_h collar compared to R_a collar – if more litter fell into the dead collar vs living collar, then the dead collar

would have a higher-than-normal flux all else being equal. For instance, at CRT plot H, the soil collars were placed with no close living trees nearby other than sapling balsam firs which have roots that do not extend that far. The roots could have extended into the R_h collar but not the R_a collar which was not part of the initial assumption that soil in both collars were the same with the exception of roots. Plot H had a dead larch that had bark and woody biomass falling off – some of which might have gone into one collar and not the other.

(Figure 31) CRT forest R_h box is much smaller compared to R_t and R_a boxes, suggesting all of the data was clustered together and had a similar flux value throughout all of the surveys ranging from 1.9 – 3 $\mu mol/m^2/s$. There is a single outlier in the R_h distribution but the triplicate flux readings were all within 0.5 $\mu mol/m^2/s$ of each other and the outlier is assumed to be a valid reading. Comparatively, R_t and R_a had a greater range but no outliers.

The alvar regression equation in table 13 shows when the temperature is 0°C, R_h in the deciduous alvar has the highest flux while total – combined coniferous and deciduous alvar R_h, has the lowest flux with the flux at the deciduous alvar being 5× larger. When temperatures reach 10°C, the combined alvar R_h, R_t and R_a are 1.2, 1.8, and 0.6 $\mu mol/m^2/s$, respectively. At 20°C, the combined alvar R_h, R_t, R_a is 2.3, 3.4, and 1.1 $\mu mol/m^2/s$, respectively. For the coniferous alvar Rt regression equation, temperatures at 0°C, 10°C and 20°C correlated to fluxes of 0.07, 1.7 and 3.3 $\mu mol/m^2/s$, respectively. The deciduous alvar R_h and R_t for temperatures at 0°C, 10°C and 20°C are 0.3, 1.4 and 2.6 $\mu mol/m^2/s$ respectively (R_h), and 0.1, 1.7, and 3.2 $\mu mol/m^2/s$ respectively (R_t). The regression equation slope is the greatest at combined alvar R_t and the smallest in combined alvar R_a, indicating the fastest rate of change – the flux response to increasing temperature.

4.2.4 – Field litter Pucks

The field litter pucks were left in situ to understand how much of the litter decomposed and how much flux was due to the litter only. Decomposition rates vary between species due to the difference of lignin and cellulose content present. Litter with high nitrogen content and a lower CN ratio will decompose faster due to the way microorganisms responsible for decomposition, utilize N to break down C (Wotherspoon et al., 2014). HB litter puck flux was highest in plot D followed by plot H. The average field litter puck flux was 0.81 $\mu mol/m^2/s$ at HB compared to 1.1 $\mu mol/m^2/s$ at CRT – a difference of 26%. The difference could be attributed to the CRT having more litter, approximately double the amount of HB litter. In a litter removal experiment by Han et al, (2015), 33% of total soil respiration was a result of litter and doubling the litter showed a 77% increase in total soil respiration. The 26% litter flux

difference between CRT and HB is similar to 33% litter flux from Han et al, (2015). Comparing the spread of field litter data of HB to CRT, the former has larger box and whisper plots compared to CRT, signalling the flux data is highly variable while the latter has a much smaller range – data is more homogeneous and grouped together – with less outliers. Comparing CRT and HB litter respiration to other coniferous litter respiration (0.88 ± 0.12 µmol/m^2/s pine forests), our values are within the average range (Han et al., 2015). The average percentage of R_h flux that comes from the forest litter for CRT plots B–H is 34% while the 66% comes from the forest soils. For HB, the values are lower at 28% and 72% for litter and soil R_h respectively. Comparing these to a litter removal experiment by, Han et al, (2015), shows that 33% of total soil respiration was a result of litter, implying 67% is the result of soils only. This value is very close to both CRT and HB litter R_h to soil R_h ratios. Han et al., (2015) also showed that doubling the amount of litter caused a 77% increase in total soil respiration. It is possible that doubling the quantity of our litter will yield similar results, a possible future research avenue. Some pucks contained woody detritus matter such as small twigs and sticks which have a decomposition rate that is based on moisture. When summer temperatures average 25°C, the average wood respiration was 1.2 µmol/m^2/s hours after a rainfall event and the wood dried, the respiration dropped to 0 (Law et al., 2001).

The average change in litter puck biomass is lower at HB by 50% compared to CRT – 153 and 308 g/m^2, respectively. HB litter puck biomass decrease for all locations averaged 11.4% over the study period while CRT averages 11%. Proportionally, there is barely any change in the rate of litter decomposition between the two sites – only 0.4% more at HB. The greatest change in litter puck biomass occurred at plot H (CRT) and plot A (HB) with a decrease of litter by 22% and 44% respectively. This could have been due to animal intervention as both pucks did show some small tears where litter could have escaped and not decomposed. While the CRT and HB study sites were within 75km of each other, climate conditions may vary especially since the HB site was situated beside a freshwater bay while CRT was inland. Decomposition of litter depends on the climate, litter quality and the number of microbes present (Couˆteaux et al., 1995). Under favourable decomposition conditions, litter quality is the main influence of decomposition rate while under unfavourable conditions, climate is the dominant influence (Couˆteaux et al., 1995). Seasonality effects the difference between R_h and temperature due to changes in the litter. Spring fluxes are lower than autumn fluxes due to the lack of freshly fallen litter. Autumn has the benefit of fresh litter – a newer substrate with higher lability compared to the spring which has a lower litter lability due to a winter of decomposition. The rate of litter decomposition varies per species with deciduous species (Red Alder) loosing litter mass at rate of 50% faster than coniferous species (Western Red Cedar and Western Hemlock; Richardson et al., 2004). Due to the high amount of nitrogen

in Alder leaves, it decomposed faster than the coniferous leaf species (Richardson et al., 2004). Western Red Cedar had one of the slowest litter decomposition rates due to high ratios of Klason lignin to nitrogen content (Moore et al., 1999). For litter decomposition to occur, two processes must occur simultaneously, the mineralization and humification of cellulose, lignin and other compounds via microorganisms and, the downwards leaching of soluble compounds in soil which immobilizes and mineralizes nitrogen and carbon (Couˆteaux et al., 1995). The amount of nitrogen in the decomposition process alters the competitive outcome between potent and less potent decomposers, specifically the ones that metabolize lignin as throughout the lignin decomposition process, toxic inhibitory byproducts known as browning precursors are formed, which inhibits certain less potent microorganisms from gaining access to the nutrients in the litter (Couˆteaux et al., 1995). Active litter breakdown is partially contributed to the natural soil fauna which increases the litter surface area by grinding down plant residual matter, increasing the soil structure and mixing the soils of the A and B horizons (Couˆteaux et al., 1995).

The amount and type of litter present effects the microbial population. Experiments that removed litter saw an increase in gram positive bacteria by 21.6% and a decrease in gram negative bacteria by 32.8% (Wang et al., 2013). As both carbon and nitrogen increase from litterfall, fungi growth patterns were stronger than bacteria growth patterns. This is due to the dependence of gram-negative bacteria on inputs of fresh organic matter while fungi are able to extract nutrients out of fresh litter and old litter – including high lignin litter (Wang et al., 2013). Increases in bacteria, fungi and actinomycetes were 28.8%, 161.2% and 32.5%, respectively, following root trenching, suggesting that the nutrients stored within the severed roots is more easily decomposed via fungi systems compared to gram-positive and gram-negative bacteria species (Wang et al., 2013). Litter decomposition makes up 22.3% of total soil flux while, root respiration and mineral soil respiration makes up 20.1% and 57.6% of total soil respiration in a subtropical coniferous forest, respectively (Wang et al., 2013).

4.2.5 – Lab Litter Experiments

The litter lab pucks had the same design and composition as the field pucks with the exception that temperature and moisture could be individually manipulated to test how temperature and moisture effects the rate of litter respiration only. Litter respiration varied based on temperature, moisture and litter quality. Regression of flux against temperature (Tchamber) and evaporation rate (H20 range), were significant at CRT ($P < 0.05$, $R^2 = 0.05$) but biomass and GMC were not significant. Regression of flux against biomass (g/m^2), gravimetric moisture content (GMC), Tchamber and H20 Range, were all highly

significant with a minimum of $P < 0.05$ and R^2 value of 0.52, at HB. There is reason to suspect that the biomass and GMC should have been significant given the HB values how high significance between flux, biomass and GMC, and considering that Han et al., (2015) and Sha et al., (2021), showed litter contributing 33–37% of total soil flux and doubling the litter biomass, resulted in doubling the litter flux.

There are two main reasons as to why the CRT pucks had such a massive difference in litter flux compared to HB and amongst themselves. They contained twice the amount of litter at HB and – the unaccounted for – buildup of CO_2 within the resealable bags used to prevent moisture loss between puck flux readings. The buildup was especially high in the CRT pucks where two of the three triplicate readings had a flux of 15–20 $\mu mol/m^2/s$. The average field litter pucks were 0.81 $\mu mol/m^2/s$ at HB and 1.1 $\mu mol/m^2/s$ at CRT while the average lab litter puck flux were 1.71 $\mu mol/m^2/s$ (HB) and 4.7 $\mu mol/m^2/s$ (CRT) – the lab pucks being 2× larger at HB and 4× larger at CRT compared to the field pucks. In the field, constant air circulation prevented the accumulation of CO_2 within the litter pucks. The lab pucks did not undergo any air circulation and were actively prevented from that by sealing them in airtight bags. This was to keep the moisture constant throughout all the pucks when taking growth chamber measurements. Two of the three readings per puck were removed as they were suspect due to the buildup of CO_2. The third reading for HB and CRT was used to find the regression equations but even these values might not represent steady state flux.

From both CRT and HB lab pucks, there is a significant relationship between the temperature and flux with higher temperatures causing an increase in carbon flux production. HB lab litter pucks show the highest average flux ($\mu mol/m^2/s$) at plot G and the lowest flux at plot A while CRT highest average flux is at plot E and the lowest at plot G. This does not correlate to the highest biomasses but does correlate with the lowest biomasses for both sites. Lower litter biomass could have less easily decomposable material especially considering plot A (HB) is shown to have a high average soil R_h flux in 2021 and 2022. The litter in plot A could be more labile than the other litter plots, have a higher concentration of efficient soil microorganisms, and have higher quality litter. All these factors increase rates of the litter decomposition and when coupled with the high soil fluxes and low litter biomass at plot A, it's possible that plot has a very fast turnover rate of litter. HB flux temperature box whisker plots show a pattern of increasing fluxes as temperature increases with plot A having the smallest average flux and plot G, the largest average flux. Plot A had the lowest amount of biomass while plot G had the second highest amount of biomass after plot D; a significant correlation between the amount of biomass to flux ($P < 0.05$). Under average GMC at HB, plot G had the highest flux while plot B had the lowest flux.

Flux measurements were within 1 µmol/m^2/s of each other and half of the plots had a high flux (D,E,F,G) while half had a lower flux (A,B,C,H) which could be due to better litter quality or microbial community composition. In dry sub tropical forests, the litter respiration ranges from 0.66– 0.88 µmolCO$_2$/m^2/s while in wet subtropical forests, the litter respiration ranges from 1–1.25 µmolCO$_2$/m^2/s (Han et al., 2015). Litter respiration makes up 33% of soil respiration in litter inclusion treatments and when litter was doubled, the soil respiration increased by 77% (Han et al., 2015). Excluding litter decreases soil moisture and lower soil moisture levels prevent efficient nutrient transport and metabolic processes of heterotrophic organisms, thereby slowing down the rate of respiration and decomposition. Soil microbial communities shift when litter is removed with the dominance of fungi in soil without litter compared to bacteria (Han et al., 2015). In cool temperate deciduous forests, the litter contributes 35–37% of soil carbon flux (Sha et al., 2021).

Under maximum GMC conditions at HB, plot D and G have similar fluxes but under minimum GMC conditions, plot G has a much higher average flux compared to D and a larger flux range. This suggests that there are plots that function better under different moisture regimes even from the same site. Plot G is more drought resistant than the rest of the plots while plot A is the least drought resistant and performs best under maximum GMC. The amount of type of litter effects this. The immediate period following transient drought, litter decomposition jumped from 6±3 mg[C]/m^2/ hr to 63±18 mg[C]/m^2/ hr, when water was added – a increase from 5±2% to 37±8% of litter decomposition to the total soil flux (Cisneros-Dozal et al., 2007).

4.2.6 – CN

Patterns of soil C% and N% exists at CRT with four large peaks of soil C% and N% at (35,10)A, (60,10)A, (115,10)A and (140,10)A. The large peaks of C% and N% might explain why some CRT plots (B,C, F) have large fluxes. A higher CN ratio is linked to a soil system that can accumulate more carbon per unit of nitrogen (Cotrufo et al., 2019). The CN ratio generally increases from alvar to forest except for plot B and C – transitional zones with the oldest and largest trees providing increased decomposition matter into the two plots. Plot H has the largest CN ratio likely due to the amount of balsam fir that continuously grow and senesce, providing a continuous source of nutrients into the system. A ratio range of 10–20 achieves best growth however, the ratio varies if increases to the heterotrophic biomass is the desired outcome with a CN ratio of 12:1 – 20:1 for optimal heterotrophic biomass increase (Salin & Vinh, 2023). CN ratio effects the microbial community composition with fungi species increasing with high CN ratios as addition of nitrogen into a system has been found to have negative effects on the total

heterotrophic biomass and decrease the fungi to bacteria ratio (Wan et al., 2015). Fungi communities are more sensitive to the addition of nitrogen compared to bacteria communities (Wan et al., 2015). A factor that effects the CN ratio is tree species with deciduous species having higher nitrogen ratios compared to coniferous species (Devi, 2021). Averages in world soil CN ratio ranges from 9.9 to 25.8 (Cotrufo et al., 2019). Coniferous soils had the largest soil CN ratios of 22.5±7.1, deciduous forests 13.8±4.0 and, deciduous grasslands 11.0±2.1 (Cotrufo et al., 2019). Plants have a wider range of acceptable CN ratios compared to soil heterotrophs with fungi CN ratio ranging from 4.5 – 15 and bacterial CN ratio ranging from 3 – 5 (Cotrufo et al., 2019). The average CN ratio at CRT forest, coniferous alvar and deciduous alvar are 22.08, 15.85, and 11.50, respectively. A study done in the Bruce Peninsula on five alvar habitats show the average C and N (%) in alvar soil to be 19.9±0.8 and 0.77±0.05, respectively for a mean soil depth of 2.6 cm – a ratio of 25 (Stark et al., 2004). The average C% in young (<100 years post biomass disturbance) and old (>280 years) alvars are 21.1±1.1 and 19.2±1.1, respectively (Stark et al., 2004). Total soil carbon averaged 20% while the percentage of organic and inorganic carbon ranged from 12–18% and 5.7–7%, respectively (Stark et al., 2004). Stark et al, (2004) alvar values are larger than both the deciduous and coniferous CRT alvar values by a factor of 2.1 and 1.5, respectively.

The CN ratio at CRT increases from plot B to plot H in forested plots. The ratio is highest in plot H and the lowest in plots A deciduous alvar. Deciduous and coniferous alvar CN ratios are 48% and 28%, respectively smaller than coniferous forest CN values. The average N% in coniferous forests for stem wood, foliage, branch and bark are 0.075, 1.289, 0.318, and 0.314 respectively (Paré et al., 2013). The average soil N% in pure cedar forests is 0.70 (Ferrari, 1999). AT CRT, the average N% is 0.66 which falls within the average. The amount of C and N in pine forests is 523 and 9.1 mg/g with a CN ratio of 58 (Han et al., 2015). The amount of nitrogen mass in leaf litter is higher in deciduous species (17.4–18.9 mg/g) than coniferous species (8.0–9.2 mg g) and CN ratio of leaf litter in deciduous forests (25.6–29.4) are less than half of the CN ratio in coniferous forests (58.7–70.0) (Masuda et al., 2022). At CRT, mean N% in the deciduous alvar was lower than coniferous alvar by 9%. The literature states that deciduous species (*Mytilaria laosensis*, 17.9) should have a higher CN ratio than coniferous species (*Cunninghamia lanceolata*, 16.2) (Wan et al., 2015). Dissolved carbon and nitrogen might explain this phenomenon since the deciduous alvar floods annually during the spring melt and the meltwater could have carried carbon, nitrogen and any partially decomposed leaf-fall litter, to lower topographies. In young soil profiles, the rate of C accumulation is predominantly controlled by the amount of N present as plants have a restricted CN ratio (Amundson, 2001).

Tree species and composition effects the CN ratio in topsoil and the forest floor while in deeper mineral soils, the soil type is the main effector of CN ratios (Cools et al., 2014). Tree species influence the microbial community with microbes feeding on high lignin, low nitrogen materials, decomposing the slowest (Cools et al., 2014). Coniferous species have high CN ratios in comparison to deciduous species as, on average, deciduous plants have more nitrogen fixing bacteria species than coniferous ones (Cools et al., 2014). Soils with lower CN is associated with increased soil N_2 emissions (Cools et al., 2014). Lower CN ratios are found in fine textured soils compared to coarse textured soils as labile carbon has already been used by heterotrophic decomposers which break down coarse textured soils into finer textured soils. Deciduous species are found more frequently with fine textured soils and have a tendency to leach more N than coniferous species (Cools et al., 2014). Old growth forest soils show a higher CN ratio than former agriculture soils. Forests that have been logged or burned show increased amounts of soil CN compared to unburned, unlogged old growth forests (Cools et al., 2014). The CRT and HB have been burned and logged respectively. The CRT forests have evidence of burnt logs and charred stumps, but it is unknown if the fire reached the deciduous alvar for two main reasons; the low elevation and spring melt caused the alvar to flood with a water level up to 50 cm in some areas, preventing fire from burning. There was a lack of charred tree remnants at the deciduous alvar. The highest CN ratio at CRT is in plot H which had the greatest frequency of snags (Balsam Fir). The number of dead snags contributes to the increased CN ratio as recently fallen; high lignin materials directly correlate to the amount of CN in the organic O horizon layer. The greater amount of branch and litter fall, the higher the CN ratio. Snags are mostly lignin, attributing to increased CN ratios.

The average CN ratio increases from deciduous alvar to coniferous alvar to coniferous forest (Table 18) and the regression between C% and N% shows a highly significant R^2 of 0.82. This linear regression is valid as Wibowo, & Kasno, A. (2021), compared over 860 data points in Indonesia to show a positive correlation between C and N with R values of 0.842, 0.9, 0.895. The soil and litter composition at the CRT varied between the plots with plot H having the greatest amount of AGB and wood biomass which may have attributed to the high CN ratio as woody tissue have lignin a compound that is high in carbon and more difficult to break down compared to leaf tissue. The accumulation of woody matter within the plot could account for the high C content. The supply of carbon into the soil system can come from either aboveground litterfall which is comprised predominantly of autumnal dead leaf-fall but includes the rest of the tree with bark, branches, twigs, cones, and seeds – or from belowground where transportation of C via phloem to roots occurs and when the roots die, the carbon becomes incorporated into the soil (Marshall et al., 2021). The CN ratio in fresh, undecomposed leaves is mainly affected by the

nitrogen ratio which fluctuates between species depending on age and location on the tree, and across different species (Ostrowska & Porębska, 2015). A decrease in SOC and nitrogen is higher in coniferous forests than deciduous forests and if the rate of change is fast in one over the other, the CN ratios will vary (Ostrowska & Porębska, 2015). The largest decrease of C and N, occurs in the O and A horizons due to the connection between litter decomposition and downwards migration of smaller, decomposed particles of organic matter, deeper into the soil (Ostrowska & Porębska, 2015).

4.3 – Carbon Budget

The soil carbon budget can be defined as inputs minus outputs equals the change in storage (I – O = ΔC). Inputs include leaf-fall, the shedding of dead above and below-ground biomass and fine root turnover while the output is heterotrophic soil respiration. The rate of change of soil organic matter reflects balance between inputs and outputs. The factors that control the amount of organic matter in the soil include climate, topography, quality and quantity of parent material, biota, human activity, and time (Amundson, 2001). When mean annual temperature and precipitation increases, the residence time of SOC decrease. With every 10°C increase in temperature, microbial activity doubles (Amundson, 2001). Aerobic respiration drives the decomposition process but anerobic conditions will greatly reduce decomposition rates. Annual soil carbon flux was binned at 5°C intervals from 0–30°C to create regression equations to calculate flux given temperature and to eliminate noise in the data for a better, monthly estimate. CRT forest has the highest flux for when temperature is 0°C while CRT coniferous alvar has the lowest flux at the same temperature. Binned sites regression equations for estimating the soil output flux, have reliable R^2 values between 0.78 – 0.97 with CRT coniferous alvar having the lowest R^2 value while HB coniferous forest has the highest R^2 value. HB has the highest sensitivity to temperature. According to the regression model, when temperatures reach 20°C, the soil output becomes 2.9, 2.4, 1.7, and 1.57 µmol/m^2/s for HB forest, CRT forest, coniferous alvar and deciduous alvar respectively. Now deciduous alvar has the lowest flux while HB forest has the highest flux. The flux responds differently to changes in temperature at each of the sites.

4.3.1 – Measured Leaf Fall Gains and Soil Respiration Losses

Leaf fall was the only directly measured input in the soil carbon budget. The leaf-fall inputs at HB were almost 2× larger than the CRT. This could be due to the interannual variability associated with leaf-fall, the forest composition and age, or the coastal environment of HB causing increased leaf mortality by high winds and harsh storms. It is unlikely the interannual variability of leaf-fall is the cause. Two and three years of leaf-fall data at CRT and HB respectively, show the average amount of leaf-fall at CRT is smaller by 34%. More annual leaf-fall should be collected to validate this claim. The coniferous alvar leaf-

fall was 43% smaller than the deciduous alvar. One of the reasons for this is the different leaf-fall patterns of deciduous species. It is assumed all leaves senesce and fall annually in a deciduous environment while only 1/5th of the coniferous leaves falls annually. The turnover of vegetation is determined by the stand age, density and other factors including the allocation of biomass under different climatic conditions. In cold, dry climates, root biomass allocation is prioritized over foliage (Wang at al., 2018). The decline of NPP occurs in forests stand as trees age due to limitation of nutrients, stomatal constraints and stand development photosynthetic decline (Wang at al., 2018). The soil heterotrophic respiration rates vary between young (0–10 years, 9.7 Mg[C]/ha/year) and old (121–200 years, 2.8 Mg[C]/ha/year) forests, and R_h increases post disturbance (Wang at al., 2018). Decreased NPP and R_h with forest age, combined with increased above and belowground carbon pools, leads to the increase of vegetation turnover rates with stand age and development. It was assumed that HB and CRT forest stands are the same age given the 1908 fire and the intensive logging but there was no set year in which the logging at HB stopped entirely, suggesting that HB soils might be older than CRT. Within a forest comprised of a single species, increased elevation caused the turnover rate to decrease (Stephenson & Mantgem, 2005).

The leaf-fall inputs to the coniferous alvar were 43% smaller than the inputs to the deciduous alvar. The coniferous alvar species composition was predominantly gymnosperms which have lower vegetation turnover rates compared to the deciduous alvar, made up of angiosperms that have a high vegetation turnover rate (Stephenson & Mantgem, 2005). The coniferous alvar was at a higher elevation than the deciduous alvar due to the latter flooding during the spring melt while the former did not. Creeping juniper do not survive waterlogged or flooded soils. While the turnover rate of forest vegetation is primarily governed by biotic factors such as stand age and species while abiotic, climatic factors govern the soil turnover rate. The soil turnover rate was the longest at HB and the shortest in the coniferous alvar. Even between CRT and HB forests, the turnover rate via losses was 31.7 and 19 years respectively – HB 1.6× shorter than CRT.

The global soil carbon flux varies between life ecoregions with warm temperate forests containing annual soil C flux of 0.826 kg/m^2/year while cool temperate forest soil C flux are 0.912 kg/m^2/year (Amundson, 2001). The annual soil losses at HB (0.50 kg[C]/m^2/y) and CRT (0.58 kg[C]/m^2/year) are much smaller than Amundson, (2001) values, suggesting that, globally, the amount of carbon flux from soil is much higher than in the Bruce Peninsula. The mean soil C content in temperate cool and warm forests are 12.7 and 7.1 kg/m^2, respectively (Amundson, 2001). Cooler temperatures

inhibit decomposition. Soil turnover rates vary based on forest origin and type with old forests having a longer soil C turnover rate compared to young and middle-aged stands. Soil turnover rates in different forest types are, evergreen broadleaf forest (15.4 years), deciduous broadleaf forest (23.5 years), evergreen needleleaf forest (24.3 years), mixed needle and broadleaf forest (37.9 years), and deciduous needle leaf forest (53.8 years) (Wang et al., 2018). The rate of carbon turnover is correlated with latitude – high latitude forests have a slower turnover rate compared to low latitudes (Wang et al., 2018). Increasing precipitation will increase the soil turnover rate by increasing the aboveground and belowground carbon inputs, simulating microbial decomposition, and cause increase availability of nitrogen (Wang at al., 2018). Under global enhanced precipitations models, an increase of mean annual precipitation of 28% will cause annual soil respiration to increase by 16% while decreases in precipitation correlates to a reduction of soil respiration by 17% (Wang at al., 2018).

4.3.2 – Calculated Root Input

The fine root biomass turnover rates were calculated using the relationships of Chen et al. (2004) for the assumed age (114 y) of the forest and mean annual temperature of 6.5°C. These indicate an annual fine root turnover of 9.0% and 5.5%. at CRT and HB. The relative fine root pool sizes and fine root turnover rates somewhat offset each other such that annual production of soil carbon from fine roots is 0.10 and 0.13 kgC/m^2/y at the two sites, respectively (Table 24). The fine root pools represent 16.8% and 24.1% of their foliage pools.

A direct comparison of the calculated soil carbon budgets here to those of Bao (2021) at Hay Bay are not valid because fine root turnover was not included as an input in that study and as well Rh fluxes were likely influenced by CO_2 leakage from poorly sealed collars. In 2022–23 special attention was paid to capping and sealing the dead-root soil collar bases at Hay Bay. Root biomass sampled in the field was made difficult because the manual corer wasn't sharp enough to > 10 mm in diameter. It was impossible to cut through large roots or large pieces of buried deadwood. This was an issue at both HB and CRT as the ground at both sites was very springy – as if the interconnected root system formed a mattress spring effect. The serrated power corer employed at CRT seems to have alleviated this problem. The percentage of roots varies in the literature from 5% to 40% depending on forest type and composition (Nickels & Prescott, 2021; Brunner et al., 2015).

Nickels & Prescott (2021) suggest forest floor composition for deciduous forest and deciduous grass was predominantly grasses and shrubs while the coniferous forest floor was comprised of mosses. Root biomass was greater in the deciduous forest than the deciduous alvar grasses due to the lack of

very fine roots (<2mm). At the deciduous forest site, very fine roots made up 50% of total root biomass while the coniferous forest contained 40% coarse (>2mm) roots (Nickels & Prescott, 2021). The pH of the deciduous grass site was 7.0 while the coniferous forest and deciduous forest were 6.5 and 6.4, respectively (Nickels & Prescott, 2021).

Obtaining field data on the fine root systems of the CRT would be a major undertaking. However, Achidago's, (2023), work on modeling the total GPP in the Bruce Peninsula, was used to calculate the structural root annual growth in the CRT using an assumed 20% belowground proportion of living biomass. In broadleaf deciduous forests, the fine root biomass made up 8% of belowground biomass (Vogt et al., 1995). In predominant *Pinus koraiensis* (Korean Pine) coniferous forests, the root biomass made up 22% of total aboveground biomass (He et al., 2018). In cold temperate regions, needleleaf evergreen forest root biomass made up 22% of aboveground biomass (Vogt et al., 1995). Root biomass in a mature *Pinus sylvestris L*. (Scots pine) forest made up 18% of aboveground biomass (Urban et al., 2014). Root biomass is 20% of aboveground biomass in a temperate bog environment (Murphy & Moore, 2010). Averaging these percentages out, the total root biomass in a coniferous forest makes up approximately 20% of total aboveground biomass.

Root growth was not sampled – rather it was estimated. Achidago, (2023) modelled GPP for the Bruce Peninsula with satellite data from the past 20 years to generate annual GPP for site CF10 – the site that most closely resembles the CRT and HB, with 89% coniferous tree forest composition. The GPP over 20 years at CF10 is 3.55 ± 2.26 g[C]/m^2/day (12957 kg[C]/ha/year) while annual 2022 heterotrophic respiration is 2.19 µmol/m^2/s (8294 kg[C]/ha/year) (CRT) and 2.07 µmol/m^2/s (7840 kg[C]/ha/year) (HB). When GPP is greater than respiration, carbon accumulates in the ecosystem. Assuming 20% of total living biomass increase is root input and the small inputs of aboveground and belowground dead organic matter to the soil carbon budget, the soil turnover rates (years) for HB coniferous forest and CRT coniferous forest are longer than if the only input to the carbon budget was leaf-fall. Comparing the inputs in Table 24, the HB forest has 25% more annual input than the CRT. There is a large inter annual variability for leaf-fall and fine root biomass. Factors that effect the annual amount of leaf and root input is based on temperature, moisture, age of the stand and species.

At both sites, the calculated carbon budgets are negative, and inputs are smaller than the outputs, leading to the decline of soil C pool over time. HB has larger soil C gains to balance R_h losses yielding 0.58 kg[C]/m^2/year change in storage compared to CRT 0.50 kg[C]/m^2/year. The reasons for this could be due to the variability of annual leaf-fall considering the interannual leaf-fall discrepancy of 1/5th

and $1/8^{th}$ of canopy foliage falling and the mean annual leaf-fall for three years being consistently higher at HB compared to CRT. However, more yearly leaf-fall data must be collected over multiple years to give a concrete explanation. There was a bias in leaf-fall collection trap design as the 25×35 cm baskets were designed to catch leaf-fall but not any deadwood input such as branches. On the rare occasion when a branch or twig landed on a basket it was clipped at the boundaries and included as litterfall. Falling branches and trees occur episodically and are highly location specific. The structural root estimates were made using Achidago, (2023) GPP estimates for CF10 for both HB and CRT since there was no comparable data from the HB site.

We assumed both CRT and HB sites were 115 years old due to fire and lumber practices in the early 1900s and average temperatures were 6.5°C. In fact, the fine root estimates were not particularly sensitive to stand age or annual temperature. The fine root turnover at HB is 30% larger than that at CRT, suggesting an increased amount of labile soil carbon as the result of fine root turnover and root slough decomposition. The AGBDOM and BGDOM at both sites were approximately the same with 0.04 and 0.07 kg[C]/m^2/y of deadwood inputs for both sites, suggesting an equal amount of deadwood contributing to the soil carbon budget. But the AGBDOM falling to the forest floor was assumed to equal the AGBDOM incorporated into the soil carbon budget as an input. This effectively means that the deadwood pool remains relatively constant over time which we have no method of verifying as a valid assumption. When the definition of the soil carbon pool is modified to include deadwood, the issue that arises is that measurements of R_h respiration losses do not include R_h from unburied deadwood lying on or supported above the ground.

Waring et al., (1998), after reviewing an extensive number of forest productivity studies, show the NPP/GPP ratio averages 0.47±0.04. The difference between forest GPP and NPP is due to autotrophic tree respiration, which includes respiration losses from the leaves, stems, branches, bark and roots. Applying the 0.47 proportion to modelled 20-year average GPP by Achidago (2023) for his study location CF10 (which includes Crane River Tract) of 1290 kg[C]/m^2/y, gives 20-year average NPP as 606 g[C]/m^2/y while generating 684 g[C]/m^2/y in losses as autotrophic respiration, R_a. The vegetation provides a net sink of 606 g[C]/m^2/year because gross photosynthesis of the trees is being partially offset by leaf, bark stem and root autotrophic losses.

From this study, the soil decomposers at CRT annually produce 580 g[C]/m^2/y as R_h and the roots release 540 g[C]/m^2/y autotrophically. Therefore, the combined respiration from the forest floor $R_G = R_a + R_h = 540 + 580 = 1120$ g[C]/m^2/y. This is larger than ecosystem losses of 684 g[C]/m^2/y indicating that

only 61% of ground emitted CO_2 reaches the atmosphere on an annual basis at CRT. This suggests that 39% of ground emitted CO_2 is taken up by the plant canopy. The forest ecosystem at the Crane River Tract is still serving as a net sink for atmospheric carbon dioxide.

If we were to use the same GPP and NPP values for Hay Bay vegetation (Note: HB is not within grid location CF10) because it is also dominated by coniferous trees, then the total forest autotrophic respiratory losses are the same at HB. Combining root losses and soil decomposition losses from the ground, R_G = 500 + 470 = 970 g[C]/m^2/y (Table 24). This exceeds ecosystem losses by 290 g[C]/m^2/y suggesting that 29.5% of ground emitted CO_2 is taken up by the plant canopy at HB. The forest ecosystem at Hay Bay is still serving as a slightly stronger net sink for atmospheric carbon dioxide at 540 g[C]/m^2/y.

There is a seasonal variability for fine root biomass in temperate deciduous stands with a 20% difference in fine root biomass over a 9-month period from April to January (Meinen et al., 2009). Average fine root biomass in mixed species stand (370 g/m^2) was higher than a monospecies stand (265 g/m^2) and most fine roots are found within the first 20 cm of soil depth (Meinen et al., 2009). The seasonality of root growth varies based on temperature with optimal root growth temperatures of 20°C for *Fagus* and *Tilia* species while optimal temperatures for *Carpinus* root growth is between 25 – 30°C (Meinen et al., 2009). Temperate deciduous root growth mainly occurs during the months of April to June and from July thorough January, the root biomass stays constant, suggesting two months of root growth while the rest of the year is dedicated to root maintenance (Meinen et al., 2009).

One of the reasons why Archidago, (2023), found the GPP in the Bruce Peninsula forests to be at the high end for forests in general, is the age of the forest. The CRT Forest is 114 years from the time of the last fire. Stand age effects the growth rate of the forest with younger forests having a greater GPP compared to older forests. Stand age effects the fine root biomass with Norway spruce stands aged 10, 30, 60 and 120 years, having a fine root biomass of 22, 217, 107 and 75 g/m^2, respectively (Børja et al., 2008). Extrapolated from this, the 30–60-year-old forest stands have the largest amount of fine root biomass due to the successional stage the forest is at. When the stand is 10 years, it is still covered with pioneer species and some intermediate species which induces heavy competition. Metabolic energy allocated to fine roots would be detrimental to survival as the fine roots are incredibly delicate and prone to breakage. Instead, energy would be used for growth of the tree stem and foliage to outcompete other species. At the 30-year mark, competition is lessened and more of the metabolic energy can be allocated to fine root production (Ghedini et al., 2018).

The estimate of fine root biomass in temperate forests is 775±474 g/m^2 (0.387 kg[C]/m^2) and the fine root biomass in temperate coniferous and temperate deciduous forests are 440 (0.22) and 420 g/m^2 (0.21 kg[C]/m^2) respectively (Finér et al., 2011). Moisture regimes influence fine root biomass. Two drought summers cause a decrease in fine root biomass from 200–400g/m^2, under normal conditions in coniferous boreal forest, to 4–5g/m^2 under two drought summers for *Larix sibirica* (Chenlemuge et al., 2013). In a *Pinus oaxacana* forest, drought caused the fine root biomass within the first 20 cm of soil to decrease to 18.1 g/m^2 from 59.4 g/m^2, in a wet year (Chenlemuge et al., 2013). Drought conditions are unfavourable for fine roots due to the reduced respiration and transpiration rates to prevent water loss. The tip and length of roots also reduce during drought conditions (Brunner et al., 2015). Young roots are better at absorbing water than old roots. Fine roots can survive in mild drought conditions (-0.06 MPa soil water matrix potential) and have higher rates of fine root production when a mild drought occurs, suggesting a response to increased mortality of old fine roots to drought by stimulating production of new fine roots which have a higher water absorption capacity than odd roots (Brunner et al., 2015). Under severe drought conditions (-0.12 MPa soil matrix water potential), there was a lack of replacement when fine root mortality occurred (Brunner et al., 2015).

The annual soil respiration losses at CRT are 16% larger than HB. This could be due to almost double the amount of litter present at CRT compared to HB. This a possibility since there's ample proof of interannual variability of the inputs. The 2022–23 study year could have been an abnormally dry year, a shorter growing season, harsher summer and winter temperatures.

There are two reasons why the soil carbon pool is larger at HB compared to CRT. The removal of soil via the 1908 fire and the accumulation of soil is faster at HB compared to CRT. Anecdotal evidence from the 1908 fire stated that it did not burn through the northern section of St. Edmund township, only the southern section. The Hay Bay site is location on the northern part of the St. Edmund township and have no evidence of fire scars, insinuating the soils did not burn. No soil carbon was lost to the atmosphere because of the fire at HB. The CRT soils had evidence of fire in the form of charred logs. HB, despite evidence of logging, has a larger soil carbon pool and aboveground biomass pool compared to CRT. The soil carbon at HB could have had a greater amount of time to build up and systematic logging selects only the largest trees to be logged while smaller trees would be uncut and continue to contribute to the accumulation of soil carbon. HB stem density is higher than CRT by 32% while HB leaf-fall is higher than CRT. Increased stem density leads to higher AGB and higher leaf-fall. HB AGB is larger than CRT, the foliage is higher which leads to increased leaf fall. For belowground, increased biomass at HB leads to

greater amount of root slough which increases the AGDOM and BGDOM. When leaf-fall increases, there is a greater potential for the soil to build up faster as the inputs to the system are larger at HB due to higher AGB, more trees, deeper soils, more leaf shedding, and a lack of fire. The only pool that is larger at CRT compared to HB is the litter pool. There is more litter at CRT despite having lower leaf fall. The reason for this could be due to the differences in litter type via species. CRT litter is mainly comprised of Red and White Pines while HB is Eastern White Cedar. Cedar leaves could be more easily decomposable than White or Red Pine leaves, thereby decreasing the HB litter pool.

The faster disappearance of soil at CRT compared to HB could be the result of higher respiration rates in the former. There is more respiration and less leaf-fall at CRT compared to HB. This pattern generates less available biomass and carbon for heterotrophic decomposers, thereby producing less carbon dioxide as a byproduct. The litter decomposing slower at HB could be a result of the homogenous litter comprised of cedar leaves while CRT has mixed litter of cedar and pine which results in more airflow through the litter due to the lack of compression and packing litter typically seen with leaves of the same species.

5.0 – Conclusions
5.1 – Summary of Research and Implications for Future Research

The research aimed to identify the carbon pools, carbon dynamics and carbon budget of the Bruce Peninsula, a UNESCO world heritage site and biodiversity hotspot – by answering the following questions:

1) How is the soil carbon budget evolving and are the soil carbon pools and dynamics in a steady state?
2) What factors are responsible for the steady state or lack thereof between the carbon pools and dynamics?

The results show the forest soil carbon budget was not at steady state at either CRT or HB sites. Both were losing soil carbon with gains being less than losses for the 2022–2023 study year, although both CRT and HB have positive ecosystem carbon budgets and are sequestering atmospheric carbon.

Most pools are consistently smaller at CRT compared to HB by 28% (soil carbon pool) and 28.6% (AGB). The exception is the litter pool is larger at CRT by 12.7%. Average R_h is higher at CRT (2.19 $\mu mol/m^2/s$) compared to HB (2.07 $\mu mol/m^2/s$), which could explain the output variability in soil carbon pool sizes. Foliage turnover rates varied from $1/5^{th}$ in 2021–22 and $1/8^{th}$ in 2022–23 study year. Doubling

the field litter quantity increased R_h by 26%. The factors that are responsible for the lack of steady state between the carbon pools and dynamics are climate and interannual variability associated with climatic changes, stand age and composition, litter quality and quantity. Temperature significantly impacts soil and litter flux in both field and lab experiments. GMC was significant for the HB lab litter pucks but not for CRT lab litter pucks although this was suspected to be an error in experimental design that trapped flux buildup in order to prevent moisture loss. Areas of research that should be investigated for future research are measured root inputs to the carbon budget and how deadwood contributes to the carbon budget. The root inputs are important to the carbon budget and estimated in this thesis, but models need to be verified by field work in this biodiversity hotspot. The interannual variability of leaf-fall and foliage are large– this needs to be addressed over a period of several years as 2021–22 and 2022–23 leaf-fall inputs are very discrepant, and a long-term value is required. A mechanism for better classifying the deadwood decay rate needs to be developed if this input to the soil carbon budget is to be evaluated in a site-specific way.

5.2 – Limitations of the Study

There were a few limitations that impacted the study. The R_h flux was measured using Infrared Gas Analyzer (IRGA) connected to a datalogger. Each of the IRGAs cost ~$40,000 and there were two running simultaneously – one at CRT and the other at HB. Ideally, there would be eight survey chambers multiplexed to the IRGA running simultaneously at the CRT site, each one surveying the plots in real time so if a precipitation event occurred, all of the fluxes from each plot could be compared to truly see if there are significant flux differences between the transitional zones of forest and alvar, compared to pure forest or pure alvar.

Another issue was the lack of power during long stretches of overcast weather. Due to the lack of a power outlet and a constant supply of electricity, solar panels had to be installed to charge the 12V batter which powered the IRGA and datalogger. On clear, sunny days, this was no issue, and the equipment would run smoothly. However, during overcast conditions that lasted for 3–5 days, the battery was drained and the datalogger and IRGA would stop working and collecting data. Occasionally, there are a few gaps in the continuous data due to this unpredictable phenomenon.

Since the Bruce Peninsula is a maritime climate, it sees large amounts of snow during the winter months. The CRT site is located near the side of the road which has a culvert that drains into the lower lying area. Due to this topographical feature, the snow accumulation reached over half a meter in some areas of the study site, making transportation, use and data collection of the IRGA impossible in the

winter months. Unfortunately, no flux measurements were collected during snow bound winter months. Spring flooding also caused accessibility issues into the site as the water levels were 60 cm deep in some areas of the coniferous alvar. Due to these two limitations, flux data was collected from April to December. The conclusions drawn from this thesis are strictly only applicable to the soils of the Bruce Peninsula and, more specifically, at the two study sites (CRT and HB) due to the sample size being relatively small, time and budget constraints. It would be inaccurate to assume that this study on soil carbon can be more generally applied to the forests elsewhere in Ontario or, to generalize any patterns found on soil carbon of CRT or HB and apply it to the rest of Canada.

The lab experiments for litter respiration need a better mechanism for securing steady moisture levels throughout the experiment while allowing CO_2 produced during growth chamber adjustment periods to dissipate and not accumulate to levels which are not replicated in nature.

Closing these gaps in knowledge are critical to reduce the uncertainties surrounding the soil carbon budget results from this experiment which suggest that presently the forest soil carbon reservoir is decreasing in a relatively young ecosystem following the fire of 1908.

Bibliography

Achidago, Lord-Emmanual, (2023). **Quantifying the Effect of Stressors on CO2 Uptake in the Bruce Peninsula**. MSc Thesis, Graduate Program in Geography, Faculty of Environmental and Urban Change, York University, October 2023, 99pp.

Adair, E. C., Parton, W. J., Del Grosso, S. J., Silver, W. L., Harmon, M. E., Hall, S. A., & Hart, S. C. (2008). **Simple three-pool model accurately describes patterns of long-term litter decomposition in diverse climates**. Global change biology, 14(11), 2636-2660.

Alexander, M. E., & Cruz, M. G. (2012). **Modelling the effects of surface and crown fire behaviour on serotinous cone opening in jack pine and lodgepole pine forests**. *International Journal of Wildland Fire*, *21*(6), 709. https://doi.org/10.1071/wf11153

Amundson, R. (2001). **The carbon budget in soils**. Annual Review of Earth and Planetary Sciences, 29(1), 535-562.

An, J. Y., Park, B. B., Chun, J. H., & Osawa, A. (2017). **Litterfall production and fine root dynamics in cool-temperate forests**. PLoS One, 12(6), e0180126.

Arrouays, D., Deslais, W., & Badeau, V. (2006). **The carbon content of topsoil and its geographical distribution in France**. Soil Use and Management, 17(1), 7–11. https://doi.org/10.1111/j.1475-2743.2001.tb00002.x

Baird, M., Zabowski, D., & Everett, R. L. (1999). **Wildfire effects on carbon and nitrogen in inland coniferous forests.** Plant and Soil, 209(2), 233–243. https://doi.org/10.1023/a:1004602408717

Bao, K. (2021). **Heterotrophic respiration and the soil carbon budget of Eastern White Cedar forests in the Northern Bruce Peninsula**. BSc Thesis Department of Geography, York University, May 2021.

Barr, A. G., Black, T. A., Hogg, E. H., Kljun, N., Morgenstern, K., & Nesic, Z. (2004). **Inter-annual variability in the leaf area index of a boreal aspen-hazelnut forest in relation to net ecosystem production.** Agricultural and forest meteorology, 126(3-4), 237-255.

Bealde, C. L., Talbot, H., & Jarvis, P. G. (1982). **Canopy Structure and leaf area index in a mature Scots Pine Forest.** Forestry, 55(2), 105–123. https://doi.org/10.1093/forestry/55.2.105

Boča, A., & Van Miegroet, H. (2017). **Can carbon fluxes explain differences in soil organic carbon storage under aspen and conifer forest overstories?** Forests, 8(4), 118. https://doi.org/10.3390/f8040118

Børja, I., De Wit, H. A., Steffenrem, A., & Majdi, H. (2008). **Stand age and fine root biomass, distribution and morphology in a Norway spruce chronosequence in southeast Norway.** Tree physiology, 28(5), 773-784.

Bou, J., Caritat, A., & Vilar, L. (2015). **Litterfall and growth dynamics relationship with the meteorological variability in three forests in the Montseny natural park**. Folia Forestalia Polonica, 57(3), 145-159.

Bradford, M. A., Watts, B. W., & Davies, C. A. (2010). **Thermal adaptation of heterotrophic soil respiration in laboratory microcosms.** Global Change Biology, 16(5), 1576-1588.

Brunner, I., Herzog, C., Dawes, M. A., Arend, M., & Sperisen, C. (2015). **How tree roots respond to drought.** Frontiers in plant science, 6, 547.

Burgess-Conforti, J. R., Moore, P. A., Owens, P. R., Miller, D. M., Ashworth, A. J., Hays, P. D., & Anderson, K. R. (2019). **Are soils beneath coniferous tree stands more acidic than soils beneath deciduous tree stands?** Environmental Science and Pollution Research, 26, 14920-14929.

Camarero, J. J., Gazol, A., Sánchez-Salguero, R., Sangüesa-Barreda, G., Díaz-Delgado, R., & Casals, P. (2020). **Dieback and mortality of junipers caused by drought: Dissimilar growth and wood isotope patterns preceding shrub death**. Agricultural and Forest Meteorology, 291, 108078.

Canada, N. R. (2020). **Fire ecology**. *Natural Resources Canada*. Retrieved March 29, 2023, from https://natural-resources.canada.ca/our-natural-resources/forests/wildland-fires-insects-disturbances/forest-fires/fire-ecology/13149

Chen, W., Zhang, Q., Cihlar, J., Bauhus, J., & Price, D. T. (2004). **Estimating fine-root biomass and production of boreal and cool temperate forests using aboveground measurements**: A new approach. Plant and Soil, 265, 31-46.

Chenlemuge, T., Hertel, D., Dulamsuren, C., Khishigjargal, M., Leuschner, C., & Hauck, M. (2013). **Extremely low fine root biomass in Larix sibirica forests at the southern drought limit of the boreal forest**. Flora-Morphology, Distribution, Functional Ecology of Plants, 208(8-9), 488-496.

Chiti, T., Díaz-Pinés, E., & Rubio, A. (2012). **Soil organic carbon stocks of conifers, broadleaf and evergreen broadleaf forests of Spain**. Biology and Fertility of Soils, 48(7), 817–826. https://doi.org/10.1007/s00374-012-0676-3

Cisneros-Dozal, L. M., Trumbore, S. E., & Hanson, P. J. (2007). **Effect of moisture on leaf litter decomposition and its contribution to soil respiration in a temperate forest**. Journal of Geophysical Research: Biogeosciences, 112(G1).

Conant, R. T., Klopatek, J. M., Malin, R. C., & Klopatek, C. C. (1998). **Carbon pools and fluxes along an environmental gradient in northern Arizona.** Biogeochemistry, 43, 43-61.

Cools, N., Vesterdal, L., De Vos, B., Vanguelova, E., & Hansen, K. (2014). **Tree species is the major factor explaining C: N ratios in European forest soils**. Forest Ecology and Management, 311, 3-16.

Cotrufo, M. F., Ranalli, M. G., Haddix, M. L., Six, J., & Lugato, E. (2019). **Soil Carbon Storage informed by particulate and Mineral-Associated Organic matter**. Nature Geoscience, 12(12), 989–994. https://doi.org/10.1038/s41561-019-0484-6

Couˆteaux, M. M., Bottner, P., & Berg, B. (1995). **Litter decomposition, climate and litter quality.** Trends in Ecology & Evolution, 10(2), 63-66.

Demoling, F., Ola Nilsson, L., & Bååth, E. (2008). **Bacterial and fungal response to nitrogen fertilization in three coniferous forest soils.** Soil Biology and Biochemistry, 40(2), 370–379. https://doi.org/10.1016/j.soilbio.2007.08.019

Devi, A. S. (2021). **Influence of trees and associated variables on Soil Organic Carbon: A Review**. Journal of Ecology and Environment, 45(1). https://doi.org/10.1186/s41610-021-00180-3

Dilustro, J. J., Collins, B., Duncan, L., & Crawford, C. (2005). **Moisture and soil texture effects on soil CO2 efflux components in southeastern mixed pine forests**. Forest Ecology and Management, 204(1), 87-97.

Dymond, C. C., Beukema, S., Nitschke, C. R., Coates, K. D., & Scheller, R. M. (2016). **Carbon sequestration in managed temperate coniferous forests under climate change**. Biogeosciences, 13(6), 1933–1947. https://doi.org/10.5194/bg-13-1933-2016

Ferrari, J. B. (1999). **Fine-scale patterns of leaf litterfall and nitrogen cycling in an old-growth forest**. Canadian Journal of Forest Research, 29(3), 291-302.

Finér, L., Ohashi, M., Noguchi, K., & Hirano, Y. (2011). **Factors causing variation in fine root biomass in forest ecosystems**. Forest Ecology and Management, 261(2), 265-277.

Gao, Y., Cheng, J., Ma, Z., Zhao, Y., & Su, J. (2014). **Carbon storage in biomass, litter, and soil of different plantations in a semiarid temperate region of northwest China**. Annals of Forest Science, 71(4), 427-435.

Geng, Y., Yu, X., Yue, Y., Li, J., & Zhang, G. (2009). **Active organic carbon pool of coniferous and broad-leaved forest soils in the mountainous areas of Beijing**. Forestry Studies in China, 11(4), 225–230. https://doi.org/10.1007/s11632-009-0035-0

Ghedini, G., White, C. R., & Marshall, D. J. (2018). **Metabolic scaling across succession: do individual rates predict community-level energy use?** Functional Ecology, 32(6), 1447-1456.

Goodale, C.L., Apps,M.J., Birdsey, R.A., Field, C.B., Heath, L.S., Houghton, R.A., Jenkins, J.C., Kohlmaier, G.H., Kurz, W., Liu, S., Nabuurs, G.-J., Nilsson, S., Shvidenko, A.Z., (2002). **Forest carbon sinks in the northern hemisphere**. Ecol. Appl. 12, 891–899.

Gower, S. T., Reich, P. B., & Son, Y. (1993). **Canopy dynamics and aboveground production of five tree species with different leaf longevities**. Tree physiology, 12(4), 327-345.

Gower, S., Hunter, A., Campbell, J., Vogel, J., Veldhuis, H., Harden, J., Trumbore, S., Norman, J. M., & Kucharik, C. J. (2000). **Nutrient dynamics of the southern and northern Boreas boreal forests**. Écoscience, 7(4), 481–490. https://doi.org/10.1080/11956860.2000.11682620

Hall, S. A., Burke, I. C., & Hobbs, N. T. (2006). **Litter and dead wood dynamics in ponderosa pine forests along a 160-year chronosequence.** Ecological Applications, 16(6), 2344-2355.

Han, T., Huang, W., Liu, J., Zhou, G., & Xiao, Y. (2015). **Different soil respiration responses to litter manipulation in three subtropical successional forests**. Scientific reports, 5(1), 18166.

He, H., Zhang, C., Zhao, X., Fousseni, F., Wang, J., Dai, H., Yang, S., & Zuo, Q. (2018). **Allometric biomass equations for 12 tree species in coniferous and broadleaved mixed forests, northeastern China.** PLOS ONE, 13(1). https://doi.org/10.1371/journal.pone.0186226

Hepburn, G. F. (1981). **The Bruce Peninsula Bush Fire of 1908**. In Bruce County Historical Society 1981 yearbook (pp. 20-25). Wiarton: The Society.

Hepburn, G. F. (1981). **The Bruce Peninsula Bush Fire of 1908**. In Bruce County Historical Society 1981 yearbook (pp. 20-25). Wiarton: The Society.

Hicks Pries, C. E., Castanha, C., Porras, R. C., & Torn, M. S. (2017). **The whole-soil carbon flux in response to warming.** Science, 355(6332), 1420–1423. https://doi.org/10.1126/science.aal1319

Hobbie, S. E., & Vitousek, P. M. (2000). **Nutrient limitation of decomposition in Hawaiian forests.** Ecology, 81(7), 1867-1877.

IPCC (2006). **2006 IPCC Guidelines for National Greenhouse Gas Inventories**, Prepared by the National Greenhouse Gas Inventories Programme, Eggleston H.S., Buendia L., Miwa K., Ngara T. and Tanabe K. (eds). Published: IGES, Japan.

Johnston, W. F. (1979). **Thuja occidentalis** L. Retrieved December 28, 2022, from https://www.srs.fs.usda.gov/pubs/misc/ag_654/volume_1/thuja/occidentalis.htm

Kauffman, J. B., Hughes, R. F., & Heider, C. (2009). **Carbon Pool and biomass dynamics associated with deforestation, land use, and agricultural abandonment in the Neotropics**. Ecological Applications, 19(5), 1211–1222. https://doi.org/10.1890/08-1696.1

Keeley, J. E. (2009). **Fire intensity, fire severity and burn severity: A brief review and suggested usage.** *International Journal of Wildland Fire*, *18*(1), 116. https://doi.org/10.1071/wf07049

Khan, K., Iqbal, J., Ali, A., & Khan, S. N. (2020). **Assessment of sentinel-2-derived vegetation indices for the estimation of above-ground biomass/carbon stock, temporal deforestation and carbon emissions estimation in the moist temperate forests of Pakistan**. Applied Ecology and Environmental Research, 18(1), 783–815. https://doi.org/10.15666/aeer/1801_783815

Kriiska, K., Frey, J., Asi, E., Kabral, N., Uri, V., Aosaar, J., Varik, M., Napa, Ü., Apuhtin, V., Timmusk, T., & Ostonen, I. (2019). **Variation in annual carbon fluxes affecting the SOC pool in hemiboreal coniferous forests in Estonia**. Forest Ecology and Management, 433, 419–430. https://doi.org/10.1016/j.foreco.2018.11.026

Krishna, M. P., & Mohan, M. (2017). **Litter decomposition in forest ecosystems: a review**. Energy, Ecology and Environment, 2, 236-249.

Kurz, W. A., and M. J. Apps. (1999). **A 70-year retrospective analysis of carbon fluxes in the Canadian forest sector.** Ecological Applications 93526547.

Kurz, W. A., Shaw, C. H., Boisvenue, C., Stinson, G., Metsaranta, J., Leckie, D., Dyk, A., Smyth, C., & Neilson, E. T. (2013). **Carbon in Canada's Boreal Forest — a synthesis**. Environmental Reviews, 21(4), 260–292. https://doi.org/10.1139/er-2013-0041

Lambert, M., Ung, C., & Raulier, F. (2005). **Canadian national tree aboveground biomass equations**. Canadian Journal of Forest Research, 35(8), 1996-2018. doi:10.1139/x05-112

Lavigne, M.B., Ryan, M.G., Anderson, D.E., Baldocchi, D.D., Crill, P.M., Fitzjarrald, D.R., Striegl, R.G., (1997). **Comparing nocturnal eddy covariance measurements to estimates of ecosystem respiration made by scaling chamber measurements at six coniferous boreal sites.** J. Geophys. Res.: Atmos. 102 (D24), 28977–28985.

Law, B. E., Thornton, P. E., Irvine, J., Anthoni, P. M., & Van Tuyl, S. (2001). **Carbon storage and fluxes in ponderosa pine forests at different developmental stages**. Global Change Biology, 7(7), 755–777. https://doi.org/10.1046/j.1354-1013.2001.00439.x

Liipere, S. (2014). **Community Conservation and Stewardship Plan for the Bruce Peninsula**. Bruce Peninsula Biosphere Association, Lion's Head, Ontario.

Liu, M., Sui, X., Hu, Y., & Feng, F. (2019). **Microbial community structure and the relationship with soil carbon and nitrogen in an original Korean pine forest of Changbai Mountain**, **China.** BMC Microbiology, 19(1). https://doi.org/10.1186/s12866-019-1584-6

Liu, S., An, N., Yang, J., Dong, S., Wang, C., & Yin, Y. (2015). **Prediction of soil organic matter variability associated with different land use types in mountainous landscape in southwestern Yunnan province, China**. Catena, 133, 137-144.

Lyu, H., Watanabe, T., Zhong, R., Kilasara, M., Hartono, A., & Funakawa, S. (2021). **Factors controlling sizes and stabilities of subsoil organic carbon pools in tropical volcanic soils.** Science of The Total Environment, 769, 144842.

Marshall, J. D., Peichl, M., Tarvainen, L., Lim, H., Lundmark, T., Näsholm, T., & Linder, S. (2021). **A carbon-budget approach shows that reduced decomposition causes the nitrogen-induced increase in soil carbon in a boreal forest.** Forest Ecology and Management, 502, 119750.

Maser, C., Anderson, R.G., Cromack Jr., K., Williams, J.T., Martin, R.E, (1979). **Dead and down woody material**. In: Thomas, J.W. (Ed.), Wildlife Habitats in Managed Forests: The Blue Mountains of Oregon and Washington. USDA Forest Service Agriculture Handbook, vol. 553, pp. 78–95

Masuda, C., Kanno, H., Masaka, K., Morikawa, Y., Suzuki, M., Tada, C., & Seiwa, K. (2022). **Hardwood mixtures facilitate leaf litter decomposition and soil nitrogen mineralization in conifer plantations.** Forest Ecology and Management, 507, 120006.

Meinen, C., Hertel, D., & Leuschner, C. (2009). **Root growth and recovery in temperate broad-leaved forest stands differing in tree species diversity**. Ecosystems, 12, 1103-1116.

Millar, C. S. (2012). **Decomposition of coniferous leaf litter. Biology of plant litter decomposition**, 1, 105-128.

Moore, T. R., Trofymow, J. A., Taylor, B., Prescott, C., Camire, C., Duschene, L., & Zoltai, S. (1999). **Litter decomposition rates in Canadian forests.** Global Change Biology, 5(1), 75-82.

Moroni, M. T., Morris, D. M., Shaw, C., Stokland, J. N., Harmon, M. E., Fenton, N. J., & Hagemann, U. (2015). **Buried wood: a common yet poorly documented form of deadwood.** Ecosystems, 18, 605-628.

Murphy, M. T., & Moore, T. R. (2010). **Linking root production to aboveground plant characteristics and water table in a temperate bog**. Plant and soil, 336, 219-231.

Nazari, M., Pausch, J., Bickel, S., Bilyera, N., Rashtbari, M., Razavi, B. S., & Zarebanadkouki, M. (2023). **Keeping thinning-derived deadwood logs on forest floor improves soil organic carbon,**

microbial biomass, and enzyme activity in a temperate spruce forest. European Journal of Forest Research, 142(2), 287-300.

Nickels, M. C., & Prescott, C. E. (2021). **Soil carbon stabilization under coniferous, deciduous and grass vegetation in post-mining reclaimed ecosystems.** Frontiers in Forests and Global Change, 4. https://doi.org/10.3389/ffgc.2021.689594

Obbard, M., Howe, E., Kyle, C., Haselmayer, J., & Scheifley, J., (2016). **Estimating the abundance of American black bears (Ursus americanus) on the Bruce Peninsula, Ontario**. Science and Research Technical Report, TR-13. Ontario Ministry of Natural Resources and Forestry.

Ontl, T. A. & Schulte, L. A. (2012) **Soil Carbon Storage**. *Nature Education Knowledge* 3(10):35

Ostrowska, A., & Porębska, G. (2015). **Assessment of the C/N ratio as an indicator of the decomposability of organic matter in forest soils**. Ecological Indicators, 49, 104-109.

Ott, C. A., & Chimner, R. A. (2016). **Long-term peat accumulation in temperate forested peatlands (Thuja occidentalis swamps) in the Great Lakes region of North America.** Mires & Peat, 18.

Palmer, J., Thorburn, P. J., Biggs, J. S., Dominati, E. J., Probert, M. E., Meier, E. A., Huth, N. I., Dodd, M., Snow, V., Larsen, J. R., & Parton, W. J. (2017). **Nitrogen cycling from increased soil organic carbon contributes both positively and negatively to ecosystem services in wheat Agro-Ecosystems**. Frontiers in Plant Science, 8. https://doi.org/10.3389/fpls.2017.00731

Palosuo, T., Foereid, B., Svensson, M., Shurpali, N., Lehtonen, A., Herbst, M., Linkosalo, T., Ortiz, C., Rampazzo Todorovic, G., Marcinkonis, S., Li, C., & Jandl, R. (2012). **A multi-model comparison of soil carbon assessment of a coniferous forest stand**. Environmental Modelling & Software, 35, 38–49. https://doi.org/10.1016/j.envsoft.2012.02.004

Paré, D., Bernier, P., Lafleur, B., Titus, B. D., Thiffault, E., Maynard, D. G., & Guo, X. (2013). **Estimating stand-scale biomass, nutrient contents, and associated uncertainties for tree species of Canadian forests.** Canadian Journal of Forest Research, 43(7), 599–608. https://doi.org/10.1139/cjfr-2012-0454

Peichl, M., Thevathasan, N. V., Gordon, A. M., Huss, J., & Abohassan, R. A. (2006). **Carbon sequestration potentials in temperate tree-based intercropping systems, Southern Ontario, Canada.** Agroforestry Systems, 66(3), 243–257. https://doi.org/10.1007/s10457-005-0361-8

Phillips, C. L., & Nickerson, N. (2015). **Soil respiration**. Reference Module in Earth Systems and Environmental Sciences. https://doi.org/10.1016/b978-0-12-409548-9.09442-2

Propriété Crane River Tract. CNC: Nous trouver - Ontario. (2022). Retrieved December 28, 2022, from https://www.natureconservancy.ca/fr/nous-trouver/ontario/projets-vedettes/crane-river-tract.html

Puric-Mladenovic D, J Gleeson and G Nielson., (2016). **Estimating Carbon Storage in Southern Ontario at the Regional and Stand Levels.** Climate Change Research Note 12, Science and Research Branch, Ministry of Natural Resources,22 pp.

Puric-Mladenovic, D. and G. Clark. 2010**. Predictive modeling and mapping of biomass and carbon for Eco-district 6e14.** University of Toronto, Faculty of Forestry. http://www.forestry.utoronto.ca/SettledLandscapes/BruceBiomassExplorer/

Quideau, S. A., Chadwick, O. A., Benesi, A., Graham, R. C., & Anderson, M. A. (2001). **A direct link between forest vegetation type and soil organic matter composition**. Geoderma, 104(1–2), 41–60. https://doi.org/10.1016/s0016-7061(01)00055-6

Reich, P. B., Luo, Y., Bradford, J. B., Poorter, H., Perry, C. H., & Oleksyn, J. (2014). **Temperature drives global patterns in forest biomass distribution in leaves, stems, and roots.** Proceedings of the National Academy of Sciences, 111(38), 13721-13726.

Reiners, W. A. (1974). **Foliage production by Thuja occidentalis L. from biomass and litter fall estimates**. American Midland Naturalist, 340-345.

Reschke, C., Reid, R., Jone, J., Feeney, T., Potter, H. (1999). **Conserving Great Lakes Alvars Final Technical Report of the International Alvar Conservation Initiative**. Nature Conservancy of Canada.

Richardson, J. S., Shaughnessy, C. R., & Harrison, P. G. (2004**). Litter breakdown and invertebrate association with three types of leaves in a temperate rainforest stream**. Archiv fur Hydrobiologie, 159(3), 309-326.

Sainepo, B. M., Gachene, C. K., & Karuma, A. (2018**). Assessment of soil organic carbon fractions and carbon management index under different land use types in Olesharo Catchment, Narok County, Kenya**. Carbon balance and management, 13(1), 4. https://doi.org/10.1186/s13021-018-0091-7

Salin, K. R., & Vinh, N. T. (2023). **Biofloc technology in aquaculture.** In Frontiers in Aquaculture Biotechnology (pp. 69-88). Academic Press.

Santa Regina, I. (2001). **Nutrient cycling in a natural beech forest and adjacent planted pine in northern Spain**. Forestry, 74(1), 11–28. https://doi.org/10.1093/forestry/74.1.11

Sauer, T. J., Cambardella, C. A., & Brandle, J. R. (2007). **Soil carbon and tree litter dynamics in a red cedar–scotch pine shelterbelt**. Agroforestry Systems, 71(3), 163–174. https://doi.org/10.1007/s10457-007-9072-7

Sauer, T. J., Wacha, K. M., Brevik, E. C., & Zamora, D. (2023). **Eastern red cedar effects on carbon sequestration and soil quality in the Great Plains.** Soil Science Society of America Journal. https://doi.org/10.1002/saj2.20534

Sha, L., Teramoto, M., Noh, N. J., Hashimoto, S., Yang, M., Sanwangsri, M., & Liang, N. (2021). **Soil carbon flux research in the Asian region: Review and future perspectives.** Journal of Agricultural Meteorology, 77(1), 24-51.

Stark, K. E., Lundholm, J. T., & Larson, D. W. (2004). **Arrested development of soil on alvars of Ontario, Canada: implications for conservation and restoration**. Natural Areas Journal, 24(2), 95-100.

Stephenson, N. L., & van Mantgem, P. J. (2005). **Forest turnover rates follow global and regional patterns of productivity**. Ecology letters, 8(5), 524-531.

Stielstra, C. M., Lohse, K. A., Chorover, J., McIntosh, J. C., Barron-Gafford, G. A., Perdrial, J. N., & Brooks, P. D. (2015). **Climatic and landscape influences on soil moisture are primary determinants of soil carbon fluxes in seasonally snow-covered forest ecosystems**. Biogeochemistry, 123, 447-465.

Su, F., Xu, S., Sayer, E. J., Chen, W., Du, Y., & Lu, X. (2021). **Distinct storage mechanisms of soil organic carbon in coniferous forest and evergreen broadleaf forest in Tropical China**. Journal of Environmental Management, 295, 113142. https://doi.org/10.1016/j.jenvman.2021.113142

Sun, X., Tang, Z., Ryan, M. G., You, Y., & Sun, O. J. (2019). **Changes in soil organic carbon contents and fractionations of forests along a climatic gradient in China**. Forest Ecosystems, 6, 1-12.

Tang, J., Bolstad, P. V., & Martin, J. G. (2009). **Soil carbon fluxes and stocks in a Great Lakes forest chronosequence.** Global Change Biology, 15(1), 145-155.

Thomas, P. A., El-Barghathi, M., & Polwart, A. (2007). **Biological flora of the British Isles: Juniperus communis L.** Journal of Ecology, 95(6), 1404-1440.

Tietema, A. (1998). **Microbial carbon and nitrogen dynamics in coniferous forest floor material collected along a European nitrogen deposition gradient.** Forest Ecology and Management, 101(1–3), 29–36. https://doi.org/10.1016/s0378-1127(97)00122-9

Urban, J., Čermák, J., & Ceulemans, R. (2014). **Above- and below-ground biomass, surface and volume, and stored water in a mature Scots Pine Stand**. European Journal of Forest Research, 134(1), 61–74. https://doi.org/10.1007/s10342-014-0833-3

Van Der Maarel, E., & Titlyanova, A. (1989). **Above-ground and below-ground biomass relations in steppes under different grazing conditions**. Oikos, 364-370.

Vashum, K. (2012). **Methods to estimate above-ground biomass and carbon stock in natural forests - A Review**. Journal of Ecosystem & Ecography, 02(04). https://doi.org/10.4172/2157-7625.1000116

Vijayakumar, S., Bazrgar, A. B., Coleman, B., Gordon, A., Voroney, P., & Thevathasan, N. (2020). **Carbon stocks in riparian buffer systems at sites differing in soil texture, vegetation type and age compared to adjacent agricultural fields in southern Ontario, Canada.** Agriculture, Ecosystems & Environment, 304, 107149. https://doi.org/10.1016/j.agee.2020.107149

Vogt, K. A., Vogt, D. J., & Bloomfield, J. (1998). **Analysis of some direct and indirect methods for estimating root biomass and production of forests at an ecosystem level.** In Root Demographics and Their Efficiencies in Sustainable Agriculture, Grasslands and Forest Ecosystems: Proceedings of the 5th Symposium of the International Society of Root Research, held 14–18 July 1996 at Madren Conference Center, Clemson University, Clemson, South Carolina, USA (pp. 687-720).

Vogt, K. A., Vogt, D. J., Palmiotto, P. A., Boon, P., O'Hara, J., & Asbjornsen, H. (1995). **Review of root dynamics in forest ecosystems grouped by climate, climatic forest type and species.** Plant and Soil, 187(2), 159–219. https://doi.org/10.1007/bf00017088

Wan, X., Huang, Z., He, Z., Yu, Z., Wang, M., Davis, M. R., & Yang, Y. (2015). **Soil C: N ratio is the major determinant of soil microbial community structure in subtropical coniferous and broadleaf forest plantations.** Plant and soil, 387, 103-116.

Wang, J. R., Zhong, A. L., Simard, S. W., & Kimmins, J. P. (1996). **Aboveground biomass and nutrient accumulation in an age sequence of paper birch (Betula papyrifera) in the Interior Cedar Hemlock zone, British Columbia.** Forest ecology and management, 83(1-2), 27-38.

Wang, J., Sun, J., Xia, J., He, N., Li, M., & Niu, S. (2018). **Soil and vegetation carbon turnover times from tropical to boreal forests.** Functional Ecology, 32(1), 71-82.

Wang, Q., He, T., Wang, S., & Liu, L. (2013). **Carbon input manipulation affects soil respiration and microbial community composition in a subtropical coniferous forest.** Agricultural and forest meteorology, 178, 152-160.

Wang, X., Sheng, L., Li, Y., Jiang, H., Lv, Z., Qi, W., & Luo, W. (2022). **Soil labile organic carbon indicating seasonal dynamics of soil organic carbon in northeast peatland.** Ecological Indicators, 138, 108847. https://doi.org/10.1016/j.ecolind.2022.108847

Waring, R. H., Landsberg, J. J., & Williams, M. (1998). **Net primary production of forests: a constant fraction of gross primary production?** Tree physiology, 18(2), 129-134.

Wei, Y., Li, M., Chen, H., Lewis, B. J., Yu, D., Zhou, L., & Dai, L. (2013). **Variation in carbon storage and its distribution by stand age and forest type in boreal and temperate forests in northeastern China.** PloS one, 8(8), e72201.

Wibowo, H., & Kasno, A. (2021). **Soil organic carbon and total nitrogen dynamics in paddy soils on the Java Island, Indonesia**. In IOP Conference Series: Earth and Environmental Science (Vol. 648, No. 1, p. 012192). IOP Publishing.

Wotherspoon, A., Thevathasan, N. V., Gordon, A. M., & Voroney, R. P. (2014). **Carbon sequestration potential of five tree species in a 25-year-old temperate tree-based intercropping system in Southern Ontario, Canada.** Agroforestry Systems, 88(4), 631–643. https://doi.org/10.1007/s10457-014-9719-0

Xu, C., Qu, J. J., Hao, X., Zhu, Z., & Gutenberg, L. (2020). **Monitoring soil carbon flux with in-situ measurements and satellite observations in a forested region**. Geoderma, 378, 114617.

Yuste, J. C., Nagy, M., Janssens, I. A., Carrara, A., & Ceulemans, R. (2005). **Soil respiration in a mixed temperate forest and its contribution to total ecosystem respiration.** Tree physiology, 25(5), 609-619.

Zhang, C., Li, W., Zhao, Z., Zhou, Y., Zhang, J., & Wu, Q. (2018). **Spatiotemporal variability and related factors of soil organic carbon in henan province. Vadose Zone Journal**, 17(1), 1-10.

Zhang, L., Chen, X., Xu, Y., Jin, M., Ye, X., Gao, H., Chu, W., Mao, J.,Thompson, M. (2020). **Soil labile organic carbon fractions and soil enzyme activities after 10 years of continuous fertilization and Wheat Residue Incorporation**. Scientific Reports, 10(1). https://doi.org/10.1038/s41598-020-68163-3

Zhou, G., Xu, S., Ciais, P., Manzoni, S., Fang, J., Yu, G., Tang, X., Zhou, P., Wang, W., Yan, J., Wang, G., Ma, K., Li, S., Du, S., Han, S., Ma, Y., Zhang, D., Liu, J., Liu, S., Chen, X. (2019). **Climate and litter c/n ratio constrain soil organic carbon accumulation.** National Science Review, 6(4), 746–757. https://doi.org/10.1093/nsr/nwz045